Doctoral Dissertations   Graduate School

Summer 2015

Nanoformulation for anticancer drug delivery: Enhanced pharmacokinetics and circulation

Gaurav Parekh
Louisiana Tech University

NANOFORMULATION FOR ANTICANCER DRUG DELIVERY:

ENHANCED PHARMACOKINETICS AND CIRCULATION

by,

Gaurav Parekh, B. Pharm., M. Tech.

A Dissertation Presented in Partial Fulfillment
of the Requirements for the Degree of
Doctor of Philosophy

COLLEGE OF ENGINEERING AND SCIENCE
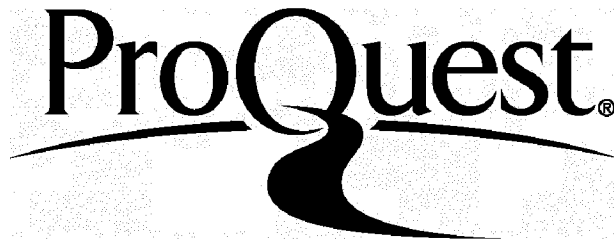LOUISIANA TECH UNIVERSITY

August 2015

ProQuest Number: 3664528

ProQuest 3664528

ProQuest LLC
789 East Eisenhower Parkway
P.O. Box 1346
Ann Arbor, MI 48106-1346

LOUISIANA TECH UNIVERSITY

THE GRADUATE SCHOOL

22nd April 2015
_____
Date

We hereby recommend that the dissertation prepared under our supervision by

GAURAV PAREKH, B. Pharm., M.Tech.
_____

entitled   NANOFORMULATION FOR ANTICANCER DRUG DELIVERY:
_____

ENHANCED PHARMACOKINETICS AND CIRCULATION
_____

_____

be accepted in partial fulfillment of the requirements for the Degree of

DOCTOR OF PHILOSOPHY IN BIOMEDICAL ENGINEERING
_____

_____
Supervisor of Dissertation Research

_____
Head of Department
BIOMEDICAL ENGINEERING
_____
Department

Recommendation concurred in:

_____

_____

_____   Advisory Committee

_____

Approved: Approved:

_____   _____
Director of Graduate Studies   Dean of the Graduate School

_____
Dean of the College

ABSTRACT

In this study, we have explored the application of the Layer-by-Layer (LbL) assembly technique for improving injectable drug delivery systems of low soluble anticancer drugs (e.g. Camptothecin (CPT), Paclitaxel (PTX) or Doxorubicin (DOX)). For this study, a polyelectrolyte shell encapsulates different types of drug nanocores (e.g. soft core, nanomicelle or solid lipid nanocores).The low soluble drugs tend to crystallize and precipitate in an aqueous medium. This is the reason they cannot be injected and may have low concentrations and low circulation time in the blood. Even though these drugs when present in the cancer microenvironment have high anti-tumor inhibition, the delivery to the tumor site after intravenous administration is a challenge. We have used FDA-approved biopolymers for the process and elaborated formation of 60-90 nm diameter initial cores, which was stabilized by multilayer LbL shells for controlled release and longer circulation. A washless LbL assembly process was applied as an essential advancement in nano-assembly technology using low density nanocore (lipids) and preventing aggregation. This advancement reduced the number of process steps, enhanced drug loading capacity, and prevented the loss of expensive polyelectrolytes.

Finally, we elaborated a general nano-encapsulation process, which allowed these three important anticancer drug core-shell nanocapsules with diameters of ca. 100-130 nm (this small size is a record for LbL encapsulation technique) to be stable in the serum and the blood for at least one week, efficient for cancer cell culture studies, injectable to

mice with circulation for 4 hrs, and effective in suppressing tumors. This work is divided into three studies. The first study (CHAPTER 4) explores the application of LbL assembly for encapsulating a soft core of albumin protein and CPT anticancer drug. In order to preserve the activity of drug in the core, a unique technique of pH reversal is employed where the first few layers of the LbL shell are assembled at acidic pH 3, and the final layers (2-3) are assembled at a slightly basic pH of 7.4. These LbL-encapsulated nanocores are not stable and immediately aggregate in water or the serum. A final layer of 5 kDa PEG was assembled to improve circulation time. It showed higher colloidal stability in PBS, high drug loading concentration of 0.5 mg/mL, and an improved drug chemical stability in Fetal Bovine Serum with high lactone fraction of 99%. It also showed 3 times improved cytotoxicity against glioblastoma cancer cells. For the first time we applied a new method of the LbL capsule assembly at different pH values, the first 4 bilayers at pH 3, and the following 3 bilayers at pH 7.4.

In the second study (CHAPTER 5), the developed LbL assembly for low solubility drug encapsulation was extended for the delivery of PTX loaded in nanomicelle cores. PTX, as a nanomicelle core, is encapsulated with fewer layers of LbL assembly, followed by an extra layer of PEG (PEGylation). A significant improvement was seen in reducing the process steps through reduction in the number of LbL layers, while smaller nano-colloids, ~100 nm, were produced with improved drug loading capacity, higher cytotoxicity, and high mice survival rate.

In the third study (CHAPTER 6), we have applied the concepts learned and the techniques developed from the previous two studies to modify the surface of the nanostructured solid lipid carriers (NLC) with LbL architecture, plus extra PEGylation.

The NLC are co-loaded with DOX and docosahexaenoic acid (DHA). This study is an attempt to further increase drug circulation time in the blood. We improved the colloidal stability with a narrow distribution size, 128 nm, polydispersity of 0.098, a higher longevity in the blood, a 1.5 times lower accumulation in the liver, a 2.25 times higher accumulation in tumors, and a significant ~3.5 times greater tumor growth inhibition in 4T1 murine tumor model in mice.

In conclusion, we developed a general model of an LbL nanoassembly core-shell drug delivery system of three anticancer drugs. The capsules had diameters of ca. 100-170 nm, were stable in the serum and the blood for three weeks, were injectable to small animals with a circulation time of 1-4 hrs., and effectively suppressed cancerous tumors in mice.

APPROVAL FOR SCHOLARLY DISSEMINATION

The author grants to the Prescott Memorial Library of Louisiana Tech University the right to reproduce, by appropriate methods, upon request, any or all portions of this Dissertation. It is understood that "proper request" consists of the agreement, on the part of the requesting party, that said reproduction is for his personal use and that subsequent reproduction will not occur without written approval of the author of this Dissertation. Further, any portions of the Dissertation used in books, papers, and other works must be appropriately referenced to this Dissertation.

Finally, the author of this Dissertation reserves the right to publish freely, in the literature, at any time, any or all portions of this Dissertation.

Author _____

Date _____

DEDICATION

To my dear parents, Mr. Subhash Kant Parekh, and Mrs. Sadhana Parekh, my brother, Prateek, and my fiancée, Ipsita.

TABLE OF CONTENTS

LIST OF TABLES

LIST OF FIGURES

ACKNOWLEDGEMENTS

CHAPTER 1

INTRODUCTION

About 40-60% of anticancer drugs developed have low bioavailability due to their

hydrophobic nature [53]. Even though they are effective when present at the tumor

microenvironment, the delivery to the site is a challenge. A lot of research is being done

to improve their delivery for different types of administrations. One of the most common

mode of chemotherapeutic delivery is through a systemic circulation. Different drug

formulation techniques are employed for delivery of such low soluble anticancer drug.

1.1   Brief overview of current low soluble drug delivery methods

Drug delivery system that use nano- and micro-carrier systems for parenteral

administration are currently under extensive study. Initial developments in micro-drops

[38, 39] and miceller nanocarriers [40-42] of hydrophobic drugs or molecules led to a

new line of research in drug delivery systems. In an article by Guzey *et al.*, an attempt

has been made to improve emulsions through Layer-by-Layer (LbL) assembly on the o/w

based emulsion system. They have also mentioned the multilayer emulsions, which have

better stability to different ambient conditions [39]. Similarly, hydrophobically modified

saccharides, such as starch, was encapsulated in oil/water (o/w) emulsion of triglyceride

oil Miglyol 812F as an oil phase and buffer solution as a water phase. Better

emulsification was observed under turbulent flow and other kinetic factors, eg. kinematic viscosity [38].

A step forward was taken where micro-drop emulsion based, micro-micelles were formulated in nano-scales. In Torchilin *et al.*, they described the formulation of polymeric micelles, which was formulated by using amphiphile copolymers [52]. It also mentions a special category of micelles formed by conjugation of hydrophilic polymers with lipids, thus forming lipid core micelles. An example is Poly-Ethylene-Glycol as copolymer with Phosphatidyl-ethanolamine (PEG-PE). It was found to have an enhanced permeability and retention (EPR) effect. The polymeric micelles had a more effective bio-distribution in mice by improving the solubility of low soluble drugs [41, 52]. It was observed that it was easy to control the size and loading capacity based on composition of water soluble polymers and the lipid. In another instance, PEG was copolymerized with polyelectrolyte, PEG with polycation, Poly-L-lysine (PLL) and polyanion, Poly(L-glutamic acid) (PGA) with PEG [40]. The major limitation of micro-drops and micellar nanocarriers was that they had a low loading capacity [58].

Another approach was to have micro-capsules with sacrificial cores. They are called microcapsule shells. The shell is composed of multilayers of polyelectrolytes. In an article by Koker *et al.*, calcium carbonate (CaCO$_3$) was used as a sacrificial template in the core and further coated by biodegradable polyelectrolyte LbL layers i.e. 2 to 4 bilayers of alternating Dextran sulfate (DS) and poly-L-arginine. The CaCO$_3$ was dissolved in resuspending microparticles in EDTA buffer solution at pH 5.4 [43]. They concluded that biodegradable polyelectrolytes based micro shells were less toxic, as tested *in vitro*. Here, based on the number of bilayers, the stability of the microcapsules

after intracellular uptake was determined. Another way to form hollow shells from LbL assembly was by lyophilizing out frozen cyclohexane in the core. LbL assembly of polyelectrolytes were done on top of it, at a temperature just below the freezing point of cyclohexane [51]. Although the hollow shell technique is quite novel, irregular release due to non-uniform destruction of hollow core and low drug loading capacity were its limitations.

A novel method of conjugating the drug with the polymer itself has been currently a major research of study for effective drug delivery. Since most of the anticancer drugs used for chemotherapy have a low half-life of systemic circulation and untargeted delivery, this leads to adverse side effects [45]. PEG conjugated with drugs was one of the first and most successful drug delivery systems, but its low biodegradability leads to toxicity. It also showed a low drug loading capacity. An effective PEG conjugate with a CPT derivative, SN-38 was formed as EZN-2208 (drug loading of 3.7%) [52].

Biopolymer based drug carrier for low soluble drugs is becoming quite common and is commercially available in the market. The most common of them are polyesters and polyamino acids, such as poly (L-glutamate) and poly (L-aspartic acid) [58]. The best example of commercially available biopolymeric drug carrier is Abraxane, in which albumin, as a biopolymer, is a carrier of PTX. The nano-encapsulations are biocompatible. LbL assembly with biopolymer based polyelectrolytes is one of the good methods to encapsulate drugs [49].

1.2   Research Goals

The objective of this research will be to make the low soluble drugs, e.g. CPT, PTX, and DOX deliverable in higher concentrations to the site of the tumor. To accomplish this objective, the formulations from these drugs are made hydrophilic in nature by encapsulating it with amphiphiles and polyelectrolytes. The increased solubility will increase the circulation time in the blood.

In this work, we developed the Layer-by-Layer (LbL) polyelectrolyte encapsulation method (initially at the Max Planck Institute, in Germany by H. Möhwald, G. Sukhorukov, F. Caruso, E. Donath, and others). Our development allows for a twenty-fold decrease of LbL capsule size, from typically 5 micrometers in the original German works to 100-170 nm in our approach [54-57]. A new improvement in LbL technique is tried on the nano-encapsulation of low soluble anticancer drugs. We made two innovations in this work: 1) Nanocore drug formulation through coacervation of drug with amphiphile including lipids; 2) Instead of repeated washing after each layer deposition, a washless technique was used for polyelectrolyte LbL assembly. This increased the drug loading capacity by 60 wt. % and made the process simpler. The following aims will be performed to test the above hypotheses 1, 2:

1) <u>To optimize the size of nanocapsules to a small size of 100-170 nm:</u> Titrated amounts of surfactants and polyelectrolytes needed per weight of drug will help in obtaining the low hydrodynamic size of the nanocapsules. It is known that particle sizes less than 200 nm easily pass the EPR at the vesicles by the tumor cells. This size is critical in order to attain longer circulation due to prevention of uptake by the liver [127].

2) <u>Washless LbL assembly under continuous sonication with capsule PEGylation:</u> We developed nano-colloids stabilized with coating of biocompatible surfactants and polyelectrolytes. First of all, the drug nano-cores developed were often lighter than water. Secondly, the washless technique reduced the steps in formulation processing, thus reducing waste of expensive polyelectrolytes and also the drug. Examples of such substances are Bovine Serum Albumin (BSA), poly amino acids, poly saccharides and commonly used surfactants for biological activities (e.g. poly vinyl pyrrolidone, polysorbate). Further Poly Ethylene Glycol (PEG) tails were attached to the outermost surface of nanoparticles for further colloidal stability, thus increasing the circulation time.

3) <u>To restore the chemical structure and activity of the encapsulated drug:</u> CPT is present in its active form, lactone, and inactive form, carboxyl. LbL assembly will act as the diffusion barrier for exterior medium to degrade the drug. QCM can be used to study the effect of LbL assembly. The main objective of the formulation is to make the drug soluble and to restore its active form for efficient systemic circulation until it finally reaches its targeted site of action.

4) <u>To optimize the nano assembly according to the required drug release rate:</u> It is important to tune the release rate of drug from the nanocapsules to match the required dosage. The final targeted model of the nanocapsules should release sustained amounts of drug when it reached the targeted site, i.e. the tumor cells.

5) Testing LbL nano-formulation on cancer infected mice through intravenous injections (in collaboration with Northeastern University, Dept. of Pharmaceutical Sciences).

1.3   Dissertation Overview

The dissertation is divided into introduction, literature review, instrumentation, and three chapters of further results. The second chapter reviews the poorly water soluble anticancer drug formulations, their limitations for delivery, the basics of LbL assembly, specificity of its architectural encapsulation, the different techniques developed for past LbL based drug delivery systems, the industrial sonication method for nano-colloid formulations, and the washless LbL technique used to formulate different drug cores.

The third chapter briefs about the instruments used for various analytical characterization, such as UV-Vis spectroscopy, Fluorescent Spectroscopy, HPLC, FT-IR, TGA; for surface characterization, such as Contact angle and Quartz Crystal Microbalance (QMC), and for morphological characterization, such as cryo/TEM, SEM and optical microscope.

The fourth chapter describes the LbL coating based nanocapsular formulation, with CPT and BSA in the core, particle size ~200 nm. The biocompatible poly amino acid based polyelectrolytes used for LbL assembly are mentioned. During the formulation, the unique pH reversal step included is mentioned. It was employed to preserve the active form of CPT, lactone. The morphological characterizations were through the particle size analyzer, SEM, TEM; the drug chemical characterization by UV-Vis spectroscopy; the LbL architecture by zeta potential and QCM studies, and finally the *in vitro* release studies and the cell viability studies in brain glioblastoma cell culture were discussed.

The fifth chapter is about development of nano-micelle based PTX core, with non ionic surfactant, a cremophor, such as Tocopherol polyethylene glycol succinate (TPGS)

and an ionic surfactant, with further encapsulation by LbL films using the washless technique, its circulation optimization by labelling with PEG tails, and finally testing its anti-tumor activity in mice. A stable dispersion of ~100 nm was formulated with a high loading capacity of ~40%.

The sixth chapter is the application of LbL advanced technique as described in Chapters 4 and 5 for enhancement of circulation of soft lipid cores with DOX hydrochloride in the mice. An enhancement in antitumor activity is demonstrated by injecting the improved drug formulation in the tumor infected mice.

The seventh chapter concludes by pointing out the achievements made in the previous Chapters, 4, 5, and 6. It also gives an outline for the future work that has to be done in order to progress in such a research direction.

CHAPTER 2

BACKGROUND AND THEORY

This chapter is a brief introduction to water insoluble anti-cancer drugs which have not been commercially available or popular in the market. Their low solubility in the blood is the reason for short systemic circulation and negligible bioavailability. Furthermore, we will introduce a well-known nano thin film deposition process of the LbL assembly technique. We will discuss its specificity on nano sized core preparation. Then we will move forward to its application in drug delivery system development. We will discuss the industrial sonication process used in assistance with nanoparticle core preparation followed by LbL assembly. Here, during the LbL assembly process, after each polyelectrolyte (PE) film deposition step, a washing step follows to remove excess and free floating polyelectrolytes (PEs). Finally, we will give a background of the washless LbL approach, which comes into play for colloidally stable nanoparticle formulation. We will conclude by discussing the non-washing approach we will be using to formulate in this research dissertation:

1) Soft protein / CPT cores

2) Solid Lipid Nanocarriers (SLN) LbL formulation

3) Emulsion core or miceller core

2.1 Cancer and Low Soluble Anti-Cancer Drugs

More than 40% of pharmacologically active compounds exhibit poor solubility in water [34]. According to Biopharmaceutic Drug Classification, they come under Class 4 [65]. They are compounds which are have both low solubility and poor intestinal wall permeability [34]. A current emphasis of drug delivery system (DDS) research is in the development of injectable nanoparticle formulations that allow the slow release of the encapsulated drug in the bloodstream [26, 27]. A number of drugs, such as Curcumin, Tamoxifen, Lapatinib, PTX, and CPT, have been approved by Food and Drug Administration (FDA) but do not have a formulation for delivery at sufficient concentrations. Numerous drugs have been synthesized for chemotherapy, but some of these drugs are water insoluble/hydrophobic (Figure 2-1) and are difficult to administer through the systemic circulation (i.e. Intravenous (IV) pathway).
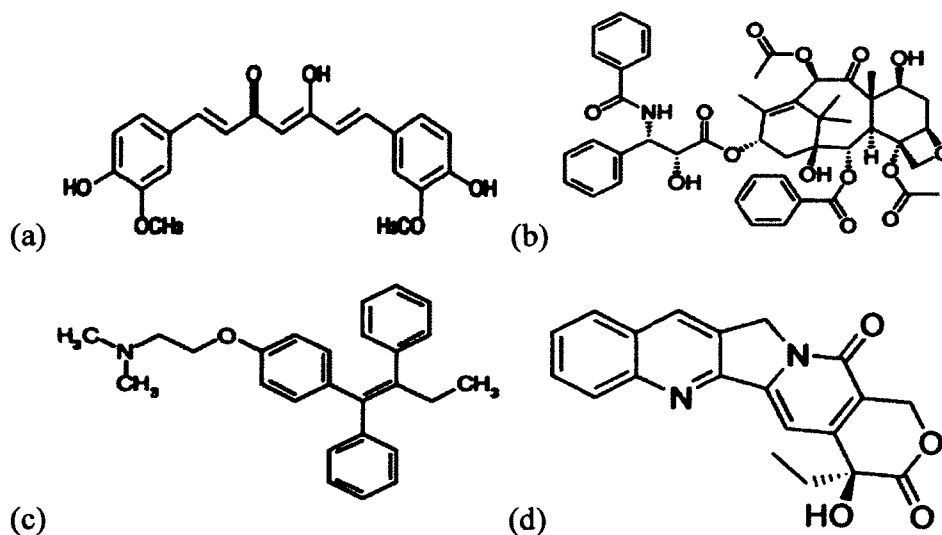
Figure 2-1: Chemical formulas of some poorly soluble anticancer drugs (a) Curcumin, (b) PTX, (c) Tamoxifen, and (d) CPT.

The respective solubility limit of these drugs in water are: Curcumin < 0.1 mg/mL, Tamoxifen 0.1 mg/mL, and for PTX and CPT < 0.001 mg/mL. Later in this chapter, we will discuss the different approaches we will take to improve the parenteral delivery of CPT, PTX and DOX as an injectable formulation. Based on the chemical stability at physiological pH and the solubility, we will use different types of nano-core carrier followed by LbL coating on top of them for better functionalization, colloidal stability, and improved circulation.

2.2 Basic Concept of Layer-by-Layer Assembly Technique

Layer-by-Layer assembly is a well-known and a common industrial approach. A short historical overview of stable coatings formation on particles of different shape and size (from microparticles to sacrificial microcores for empty microcapsules sensitive to pH and then down to shells of variable architecture formed on nanoparticles to alter their surface properties) is discussed in this section [22]. The weak and the strong PE form different film uniformity. The film growth with number of alternating polycation and polyanion deposition is either linear or exponential. This characteristic is dependent on the ionic strength of PEs being deposited. In Buron *et al.* this phenomenon was shown on a flat surface. It was demonstrated that with an increase in ionic concentrations, the polymer adsorption was decreased. The effect of bivalent ions, Ba^{2+} and Zn^{2+} was higher as compared to that by monovalent ion, Na^+ [23].

A unique approach was to deposit gold nanoparticles coated with LbL films, then slowly dissolving the inner gold with cyanide ion, thus creating a hollow nanosphere [28]. It was shown that higher number of layers, i.e. at least 20 layers (PAH/PSS) leading to 7.5 nm thick coating, was possible. It is a good example of sacrificial nanocores. It was

observed that if excess PSS destabilizes the colloidal stability of the dispersion, then it was necessary to remove the excess PE before the next layer of PE is being deposited. Another example for sacrificial core after LbL assembly of PEs is discussed in Boudou *et al.* [36]. Later, we will discuss the washing process of the LbL coating technique.

2.3 Specificity of LbL Assembly on Nanosized Cores

Limitations of length of polyelectrolytes and nature of the chain suitable for LbL coating on nanosized objects due to competition of the processes of nanocores aggregation and wrapping around a single particle was discussed [20, 39]. In practice, the low molecular weight polyelectrolytes must be <65 kDa because space for the polymer chain absorption onto the nanosphere-like structure is limited [20]. However, polyelectrolytes of high molecular weight are rarely used because their high molecular weight results in a thicker coating and rapid aggregation. Due to high charge density around the polyelectrolyte chain, it makes the chain more rigid to bend and it tends to adsorb flat on the surface. It has less effect on the thickness of the film. See Figure 2-2.

(a) Low Ionic Strength
    (high charge density / more rigid)

(b) High Ionic Strength
    (low charge density / more flexible)
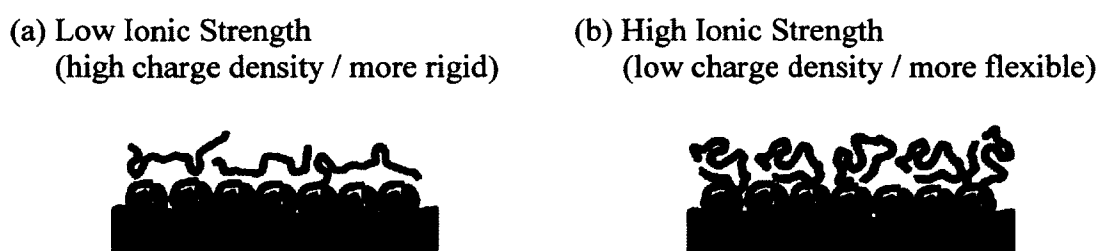
Figure 2-2: Polymer orientation on a surface based on its nature i.e. ionic strength: (a) Low ionic strength, (b) High ionic strength [20].

The pH and ionic strength strongly influence polyelectrolyte interaction and nanoparticle aggregation. The pI value determines the pH at which the net ionization of a molecule is zero. A careful selection of pH, especially for LbL assembly, is important to confirm that the charge on particle surface and the adsorbing polyelectrolytes are sufficiently high [20]. In an article by Buron *et al.*, it is shown that the concentration of polyelectrolyte and the type of salt has an influence in the colloidal stability of dispersion. The study of film deposition was done by reflectometric signal during the process, and after drying under ellipsometry [23].

Polyelectrolyte shell stability in isotonic salt solutions and *in vivo* calculation studies will be discussed [23, 31, 39]. It was observed that with an increase in salt concentration, the polyelectrolytes film thickness increased exponentially to certain concentration, i.e. 0.01 M. After that at 0.1 M concentration, the curve became linear (Figure 2-3a). It was also observed that the bivalent salt ions such as Zn^{2+} and Ba^{2+} gave a ~1.5 to ~3.0 times increased polymeric absorption after 1.6 hrs. (Figure 2-3b).

(a)   (b)   (c)
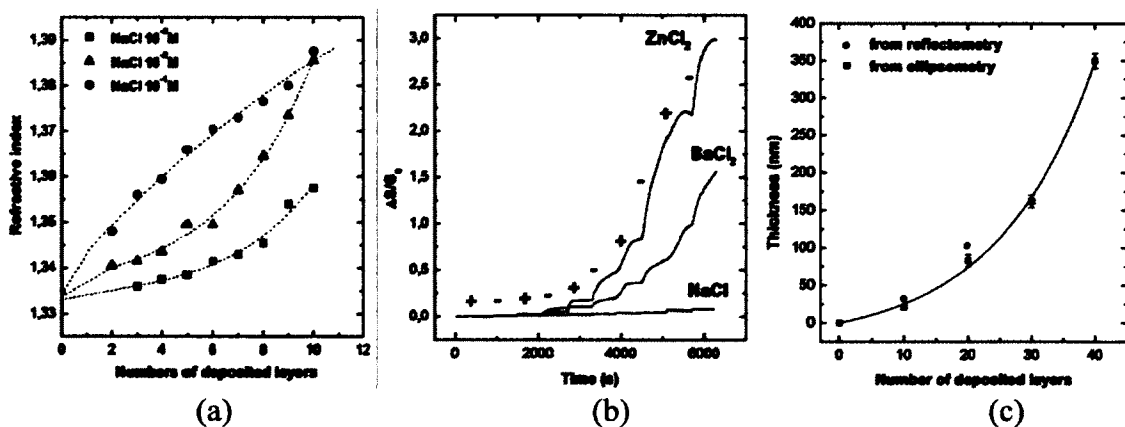
Figure 2-3: (a) Effect of different concentrations of monovalent NaCl and (b) Effect of divalent salts on quantity of polymeric absorption through reflectometric signal, (c) Comparison of reflectometry and ellipsometry measurements for film thickness with respect to number of deposited layers [23].

Chodanowski et al. used a simulation study to understand the trends in conformation of polyelectrolyte absorption on a charged particle: 1) based on the ionic concentration in the dispersion medium and 2) the particle size. They used a Monte Carlo simulation, and the electrostatic interactions were in the Debye Huckel assumptions [31]. Figure 2-4 shows that net charge, $|Q^*|$, increased linearly with particle charge, Q. An increase in the concentration of salts led to a screening effect against the particle surface charge, thus making polyelectrolyte absorption easier with an increased charge reversal. An exception was observed for an increase in particle / size ratio, $\sigma p / \sigma m > 6$ and N = 100, where the analytical data did not match the theoretical model. They suggest that this might be due to the minimum size of the polyelectrolytes needed to form a tail in the solution [31].
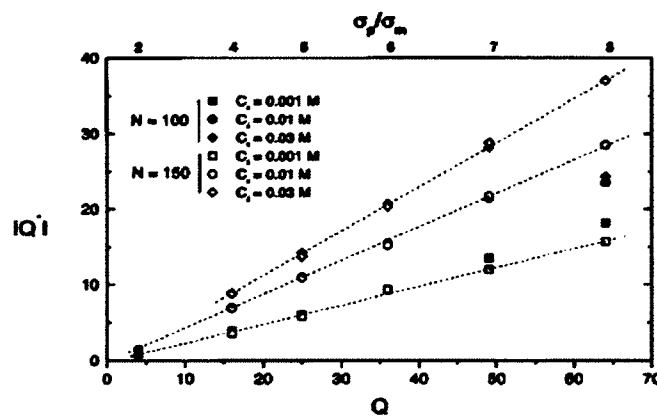
Figure 2-4: Variation of Net charge $|Q^*|$ with respect to: particle charge as Q, particle/ monomer size ratios as σ_p / σ_m and ionic concentration as Ci [31].

The polyelectrolyte concentration in LbL shell formation [39] is a critical factor to have a complete saturation of the surface. The minimum amount of PE required to coat the surface completely at a nanoscale level is simultaneously influenced by the molecular influence of the PE to the chain length, conformation at different pH or charge density,

and flexibility of the polymer chain [76]. An interesting theoretical model for estimating

critical PE concentration needed for complete surface saturation was discussed in

Mc.Clements *et al.* [77]. It assumes that the PE concentration added to the dispersion

system is completely adsorbed on all of the particle surfaces. If the polyelectrolyte

concentration is less than the saturation concentration (C_{Sat}) or the emulsion/droplet

collision concentration (C_{Ads}) i.e. $0 < C < (C_{Sat}$ or $C_{Ads})$, then

$$C_{Sat} = \frac{3\phi\Gamma_{sat}}{r} \; ; \qquad\qquad \text{Eq. 2-1}$$

$$C_{Ads} = \sqrt{\frac{60\Gamma_{Sat}^2 r_{PE}\phi}{r^3}} \; ; \qquad\qquad \text{Eq. 2-2}$$

where ϕ is the volume fraction of particles, 'Γ_{SAT}' is the surface load of PE at saturation

concentration (in kg m^{-2}), r is the radius of spherical nanoparticles (in m), r_{PE}· is the

effective radius of PE polymeric molecules in the solution (in m).

Free polyelectrolytes which are not adsorbed to the spherical nanoparticles and

are floating freely in the dispersion medium causes depletion attraction (Figure 2-5a). If

the PE concentration is less than the depletion concentration, C_{dep}, then a multilayer PE

film formation is possible. If it exceeds C_{dep}, depletion flocculation occurs. It was also

observed that a stable multilayer colloidal dispersion is less possible for very low particle

radii ($r < 0.15$ μm). See Figure 2-5 b.

(a)   (b)
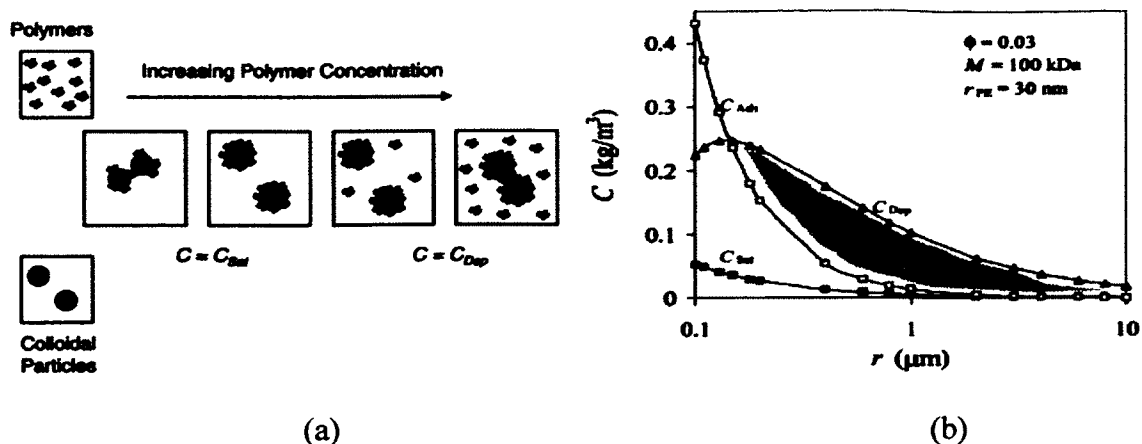
Figure 2-5: (a) Schematic shows events that happen when concentration of charged polyelectrolyte is increased in a colloidal dispersion medium, having oppositely charged particles; (b) Influence of droplet or emulsion size on critical polyelectrolyte concenration [77].

Excipients or high concentrations of solubilizers are generally used for the micro/

nanoparticle formulations. They are non-ionic polymeric excipients, which cannot be

removed from the mixture without compromising colloidal stability of dispersion. For

LbL assembly on nanocores, the amount of PE required in the presence of excipients (e.g.

polyvinylpyrrolidone, polyethylene glycol, sucrose, glycerol) is many fold more than the

PE required without excipients [10-12, 78, 79]. For example, 3-10 layers of

bio/polyelectrolytes (chondroitin sulfate, Poly L-Glutamic acid (PGA), Poly Aspartic

Acid (PAspA), Poly-L-Lysine (PLL), Poly Lactic-co-Glycolic Acid (PLGA), Dextran

Sulfate (DS), carboxymethyl cellulose, and Protamine Sulfate (PS)) were successfully

deposited on Au-modified quartz flat supports and on PROMAXX® insulin microcores

of a 1 µm diameter in aqueous solutions composed of 16% polyethylene glycol MW

3350 Da and NaCl [79].

Shells of different architecture consisting of heparin, BSA, and Poly-L-lysine-

Block-copolymer-PEG (PLB) layers were assembled on the surface of PTX and CPT

nanocrystals in aqueous solutions containing Poly Vinyl Pyrrolidone (PVP) using the non-washing LbL assembly technique [11, 12, 78]. The details of this technique will be discussed further in Section 2.6. PVP is a non-ionic surfactant, which is extensively used in pharmaceutical formulations, and is applied at the core preparation stage to enhance stability of formed drug nanocrystals. PVP does not change the amount of polyelectrolyte required for layer formation by complete ζ–potential charge reversal [12].

2.4   LbL Assembly Techniques for Drug Delivery Applications

This section will describe various techniques other than the sonication method, which was used in assistance with LbL assembly for encapsulations of micronized drugs and contrasting agents. In a review article by Ariga *et al.*, a functional hollow shell was formed out of sacrificial core of $MnCO_3$, further coated with DNA-Spermidine complexes. After the core was dissolved, the shell with DNA-Spermidine was left. A further decomposition leads to release of Spermidine, thus entrapping DNA completely [2]. Similarly, SiO_2 core structures, coated with LbL layers were used for oligopeptide antigens. In this review, an article by Fukui *et al.* has shown a novel method of combining liposomes and LbL assembly to form hollow shell structures.

Responsive materials for triggering some release in a drug delivery system play an important role. An innovative idea to apply LbL technique for the assembly of responsive polymers on a nano/micro drug carrier was utilized [3]. There can be different ways to crumble this film at a particular response such as dissolution of the cross-linker between LbL films based on pK_a of assembly or higher ionic concentration in the medium. These techniques can be used reversibly in order to make the LbL assembly more permeable for drug loading into the capsule, or irreversible for LbL film

disintegration. Here, Erel-Unal *et al.* showed that the LbL film could be destabilized with varying H-bonded bilayers having stability at different pH [59]. Poly (N-vinyl caprolactam)/poly (L-aspartic acid) combination degraded at pH ~3, while a Poly(N-vinyl caprolactam)/Tannic acid combination degraded at pH ~10. In Wohl *el al.*, work with Redox responsive films has also been described. Here, Prussian blue has been used which becomes colorless by electrochemical reduction (Fe^{3+} to Fe^{2+}). In another instance, oppositely charged forms of poly (Ferrocenyl silane) were used as LbL templates [3]. These are examples of methods for inhibiting interlayer interactions, leading to LbL film disruption. Another category of responsive LbL film is by degradation of the film components, either by mechanical or heat destruction. The swelling of encapsulated material leads to disruption of LbL film. For instance, a hydrogel is loaded with drug and then LbL is swapped. The swelling rate is controlled by the crosslinking density of the hydrogel (See Figure 2-6).

(a)   (b)
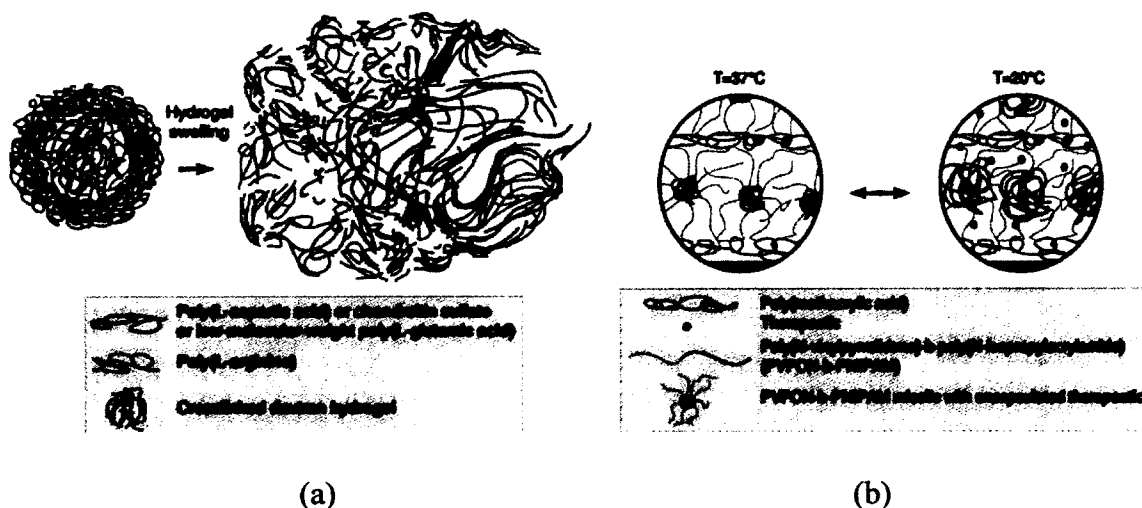
Figure 2-6: (a) Dextran hydrogel encapsulated with LbL assembly. Swelling of hydrogel leads to osmotic pressure and rupture of LbL film [3]; (b) Phase transition of PVPON-b-PNIPAM micelles due to temperature change and poly(methacrylic acid) reversibility on cooling from 37° C to 20° C [61].

Metal nano-cores absorb laser light and convert it into heat. LbL assembly on metal cores, silver, gold or TiO_2, is destroyed by layer targeting. This concept has been used in research for cell related targeting and its destruction [60]. Thermo-responsive polymers incorporated in the LbL films are another innovative way of drug encapsulation. Poly (N-isopropylacrylamide) below its lower critical solution temperature is hydrophilic in nature and is hydrophobic above it [61].

The above mentioned methods of drug delivery are based on encapsulation of drug in the core, followed by LbL assembly. A new concept of incorporating secondary drug/bioactive agent (growth promoting hormone e.g. cytokines) between the LbL assembly architecture was mentioned in multiple articles by Haidar *et al.* [62-64]. Here, bone morphogenetic protein (rhBMP-7) is entrapped between the LbL shells of alginate (AL) and chitosan (CH) assembled around a drug loaded with liposome in the core.

The formulation was nano-scalable and nontoxic with a controlled release of rhBMP-7. According to the number of bilayers, the release profile was tunable, with higher bilayers leading to a slower release. A schematic of the architecture is shown in Figure 2-7a, and a sustained release profile for 45 days is shown in Figure 2-7b.

Spray assisted LbL functionalization of printed nanoparticles is another novel technique in nanomedicine. This method of printing nanoparticles was developed to overcome the limitation of repeatability and scalability of nano-drug delivery systems. The surface molecular properties of nanoparticles are important for the desired biological effects. LbL being the most simple and effective way to coat surfaces was employed to coat such drug carriers for increased stability, targeted delivery, and tunable release properties [33].
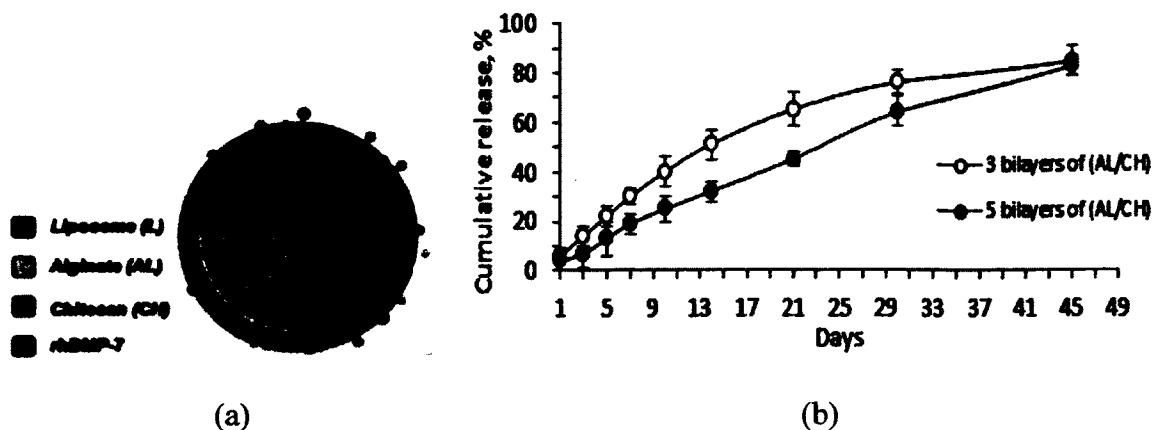
Figure 2-7: (a) Drug or bioactive agent, rhBMP-7 in the LbL shell of Alginate (AL) and Chitosan (CH) around Liposome (L) [32]; (b) An *in vitro* cumulative % release. This graph is reconstructed from the original article [32, 64].

Most drugs today are poorly water soluble, i.e. ~ 40% [34], and therefore cannot be administered orally or systemically. Especially for intravenous administration, a promising approach is to coat such drugs with LbL assembly. The PE coating acts as a barrier between the drug and the outside aqueous environment. Several methods can be used to encapsulate drugs before they are coated with LbL assembly: emulsion based core prepared by standard emulsification techniques, coating drug micro- /meso-crystals. The general process for emulsion carrier-coated LbL formulation is to form an emulsion core with a lipid soluble drug by various methods of emulsification, e.g. homogenization. The core is then coated with LbL assembly. The emulsion will have amphiphile/s along with the drug (Figure 2-8), having a net surface charge, based on which the +/ - charged polyelectrolyte is chosen for assembly [66]. Leporatti *et al.* note that the drying of such micro/nano capsules leads to their collapse [67]. LbL assembly of liposomal core (50-200 nm) with other counter polyelectrolytes around a sacrificial micro-core, e.g. of silica, was termed as capsosomes [34].
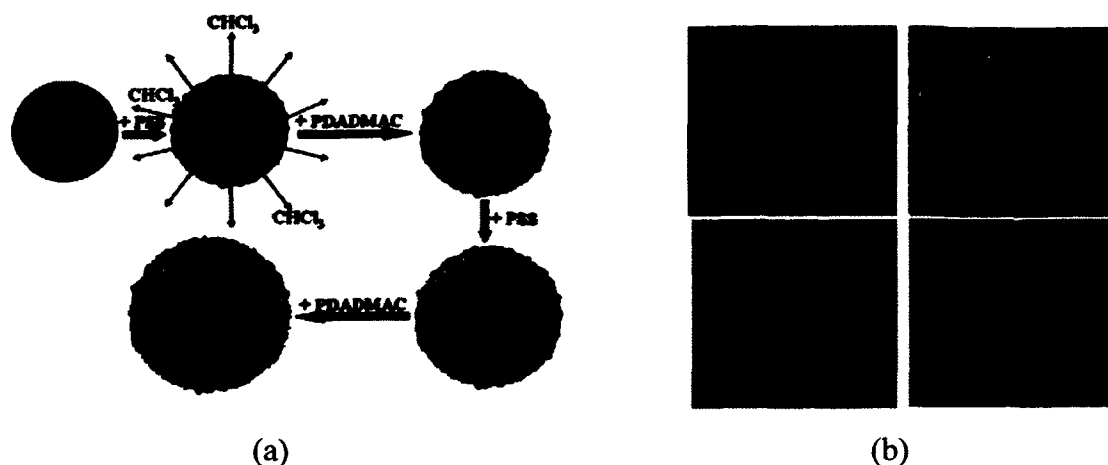
Figure 2-8: (a) Schematic of emulsion encapsulation by LbL assembly; (b) The top are the SEM images of 3 and 4 layers of PE (scale bar being 10 μm), while the bottom shows SEM images of dry encapsulations (scale bar being 20 μm and 2 μm for left and right images respectively) [66].

Formation of such emulsion systems under continuous sonication is called sonication-assisted emulsification. High-intensity ultra-sonication (20 kHz) forms microspheres that are stable for months [34]. The stability of such microspheres in blood circulation can be increased by beautifying the surface with LbL architecture. Polyelectrolyte assembly on the surface is under continuous sonication to generate a uniform assembly. The principle of cavitation is explained in the next section on industrial sonication-assisted NP core formulation. A good application of this technique was a combination of magnetic nanoparticles with protein containers as a targeted delivery [68]. LbL assembly directly on the crystals of poorly soluble drug leads to increased encapsulation capacity of the formulation. The sonication-assisted encapsulation of ibuprofen micro-crystals with chitosan as positive polyelectrolyte, dextran sulfate, carboxymethyl cellulose and sodium alginate as negative polyelectrolyte leads to electrostatically stable microcapsules [51].

The LbL approach provides greater versatility for encapsulation of low soluble

drugs and also to functionalize the surface. The technique is easy and solves many issues

of stabilization of nanocapsules. A delivery system can be easily made more

biocompatible by incorporating amino acid-based or polysaccharide-based natural PE.

The major drawback of the technique is that it is tedious [35]. In industries, process steps

are reduced by assembling multiple layers one after another without intermediate

measurements or wait time.

2.5 Industrial Sonication-Assisted NP Core Formulations- LbL Techniques

Top-down disintegration of poorly soluble drug crystals to its micro-/meso-

crystalline form is being employed to produce an effective nano-formulation with

reduced production cost. While nano-emulsions and polymeric micelles are kind of a

bottom-up approach, these formulations are further stabilized and functionalized by LbL

assembly under ultrasonication.

Nano-crystallization is an initial concept based on the Noyes-Whitney equation,

which mathematically proves that particle size reduction increases the surface area, which

in turn increases the dissolution rate [5]. The equation is

$$\frac{dC}{dt} = \frac{DS}{Vh}(C_S - C).$$

Eq. 2-3

where D is the Diffusion coefficient, h is the thickness of the diffusion layer, V is the

volume of the dissolution medium, C_s is the saturation solubility, and C is the

instantaneous concentration.

Various *Top-bottom approaches* can be used to form nano-crystals: Nano-

precipitation, high pressure homogenization, wet/dry ball milling, and ultrasonication. In

all of these cases, the application of ultra-sonication cavitation technology has been increased over the last decades. Ultra sonication cavitation of bubbles involves the expansion and collapsing of bubbles in the liquid, thus creating high pressure and temperature. These effects crush particles to smaller pieces [70, 75].

Nanoprecipitation involves restrictive growth of low soluble drug crystals. Here, the drug is dissolved in organic solvent to a supersaturated concentration, forming small crystal seeds by nucleation. The transfer of such nanocrystals with nucleation stabilizers e.g. poly vinyl pyrrolidone, Tween 80, or lecithin, into aqueous solvent, under ultrasonication, leads to nanocrystals with tunable size and stability. In Zheng *et al.* the poorly soluble anticancer drug Curcumin was dissolved in ethanol and nucleated under powerful sonication by a continuous addition of an aqueous polyelectrolyte (polycation) solution [6]. See Figure 2-9.

(a)   (b)
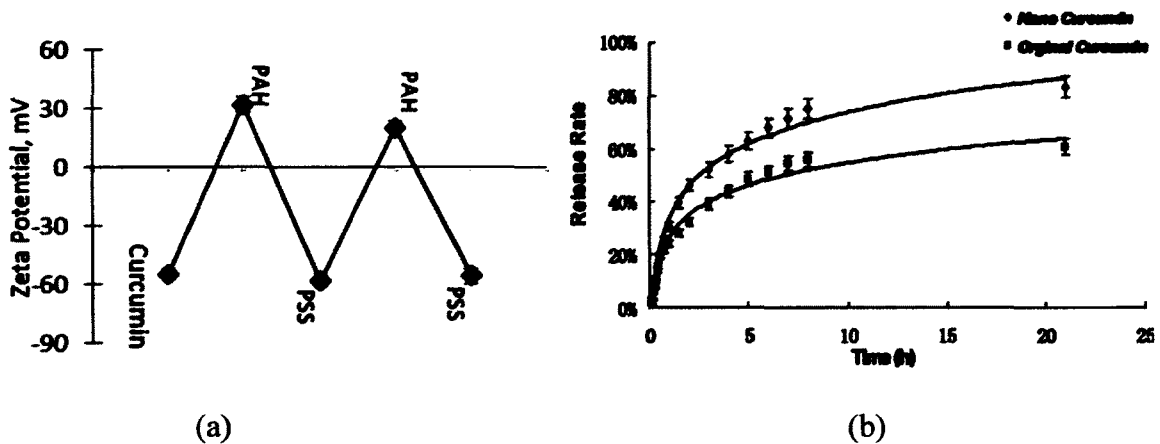
Figure 2-9: (a) Zeta Potential LbL assembly on curcumin core, at pH 6.5, with alternating PAH and PSS. This graph is reconstructed from the original article, with minor imperfections; (b) Release profile of curcumin, with UV absorbance at 480 nm [6].

The rate of addition of the aqueous medium and initial drug concentration determined the effective particle size. For 0.4 mL/min addition rate, ~320 nm particle

size and for 0.05 mL/min, ~120 nm size was obtained. See Figure 2-9b for the improved

release profile as compared to the free curcumin drug.

Another example is nano-encapsulation of PTX drug, under ultrasonication,

followed by LbL assembly of Protamine Sulfate as positive polyelectrolyte and Albumin

as negative polyelectrolyte [7, 10]. The process was done in PBS, pH 7.2. The rate of the

drug release can be tuned by changing the number of layers in the LbL assembly. To

overcome multidrug resistance for ovarian cancer targeting, combination therapeutics of

Lapatinib and PTX nanocapsules is mentioned in Vergara *et al.* [8]. See Figure 2-10.

(a)   (b)   (c)
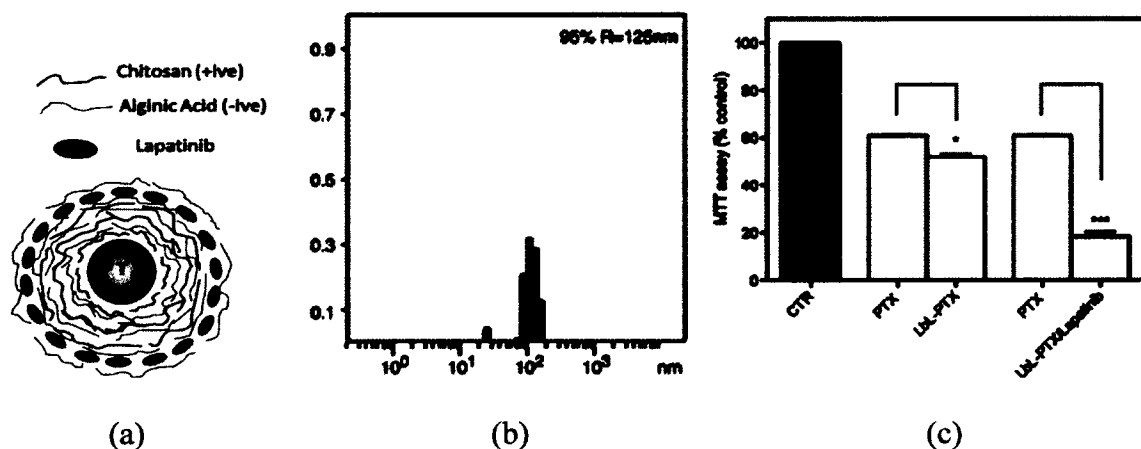
Figure 2-10: (a) Schematic of LbL architecture around PTX (PTX) nanocrytal; (b) Particle size distribution of PTX LbL formulation; (c) Lapatinib/PTX LbL nanocolloids cytotoxicity assay against P-gp overexpressed ovarian cancer cells (P < 0.05*, P < 0.01**, P < 0.0 01***); where PTX- PTX, CTR - Control [8].

High power ultrasonication was utilized to break the drug crystals into small

particles. It led to a great improvement in colloidal stability with effective particle size of

100-200 nm, a high drug loading capacity of 70% w/w, with a sustained controlled

release and an outer negative charge. It also showed an improved cytotoxicity against

overexpressed glycoprotein, P-gp (multi drug resistant protein, MDR-1) in ovarian cancer

cells OVCAR-3 [8]. Figure 2-10c shows the MTT assay results. Similarly, sonication has

been used to prepare liposomes, nano-colloids formed out of emulsions, or soft cores [9].

High pressure homogenization and media milling are the top-down disintegration

processes. High pressure homogenization is commonly used in the pharmaceutical

industry to prepare nano-crystalline drug [5]. For this method, drug and stabilizers are

mixed and passed through a narrow gap at a high pressure of 500-2000 bar. This pressure

creates an intensity of cavitation similar to that obtained in ultrasonication, with high

collision and shearing effects. The size of the nanocrystals can be manipulated based on

the number of cycles run and on the pressure and temperature of the process in the

homogenizer. An example of this method is commercially available through oral tablets,

Triglide® (Fenofibrate), an antihypercholesterolemia. The oldest method of nanocrystals

formulation is through media milling, which is done by milling pearls in the presence of

the drug, water, and stabilizers [5]. It is cost-effective, and some of the commercially

available drugs are Estrasorb ® (Estradiol), and Restasis (Cyclosporine). The limitation is

for temperature sensitive drugs, as the milling process generates heat. Also, a significant

amount of the drug is lost during the process because it adheres to the inner surface of the

milling chamber.

The top-bottom approach contrasts with the bottom-up approach, which is

becoming common in the industries. Sonication-assisted methods of nanoemulsions and

polymeric micelles are the major techniques of practice. Use of LbL assembly is also a

bottom-up approach. In general, LbL assembly is a tedious process, with a washing step

to be performed after each layer adsorption. The purpose of washing is to remove the

unbound polyelectrolytes from the dispersion mixture. A novel, less tedious method of

the washless LbL technique has now been under academic investigation. Its application

to further stabilize nanoprecipitation, nanoemulsion, and polymeric micelle-based low

soluble drug cores is discussed further in Section 2.6. Lvov *et al.* has discussed

sonication-assisted LbL assembly to convert low solubility materials to materials that are

more aqueous and stable [10]. Sonication assisted disintegration of a drug is a top-down

approach, while further architectural assembly of polyelectrolytes or other polymers is a

bottom-up approach. Sonication causes a bubble nucleation effect [73] and has been used

in combination with LbL assembly (SLbL), for stabilization of nanocolloids with poorly

soluble compounds (Table 2-1) [10]. Layer-by-Layer assembly technique is a bottom-up

nanofabrication technique. It is versatile, easy and efficient. In Ariga *et al.*, applications

of LbL as a bottom-up approach has been discussed [46]. QCM is a common technique

for the measurement of LbL assembly on any flat surface. The details of QCM will be

mentioned in the next sub-section 2.7 [69].

Table 2-1: Experimental results for ultrasonication assisted top-down LbL assembly technique for stabilization of poorly soluble organic compounds [10].

Organic compounds	Initial particle size (μm)	First layer	Second layer	Diameter after SLbL coating (nm)
PTX	15 ± 5	PAH, chitosan, PLL	PSS, alginic acid, heparin	211 ± 40
Tamoxifen	12 ± 7	PAH, PEI	PSS, PAA	220 ± 32
Curcumin	18 ± 5	PAH, PS	PSS, BSA	107 ± 17
Resveratrol	180 ± 40	Chitosan	alginic acid	200 ± 30
pigment Orange 13	19 ± 6	PAH, PS	PSS, BSA	264 ± 23
2,4-dinitrophenylhydrazine	82 ± 20	PAH, PEI	PSS	216 ± 29
2-mercaptobenzothiazole	27 ± 8	PAH, PS	PSS, BSA	290 ± 33

2.6   Non-Washing LbL Technique

The washing step after each polyelectrolyte layer deposition is done to remove the excess amounts before the addition of counter polyelectrolyte [19]. A modified version, washless LbL assembly, was developed to prevent loss of expensive polyelectrolytes. For this technique, a titrated amount of polyelectrolyte is added with simultaneous surface charge measurement by zeta potential machine. Until a certain desirable zeta potential value is reached, the polyelectrolyte is added, then similarly titration of the counter polyelectrolyte is measured. This way, the exact amount of PE layer for particular zeta potential range is estimated. In Bantchev *et al.* (2009), this assumption was applied for coating titanium dioxide (TiO_2) microcores and microfibers.

When the needed PE amount is known, the amount of the produced colloidal particle can be readily scaled up. It was explored from the study that various effects on the trend of assembly: 1) Based on the amount of particles to be coated, the amount of polyelectrolytes increases per layer for an increase in initial particle concentration; 2) Based on the length or molecular weight of the polyelectrolyte molecule, a smaller length led to less aggregation of particles; 3) The concept behind non-washing LbL assembly will be described [19] with an emphasis on the LbL procedure for extra-small and soft cores (See Figure 2-11).

(a)   (b)
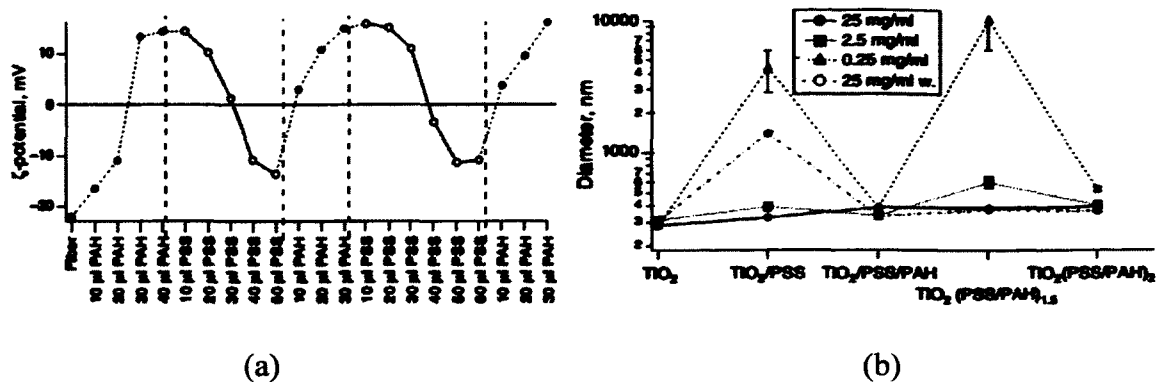
Figure 2-11: (a) Zeta potential values along the titration with PE/layer on 2.5 mg/mL of microfiber; (b) Variation in effective particle diameter along the LbL assembly for different concentrations of TiO2 particle [19].

The role of PEGylated polyelectrolytes in preserving stability of the nanoparticles in non-washing LbL assembly in the presence of salts will be discussed. The application of non-washing LbL assembly to different drug cores, discussed in this dissertation are for: 1) semi-stable crystalline drug core (PTX) [5, 11, 36, 37], 2) soft protein/CPT cores [11, 12], 3) Solid Lipid Nanocarriers (SLN) LbL formulation [13, 24, 83], and 4) Emulsion core or miceller core [15].

Semi-stable crystalline drug cores have been one of the initial methods in encapsulating drugs by LbL assembly. It involves core formation by nanoprecipitation of semi/crystalline drug nanoparticles using nucleation. Here, the drug is first dissolved in an organic solvent, in which it is most soluble. Then, adding it in a supersaturated concentration to an aqueous medium leads to drug seed formation by nucleation. Addition of the stabilizer inhibits checks on excessive crystal growth or agglomeration. A further stabilization with LbL assembly with charged polymers is becoming a common trend. The choice of solvent and ratio of drug to stabilizer controls the size of the core and also its stability.

In Shutava *et al.* (2013), an excellent demonstration of this technique has been

mentioned for formulating a stable drug encapsulation of poorly soluble anticancer drugs

PTX and CPT, separately. A PTX core was formed by a nucleation method, and the

crystal growth was restricted by 2.9 mg/mL of polyvinylpyrrolidone, 1.2 mg/mL of

dioctyl sodium sulfosuccinate (AOT) and 0.36 mg/mL of polysorbate 80 under

continuous sonication. The process was conducted at 10° C. Further bilayers of

alternating heparin sulfate sodium (HEP), as anionic polyelectrolyte, and poly-L-

lysine16kDa-b-copolyer-methoxy-PEG5kDa (PLB16-5), as cationic polyelectrolyte, were

assembled on it (Figure 2-12) [11]. While CPT, another low soluble anticancer drug, was

formed similarly, the core was formed as a soft core with albumin protein. The details of

it will be mentioned further in the discussion.

(a)   (b)
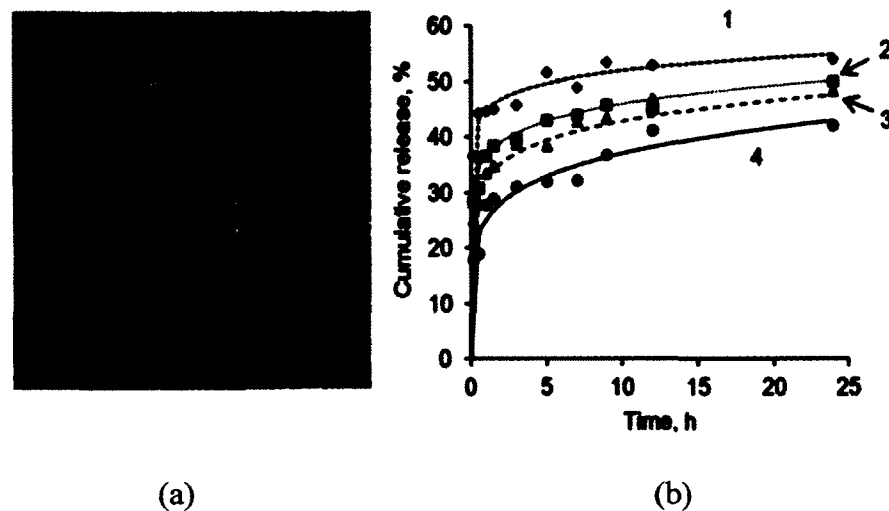
Figure 2-12: (a) TEM image of nano-PTX coating with PLB16-5/HEP)3/PLG65 5 shell. Visualization was improved by negative staining with ammonium molybdate [(NH4)2Mo2O7], (b) Release profile in water with 2% w/v Polysorbate 80 at 37° C: of 300 nm PTX nanocolloids prepared by top-down sonication assisted LbL method and coated with (PLL/Hep)n shell, where n is number of bilayers; n: 1- 0.5, 2-4, 3-8, 4-12. [11].

The role of PEGylated surfaces have been studied to provide better colloidal stability. A careful examination of the stoichiometry-related colloidal stability was given by Schneider and Decher [118]. In the conventional LbL assembly with non-PEGylated polyelectrolytes highly concentrated solutions of each polyelectrolyte are needed to recharge added particles instantly and, therefore, minimize the time of the existence of low or zero charged species [118, 119].

2.7   Core-LbL Shell Drug Nanocapsules

Nanocarriers that release the encased drugs in a prolonged or stimuli-responsive manner and target specific cells or tissue in human body are under intensive investigation. In the field of drug delivery applications, LbL-coated nanocapsules combine drug-loaded core matrix and a shell of variable architecture that can consist of polyelectrolytes, proteins, nanoparticles, and selected molecules of low molecular weight; each part of the composite bears a set of specific functions [41, 119].

200-250 nm nanocrystals of poorly soluble drugs (PTX, Tamoxifen, Curcumin, Resveratrol) prepared by top-down disintegration or nanoprecipitation technique were coated with two-layer shells of PAH 70 kDa or polyethyleneimine (PEI) of 60 kDa followed by PSS 70 kDa. For *in vitro* release studies, bio/polyelectrolytes (alginic acid, chitosan, heparin (Hep), PLL) and proteins (protamine sulfate, BSA) were used for the LbL process [6, 7, 120-122].

Emulsions stabilized by interfacial membranes consisted of sodium dodecyl sulfate/chitosan/pectin, β-lactoglobulin/carrageenan/pectin, lecithin/chitosan/pectin with an average size in the range of 300-500 nm obtained via electrostatic deposition of one

polymer after the other without the intermediate washing step show better stability to environmental stress under certain circumstances [123, 124].

The protein and cell adhesion resistance properties of LbL films and nanocapsules have been of great interest to improve the current drug delivery systems. PEG assembled in high density brush-like structures shields the underlying surface from the penetration and subsequent adsorption of proteins [125, 126].

As confirmed by QCM-R, electrophoretic measurements, and analytical technique, upon adsorption of block-copolymers of PLL and PEG, the surface remains accessible for further electrostatic binding of Hep [11, 12, 78]. The thicknesses of a PLB/Hep bilayer on flat gold surfaces are comparable for unmodified PLL and PLB copolymers. The thickness of 4.5 and 7.5 (PLB16-5/Hep) bilayer films is ca. 5.2 and 7.5 nm. The surface of PLB/Hep with a PLB outermost layer can be further modified through covalent attachment of PEG of 5-20 kDa to the film's outermost amine groups [12]. The mass of mPEG20kDa attached to the film exceeds that of mPEG5kDa by a factor of ~1.2 to 1.7. Although many amine groups remain unreacted on the surface, the further PEG attachment is hindered by neighboring PEG tails. Thus, QCM-R is a reliable and accurate method to analyze the protein resistance of PEG tails or different LbL polyelectrolyte architectural approach.

2.8   Conclusion

Many anticancer drugs are effective in a cancer microenvironment, but are not effective when applied systemically because they are poorly soluble in blood. LbL self-assembly technique has a lot of applications in the field of film coating on a flat surface. The recent applications and better understanding of how it can be employed for the

encapsulation process at the micro and nanoscale have been studied for some time recently. The introduction of sonication assisted improved washless LbL assembly technique for nano-encapsulation of drugs have been recently been applied for encapsulating nanoparticles and anticancer drugs. Few clinical experiments have been done to bring the concept into play for pharmacological experiments. Formulating LbL nanocapsules less than 200 nm size is crucial for effective IV delivery with improved bioavailability.

In Chapters 4, 5 and 6, washless LbL assembly with surface modification with poly ethylene glycol (PEG) tails has been used to encapsulate different forms of nanocores, soft mesocrystallline drug core, nanomiceller core, and nano structured lipid cores. The hypothesis is that when the particle circulates in the blood, the LbL assembly will act as a barrier between the drug core and the external environment. The PEG tails will inhibit blood protein from binding to them. These effects will significantly improve the colloidal stability, preserve the anticancer activity of the drug, improve the circulation time, and increase the amount of drug delivered to the cancer site.

CHAPTER 3

INTRUMENTATION

3.1   Ultrasonication

Ultrasound technology has been an effective way to process or clean materials in medicine and also in industries. A Branson 1510 ultrasonicator (Branson Ultrasonics, US) was used to prepare the different nanocores followed by the LbL assembly and extra PEGylation.

3.2   Zeta-Potential Analyzer

A ζ-Plus Microelectrophoretic instrument (Brookhaven Instruments, Co.) was used to measure the hydrodynamic diameter and the surface charge of nanoparticles during each layer deposition of the LbL assembly. The instrument was calibrated using a standard sample from the manufacturer. For each measurement of the sample, 20 μL of the sample was diluted up to 2 mL by using the required solvent. The ζ-potential was measured in the range of 200 mV to -200 mV. The ζ-potential can be used for certain theoretical models, which can be further used for finding out the ionic concentration (C) per unit area of the particles (m^2).

3.3   Electron Microscope

Two types of electron microscopes were used for the morphological analysis of nanoparticles: Scanning Electron Microscope (SEM) for surface morphology analysis

and Transmission Electron Microscope (TEM) from Zeiss, Co., for confirming the LbL

assembly on the nanocore. The SEM images showed the structural features of the

particles. For each preparation, the drug particles were centrifuged and resuspended in the

required solvent. A 2 mg/mL concentration of the sample was diluted 100 times in the

same solvent. Then a small drop of it was put on a clean silicon slide. It was room-dried

and then observed under SEM at 1.5 kV. While for TEM imaging the same diluted

sample was dropped on a copper grid, then a negative stain was dropped, followed by

removing the excess stain by a blotting paper. The sample was room-dried and seen

under the TEM.

3.4   Quartz Crystal Microbalance

QCM-R with motional resistance monitoring (QCM200, Stanford Research

System) is an effective method to measure the thickness and mass of each polyelectrolyte

deposition per cm^2 on the flat 5 MHz quartz crystal resonator. The quartz crystal,

subjected to an electric impulse, resonates at a well-defined frequency. As a film is

deposited on the crystal, the increase in mass decreases this frequency and increases the

viscosity resistance. To perform this measurement, the crystal must be washed after each

polyelectrolyte or film of different solution is deposited. The deposited mass is deduced

from the Sauerbrey equation:

$$\Delta f = -C_f \Delta m,$$ **Eq. 3-1**

where, Δf is the observed frequency change in Hz, Δm is the change in mass per unit area

in g/cm^2, and C_f is the sensitivity factor of the crystal (56.6 Hz μg-1cm2 for a 5 MHz AT-

cut quartz crystal at room temperature).

3.5   High Performance Liquid Chromatography (HPLC)

An Agilent 1100 (Agilent Technologies) reverse-phase high performance liquid chromatography (RP-HPLC) was used. RP-HPLC is a process of chromatographic separation technique in which the stationary phase is a hydrophobic non-polar solid phase in the column (C-18), and a polar mobile phase. The maximum rate of flow used for analysis was 0.2 mL/min.

CHAPTER 4

LAYER-BY-LAYER NANOENCAPSULATION OF CAMPTOTHECIN WITH IMPROVED ACTIVITY

This chapter describes the application of washless LbL assembly for

encapsulation of the anticancer drug CPT as a soft core conjugated with BSA. The unique

pH reversal step from 3 to 7.2 is performed to specifically preserve the active Lactone

form of CPT. The morphological characterization was assessed through a particle size

analyzer, SEM, and TEM; the drug chemical analysis was performed by UV-Vis

spectroscopy; the LbL assembly architecture was verified by zeta potential and QCM

studies. The *in vitro* release studies in PBS and FBS and the cell toxicity studies against

brain glioblastoma cells are escribed. The sections in this chapter was published as: G.

Parekh, P. Pattekari, C. Joshi, T. Shutava, M. DeCoster, T. Levchenko, V. Torchilin, Y.

Lvov, "Layer-by-Layer nanoencapsulation of CPT with improved activity," *International

Journal of Pharmaceutics*, vo. 465, no. 1-2, pp. 218–227, April 2014. Sections 4.3.9, 4 is

not included in the publication mentioned above. Results from this paper are included

only in the dissertation.

4.1   Introduction

Among delivery methods for poorly soluble substances with antitumor activity,

encasing drugs into micro and nanoparticles seems to be a promising strategy to design

implantable devices or injected directly at the tumor site; low drug loading that can be

achieved in such devices is compensated by prolonged release properties [80-82]. Several

formulations based on nanoparticle technology [58, 48, 4, 83, 49] have been developed

for oral or intramuscular injections, but only a few of them are intended for intravenous

injection as albumin-based nanoparticles containing PTX (Abraxane®) [84, 85, 86].

Another strategy, namely, injectable nanocapsules based on crystalline core of poorly

soluble anticancer drugs stabilized with a thin shell of bio polyelectrolytes assembled via

Layer-by-Layer (LbL) assembly technique, was recently reported [11].

LbL assembly provides an opportunity to form a nano-thick coating in a

controllable manner on the surfaces of variable curvature and size from interacting

oppositely charged polyelectrolyte components [11, 87, 57, 35, 28, 31, 29, 88]. Anchored

to the core surface, the thin shell of hydrophilic polyelectrolytes allows exchange of

excipients used on the core preparation. It concentrates nanocolloids without aggregation

or recrystallization and supports their high stability in physiologically relevant buffers.

Major advantages of LbL based formulation are a high, up to 70%, drug loading capacity,

and an ease of further modifying the outer shell to enhance the stealth properties of the

nanoparticles [11].

To intensify the preparation of LbL capsules on small, less than 200 nm cores, the

washless LbL technique has been developed [11, 19, 20]. Polyanions and polycations are

sequentially added to drug nanocores in the minimal amounts that completely adsorb on

the surface of the particles recharging them. No intermediate washing of non-reacted

polyelectrolytes is needed in such an approach. This removal of washing steps minimizes

the loss of all substances, like those in conventional centrifugation or filtration-based LbL

technique using step-wise sample washing. High hydrophilicity of used polymers, block-

copolymers of polyaminoacids with polyethylene glycol and polysaccharides, and also

low molecular weight i.e. < 60 kDa of the shell wall components prevented colloidal

aggregation during the LbL formation [11, 28, 31, 29, 88].

CPT combines low solubility in aqueous-based media with low stability of its

active form, lactone, which easily hydrolyses into carboxylate at neutral and slightly

alkaline pH [89-93]. Among other nanoparticulated formulations of CPT, such as

polymer-based delivery systems, lipid, liposome and solid lipid nanoparticles,

polyelectrolyte modified LbL-based nanocapsules of CPT seems to be a promising route

to obtain a concentrated dispersion, 0.5 - 1.0 mg/mL, stable in physiologically relevant

buffers and that can be injected intravenously with minimal side effects. We expect that

the LbL-coated CPT nanocapsules (Figure 4-1) will improve the chemical stability of

CPT and preserve the active lactone form of the drug by reducing its hydrolysis to an

inactive carboxylic form at neutral and alkaline conditions, especially in the presence of

albumin. It makes such nano-formulation more active and less toxic for a living body due

to lower injectable concentration.
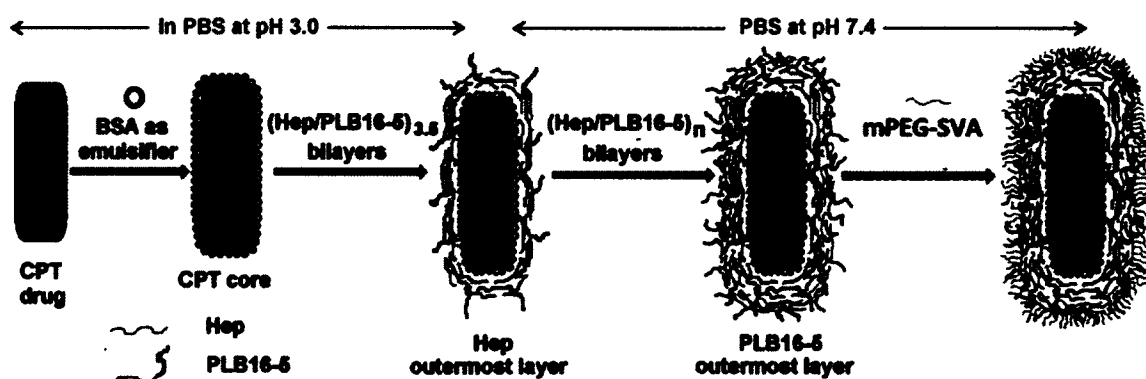
Figure 4-1: Scheme of CPT nanocapsules preparation [12].

4.2　Materials and Methods

4.2.1　Materials

CPT was obtained from LC Laboratories, USA. Heparin sodium salt (HEP), BSA, polystyrene sulfonate (PSS), polyethyleneimine (PEI), polyvinylpyrrolidone (PVP), Polysorbate 80, phosphate buffered saline (PBS), dimethyl sulfoxide (DMSO), and acetonitrile were obtained from Sigma-Aldrich and used as received. Fetal bovine serum (FBS) was obtained from Atlanta Biologicals, USA. Block-copolymers of poly-L-lysine with polyethylene glycol (PLB) of different molecular weights (PLL[16kDa]-b-PEG[5kDa] (PLB16-5) and PLL [16kDa]-b-PEG[20kDa] (PLB16-20)) were obtained from Alamanda Polymers, USA; mPEG5kDa-Succinimidyl Valerate (SVA) and mPEG20kDa-SVA were obtained from Laysan Bio, Inc., USA. For cell culture studies, rat brain glio-blastoma cells *CRL 2303* were obtained from American Type Culture Collection (Manassas, VA), DMEM from ATCC-30-2002, Thiazolyl Blue tetrazolium bromide, 98% (MTT) from Alfa Aesar, USA.

4.2.2　Drug nanocapsule preparation

4.2.2.1　Core preparation

Under continuous sonication, 200 µL of freshly prepared CPT solution in DMSO (7 mg/mL) was added to 2.58 mL of PBS buffer (pH 3) containing 0.64 mg/mL BSA and 1.44 mg/mL PVP and further sonicated for 15-20 min.

To optimize nanoparticle preparation conditions, in one series of experiments, the concentration of BSA in the mixture was varied from 0.35 to 2.50 mg/mL at C(PVP) = 1.44 mg/mL, while in another, the concentration of PVP was varied from 0 to 2.2 mg/mL and the C(BSA) was fixed at 0.64 mg/mL. Upon sonication, ζ potential (in DI water) and

hydrodynamic diameter (in PBS buffer, pH 3) of the nanocores were measured using a

ZetaPlus Brookhaven instrument.

4.2.2.2   Polyelectrolyte shell formation on nanocores

By alternating the addition of 20 μL aliquots of HEP or PLB16-5 (both 60 mg/mL

in acidic PBS, pH 3), 3.5 pairs of the polyelectrolyte layers were deposited on the cores,

with heparin being the outermost layer. Each polyelectrolyte solution was added to the

nanoparticles' dispersion under constant sonication that continues for another 30 seconds.

The obtained dispersion was kept for 5 min before the addition of the next

polyelectrolyte. No intermediate separation of nanoparticles from supernatant or rinsing

the nanoparticles with buffer was made. The assembly of polyelectrolytes was followed

by the measurements of ζ potential (in DI water) and hydrodynamic diameter of the

nanoparticles. The nanocapsules with HEP as the top layer (−20 mV) were separated by

centrifugation at 10,000 rpm for 10 min (Eppendorf 5804R centrifuge) and redispersed in

the same volume of PBS buffer, pH 7.4. More pairs of layers were assembled at pH 7.4

using 60 mg/mL solutions of polyelectrolytes by sequentially adding 20 μL aliquots of

Hep and a copolymer of PEG and PLL (PLB16-5 or PEG16-20).

4.2.2.3   PEGylation of polyelectrolyte shell

The powder of mPEG5kDa-SVA or mPEG20kDa-SVA was directly added to the

dispersion of nanoparticles with a positively charged outermost layer (PLB16-5) in PBS

buffer at pH 7.4 to achieve the PEGylator concentration of 40 mg/mL and the mixture

was vigorously shaken and sonicated for 30 s to dissolve the PEGylator. The dispersion

was kept for 10 h at 4° C. The nanoparticles were separated by centrifugation at 14,000

rpm (Eppendorf 5804R centrifuge) for 10 min and the pellet was resuspended in PBS, pH 7.4.

4.2.3   Influence of PVP on the amounts of polyelectrolytes needed for charge reversal

In this series of experiments, the dispersions of CPT cores were obtained as described above but the concentration of PVP varied from 0 to 2.2 mg/mL in different batches. Each polyelectrolyte was stepwise added to the dispersions containing a given amount of surfactants in small aliquots, 20 μL of a 6 mg/mL solution in PBS, pH 3.0. This was continued until the ζ potential of the nanoparticles reached a value of ±25 mV. The amount of polyelectrolyte needed to complete one layer was calculated as a sum of that added in all aliquots. Then, the polyelectrolyte with an opposite charge was added in a similar way. Two pairs of layers were assembled for each dispersion.

4.2.4   Analytical techniques

4.2.4.1   Amount of BSA adsorbed on nanocores

FITC-labeled BSA was used to evaluate the amount of BSA adsorbed on CPT nanocores at different stages of shell preparation. The concentrations of BSA-FITC from 0.24 to 2.50 mg/mL were used for core preparation; a HEP/PLB16-5 bilayer was coated by adding 20 μL of 60 mg/mL solutions of each polyelectrolyte to the obtained dispersion at pH 3 as described above. In another series of experiments, 3.5 HEP/PLB16-5 bilayers were assembled on nanocores at pH 3. The nanocapsules were separated from supernatant by centrifugation, washed once with PBS buffer pH 7.4, redispersed in the buffer, and then coated with one more PLB16-5/HEP bilayer. The nanoparticles were separated from the supernatant, and the concentration of BSA-FITC in the supernatant

was estimated using FITC absorbance at 490 nm (Agilent 5893 UV-vis

spectrophotometer).

4.2.4.2   Drug concentration in nanoparticles

The content of CPT in the obtained dispersions of nanocapsules was measured

after extraction of the drug with a 1:1 :: DMSO: acetonitrile mixture [90]. The insoluble

remains of polyelectrolyte shell were removed from the medium by centrifugation. The

concentration of CPT in the solution was measured using the drug absorbance band at

381 nm (extinction coefficient, $\varepsilon = 1.92 \times 10^4$ $M^{-1}cm^{-1}$) [89-93]. The BSA concentration

was measured in PBS, pH 7.4, at 280 nm, $\varepsilon = 171.6$ $M^{-1}cm^{-1}$.

4.2.5   Characterization of CPT chemical stability

The chemical stability of CPT in the core of (HEP/P16-5)5.0 nanocapsules was

studied both in PBS buffer and the buffer with BSA (25 mg/mL) at pH 3, 5, 7.4, and 9

and at room temperature (22° C). CPT dissolved in DMSO was used for comparison. The

CPT nanocapsules were dispersed in a medium at the concentration of 0.04 mg/mL. At

different time intervals, 20 µL aliquots of the mixture mentioned above were added to

1.98 mL of a 1:1 DMSO: acetonitrile solvent [90] and absorbance of the extract at 354

nm was measured.

The lactone fraction at time t (LF) was calculated as the percentage of the total

drug content:

$$LF = \frac{A_{lactone} - A_t}{A_{lactone} - A_{carboxylate}} \times 100\%$$ Eq. 4-1

where $A_{lactone}$ and $A_{carboxylate}$ are absorbances of the solutions containing CPT only in the

lactone and carboxylate form, A_t is current absorbance of the extract. The percentage of

lactone CPT that remains in the cores obtained at different pH was estimated using the

ratio of absorbances at 366 nm and 381 nm at a given pH and at pH 3.

$$LF = \frac{A_{366} - A_{381}^{pH_x}}{A_{381} - A_{366}^{pH_3}} \times 100\%. \qquad \text{Eq. 4-2}$$

4.2.6   Characterization of colloidal stability of CPT nanoparticles

A dispersion of CPT nanocapsules with a shell of a given architecture was

concentrated to 0.5 mg/mL in PBS buffer and the hydrodynamic diameter of the

nanoparticles was measured over 7 days. During the test, all samples were kept at 22° C.

4.2.7   Quartz crystal microbalance: Analysis of PLB16-5/HEP film thickness,
PEGylation and binding of serum protein

The films of PLB16-5 and HEP were formed on flat gold working surfaces of 5

MHz quartz crystal resonators from 0.5 mg/mL polyelectrolyte solutions in water in a

liquid flow cell and the film assembly was followed by QCM-R technique with motional

resistance monitoring (QCM200, Stanford Research System) [94-96]. After adsorption of

each polyelectrolyte, the cell was rinsed with DI water. After assembly of a desired

number of PLB16-5/HEP layers on a resonator, a 50 mg/mL solution of mPEG5kDa-

SVA or mPEG20kDa-SVA in water was injected into the cell for 24 h. The unreacted

PEGylator was removed from the cell by rinsing it with water. The attachment of proteins

from FBS was monitored for 20 min, and finally the cell was washed with an excessive

amount of water. The shifts of resonance frequency ΔF and motional resistance ΔR were

calculated for a resonator with a film immersed in water relatively to the empty resonator.

The mass of the deposit was calculated using the Sauerbray equation for rigid films [94-

96].

4.2.8 Characterization of release study

The release of CPT from the LbL-coated capsules with and without additional PEG layer was studied in PBS buffer, pH 7.4 or 5.0, supplemented with 2% w/v Polysorbate 80, or in FBS. The solubility of CPT in PBS-2% w/v Polysorbate 80 is ca. 1.6 µg/mL at pH 7.4 and 0.9 µg/mL at pH 5. The solubility of CPT in FBS is ca. 6.7 µg/mL. The dispersion of the nanoparticles under study was added to the release medium which was continuously stirred at 1050 rpm (Eppendorf 5804R centrifuge) at 37.4 0C. With 0.5-12 h intervals, 1 mL/2 mL aliquots were withdrawn from the mixtures of 10 mL/30 mL, as total volumes for release in PBS/FBS respectively. They were then replaced with the same volumes of fresh medium. The release was followed for 24 h. The nanocapsules with undissolved CPT were separated from the aliquots by centrifugation. The concentration of CPT dissolved in supernatant was estimated by UV-vis spectroscopy using the absorbance peaks of CPT at 370 nm (in PBS with 2% w/v Tween 80, $\epsilon = 4.0 \times 10^4$ M^{-1} cm^{-1}). All experiments were run in triplicates and the data were averaged. In the control experiment, CPT dissolved in DMSO was used.

4.2.9 TEM sample preparation

10 µL of concentrated dispersion of CPT nanoparticles in DI water was dropped on a copper grid. After 30 s it was stained with 10 µL of 1% ammonium molybdate. The excess amount of the stain was absorbed by a tip of filter paper. The sample was allowed to air dry for half an hour. The TEM images were taken on a Zeiss EM912.

4.2.10 *In vitro* cell culture study

Cell culture: Rat brain glio-blastoma cells CRL2303 (American Type Culture Collection) were cultured in 24 well plates with DMEM medium supplemented with 10%

FBS (ATCC) and penicillin/streptomycin. It was maintained at 37° C in a 5% CO2

incubator. The incubation was done overnight to get a cell density of 40,000 cells/mL for

MTT assay and 15,000 cells/mL for morphological studies [97, 98].

Treatment of cells: After required incubation, the cells were treated with varying

concentrations (0.01-10 μM) of CPT as nanoparticles coated with (HEP/PLB16-5)7

bilayers and (HEP/PLB16-5)7 bilayers -mPEG shells, or free drug. To obtain a stock

solution of free drug, its powder was sonicated for 15 min in PBS, pH 7.4, and then

centrifuged out to obtain a particle-free supernatant. It had the CPT concentration of 26.9

μM and a LF value of 96.4%. For positive control, the treatment of cells was done with

50 μg/mL copper (II) oxide nanoparticles (CuO NPs) that have high cell toxicity [97]

[98]. The morphological features were seen under an Olympus Ix51 inverted microscope.

MTT cell viability assay [99] was performed at two time points, 16 and 40 h. Four

hundred μL of 1.25 mg/mL, 3-(4,5-dimethylthiazol-2-yl)-2,5-diphenyltetrazolium

bromide (MTT) solution was made in Locke's solution at pH 7.2. It was initially pre-

warmed for 10 min in the incubator chamber. The culture medium from each well was

replaced with the same volume of MTT solution. The wells were covered with aluminum

foil and then incubated for 1 h. Then the medium was removed carefully, without

expiration of the MTT formazan precipitates. The formazan precipitates were solubilized

in 200 μL of 91% iso-propyl alcohol. Their absorbance was measured at 570 nm in a UV

plate reader Multiskan GO, Thermo Scientific. The cell viability (CV) was calculated

with respect to the average cell viability of the negative control:

$$CV = \frac{1}{n}\sum\frac{A_i \text{ at each well}}{A_{av} \text{ at negative control}} \times 100\%. \qquad \text{Eq. 4-3}$$

4.3 Results and Discussion

4.3.1 Optimization of soft nanocore preparation conditions

4.3.1.1 Influence of pH

The hydrodynamic diameter of prepared CPT cores changes drastically with the pH used (Figure 4-2a). It reaches a few tens of micrometers in the pH range from 4 to 6. In this range, the particles have a negative ζ potential, which is not sufficient for colloidal stability of the dispersions, whereas the core size at pH 7.4 is close to 400 nm as their surface charge goes beyond -20 mV. The cores exhibit the particle size of 140 ± 20 nm at pH 3. Despite the CPT nanoparticles are only slightly positively charged at this low pH, stable nanocolloids are formed.

The CPT cores were prepared under different pH conditions to evaluate the fraction of the active lactone form of the drug that retains after 20 min of intense sonication in the presence of BSA and PVP. The concentration of the lactone form in the obtained dispersion of nanoparticles reduces gradually as the pH increases from 3 to 9 (Figure 4-2b). The active lactone form of CPT and its derivatives is easily hydrolyzed into less active and toxic carboxylic form [89-93] and its preservation during preparation and storage is of high priority. Therefore, the preparation of CPT cores at pH 3 is the most reliable method to obtain smaller than 200 nm CPT particles preserving the highest content of its active lactone form.
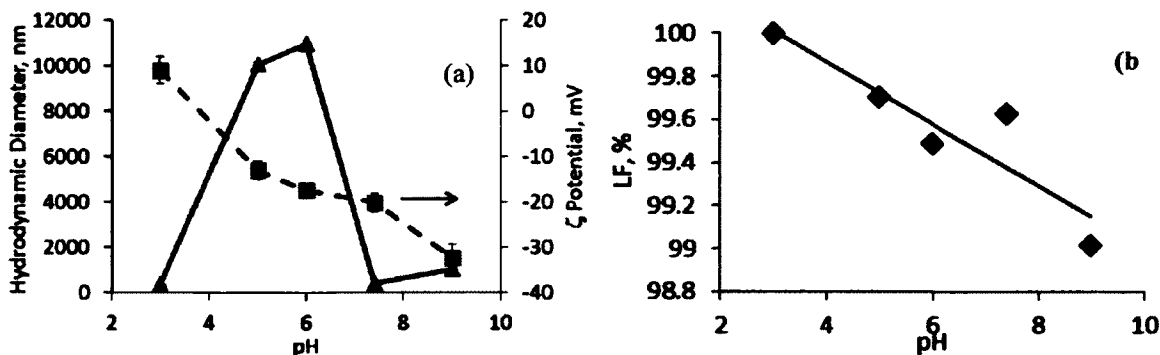
Figure 4-2: a) Influence of pH on hydrodynamic diameter and ζ potential of CPT cores. b) The content of the lactone form in the CPT cores prepared at different pH.

4.3.1.2   Amount of BSA bound to CPT nanocores

The amount of BSA-FITC bound to CPT cores coated with a Hep/PLB16-5 bilayer at pH 3.0 is 1.05 ± 0.03 mg/mg and remains the same for all concentrations of BSA above 0.64 mg/mL (Table 4-1). At this concentration, more than 90% of the added BSA-FITC binds to the core surface. If a smaller concentration of BSA is used, the protein is completely bound to the core, but the apparent diameter of nanoparticles increases sufficiently.

After changing pH from 3 to 7.4, a partial desorption of BSA-FITC from CPT nanocore's surface takes place (Table 4-1). At pH 7.4, the charge of BSA (pI = 5 [100]) is reversed to a negative value affecting adsorption of the protein. However, due to mainly hydrophobic interaction between CPT and BSA [101-103] and a variety of possible polyelectrolyte binding sites on the protein [80], a sufficient amount of the protein remains bound to the surface and to the LbL shell. The concentrations of BSA-FITC higher than 0.64 mg/mL lead to micrometer-sized particles during further LbL assembly at pH 7.4, while the nanocapsules prepared at a 0.64 mg/mL BSA concentration give

stable colloids up to 24 h with a nanoparticle diameter of 178 nm. Therefore, these conditions are considered to be the optimum parameters for the core preparation protocol.

Table 4-1: Amount of BSA-FITC bound to CPT cores at different concentration of protein.

C (BSA), mg/mL	C (BSA)/C (CPT), mg/mg	% BSA bound to the core	Hydrodymanic diameter, nm
coated with (Hep/PLB16-5) shell, pH 3.0			
0.35	0.62	97±3	254±15
0.64	1.16	91±3	167±12
1.28	1.01	43±2	180±15
1.90	1.13	30±2	303±14
2.50	4.96	100±3	1152±56
coated with a (Hep/PLB16-5)$_{4.5}$ shell, pH 7.4			
0.24	0.24	64±2	245±2
0.36	0.36	69±3	220±4
0.64	0.69	54±2	178±2

4.3.1.3   Influence of Poly vinyl pyrrolidone (PVP)

PVP was used as an excipient for the formulation to improve colloidal stability of the dispersion of CPT nanoparticles. As the concentration of PVP in the core preparation medium increases, the hydrodynamic diameter of CPT cores goes through a maximum at 0.7 mg/mL PVP concentration and then decreases significantly (Figure 4-3). It reaches 200±20 nm over the 1.4-2.2 mg/mL range, which was further used to get optimal size on CPT nanoparticles while utilizing the least amount of all excipients as possible.
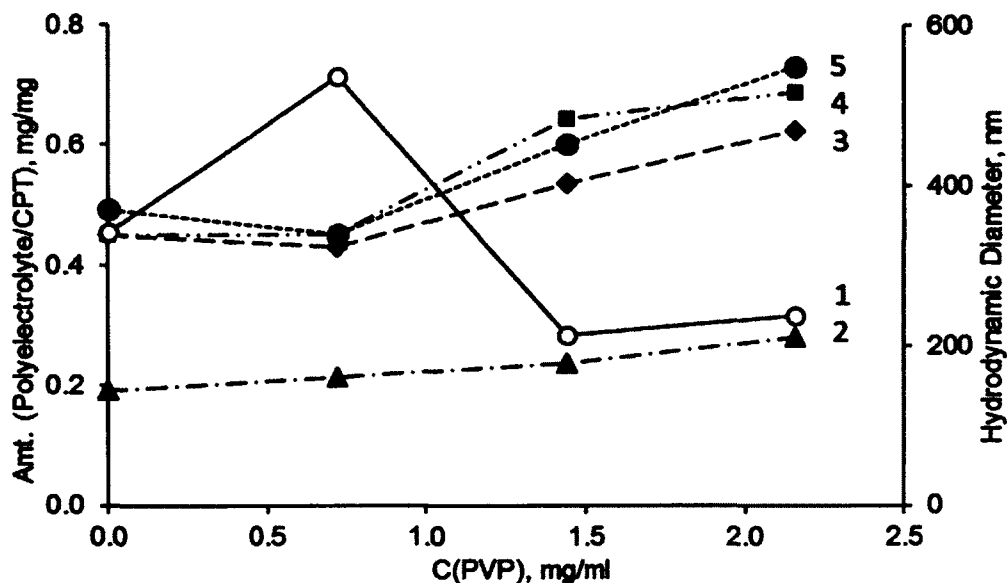
Figure 4-3: Influence of PVP concentration on hydrodynamic diameter of CPT core (1) and amounts of polyelectrolyte needed for recharging their surface upon adsorption: 2 – first step: HEP on BSA-stabilized CPT cores; 3 – second step: PLB16-5 on CPT/HEP nanoparticles; 4 – third step: HEP on CPT/HEP/PLB16-5 nanocapsules, and 5 – fourth step: P16-5 on CPT/(HEP/PLB16-5)1.5 nanocapsules. pH 3.0.

The feature of the current approach is the formation of polyelectrolyte shell on the BSA-stabilized particles directly in the medium used for preparation of CPT cores that is in the presence of polyvinylpyrrolydone. In this series of experiments, CPT cores were produced at different PVP concentration varying from 0 to 2.2 mg/mL. Besides the already mentioned effect of the excipient on the core size, we observed some dependence of the amounts of polyelectrolytes needed for ζ -potential reversal on the concentration of PVP (Figure 4-3). The light increase of the polyelectrolyte amounts needed for each layer in more concentrated PVP solutions correlates well with smaller apparent size and higher specific surface of the cores. The difference between the amounts of Hep needed to complete a charge reversal in the first and the third layer (curves 2 and 4) displays the difference in the adsorption conditions on BSA and PLB16-5 layers.

In all further experiments, each polyelectrolyte was added in one aliquot in the amount of ~ 0.7-0.8 mg per 1 mg of CPT that corresponds precisely or somewhat higher than the values in Figure 4-3. Therefore, a small amount of each polyelectrolyte remains in the supernatant. As shown previously, such excessive polyelectrolytes react with alternately charged polymer added on the next stage forming 20-50 nm Hep/PLB16-5 complexes that float free in the solution or adsorb on the nanoparticles' surface.

4.3.2   LbL assembly

Stable nanocapsules of CPT with a 140 nm diameter were prepared at pH 3.0 as described above. However, to be injectable the dispersion should be reconstituted in a physiologically relevant medium with pH 7 in isotonic PBS buffer or 0.9% sodium chloride solution.

The advantage of LbL assembly of polyelectrolytes over other surface modification techniques is the possibility of forming several pairs of layers initially at one pH and further shift pH to another value and finish the coating [87, 57, 35]. We used this approach to deposit 3.5 HEP/PLB16-5 bilayers at low pH to stabilize the colloids of the desired diameter with the highest content of lactone, and further added several layers at pH 7.4.

Previously, it was shown that to avoid complications related with material lost and nanoparticles aggregation during centrifugation-based assembly, nanoparticles can be coated with polyelectrolytes using the washless LbL technique directly in the presence of uncharged excipients [11]. Utilization of block-copolymers of polyamino acids and polyethylene glycol and polysaccharides of low molecular weight allows preserving colloidal stability of the nanoparticles. The polyelectrolytes are added in the amounts that

are needed to reverse ζ-potential to an opposite value as high as 20 mV, thus allowing

building up of the LbL shell.

The CPT cores were found to be positively charged at pH 3 (Figure 4-4). Their

positive charge is caused by BSA adsorbed on the surface [100]. The minimum amounts

of BSA which is only sufficient to support colloidal stability of the nanoparticles but

leaves almost no free protein in the supernatant on the core preparation stage was

utilized. Thereby, BSA simultaneously works as a surfactant and the first layer in the

assembly that anchors the rest of the polyelectrolyte shell.
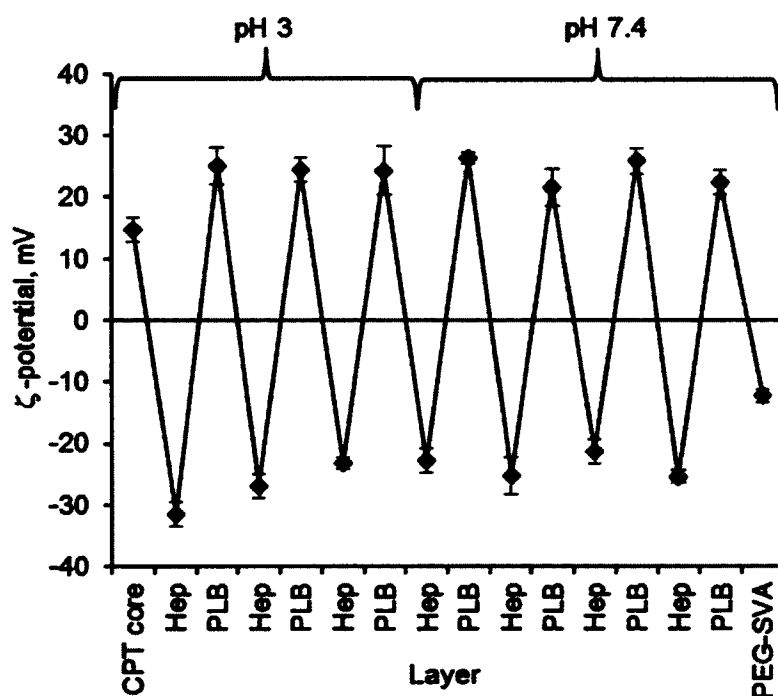
Figure 4-4: Reversal of ζ-potential value of CPT nanoparticles in the process of washless
LbL assembly of polyelectrolyte shell.

The alternation of positive and negative values of ζ-potential confirms the shell

formation on the surface of the nanoparticles (Figure 4-4) at pH 3. Three and a half

HEP/PLB16-5 bilayers allowed to obtain CPT nanocapsules of about 150 nm in size and

well dispersed in PBS at pH 3. In addition, 7.0 bilayers of (HEP/PLB16-5) were

deposited in PBS at pH 7.4 to stabilize the colloids at this physiologically relevant

condition.

TEM images of CPT nanoparticles coated with a (HEP/PLB16-5)7.0 bilayers shell

(Figure 4-5) show particles with a uniform spherical shape. The polyelectrolyte shell

material is not distinguishable from the organic core because it has the same electron

density.
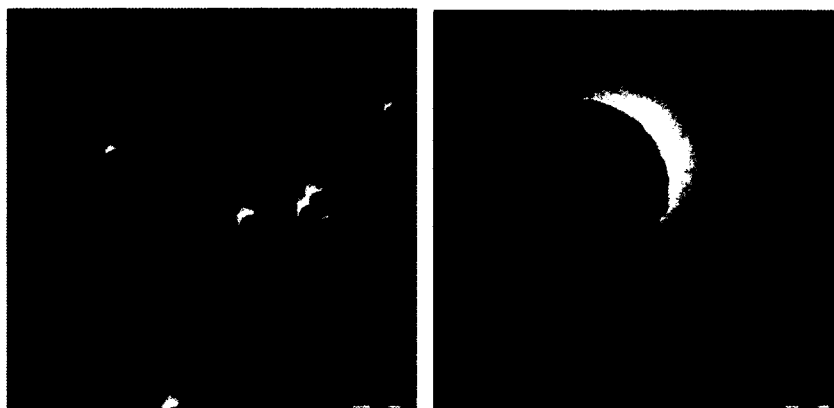
Figure 4-5: TEM image of CPT nanoparticles with a (HEP/PLB16-5)7.0 shell.

4.3.3   QCM analysis of capsule wall thickness, enhanced PEGylation and serum

protein attachment

The thickness of the nanocapsule wall was evaluated by QCM-R technique. The

mass of polyelectrolyte film deposited on the flat surface of a quartz resonator was

recalculated from its frequency decrease using the Sauerbray equation [94-96]. The

thickness of 4.5 and 7.5 (PLB16-5/Hep) bilayer films is ca. 5.2 and 7.5 nm (Table 4-2).

The difference between the films with 4.5 and 7.5 bilayers in attachment of PEG upon the

treatment with a PEGylator is negligible. Therefore, it is safe to assume that only film

outermost amine groups interact with the substances.

Table 4-2: PLB16-5/Hep thickness, amount of attached PEG.

Assembly	Bilayers (n)	dF, Hz	Absorbed mass, $\mu g/cm^2$	Thickness*, nm
LbL film				
(PLB16-5/Hep)n	7.5	51.2±10.7	0.9±0.2	7.5
	4.5	35.0±5.6	0.6±0.1	5.2
Attached PEGylator on (PLB16-5/HEP)n, Conc. mPEG-SVA=50 mg/mL				
PEG 5kDa	7.5	41.1±7.3	0.7±0.1	5.8
PEG 5kDa	4.5	49.4±16.1	0.9±0.3	7.5
PEG 20kDa	7.5	70.3	1.2	10
PEG 20kDa	4.5	58.0	1.0	8.3

* - using 1.2 g/cm^3 film density [94-96].

The mass of mPEG20kDa attached to the film is ~ 1.2-1.7 times exceeding that of

mPEG5kDa. This mass corresponds to the PEGylation degree that corresponds to the

maximum surface coverage by PEG tails. Although many amine groups remain unreacted

on the surface, the further PEG attachment is hindered by neighboring PEG tails. The

mass of these attached PEG corresponds to a layer with an apparent thickness of 6-10 nm.

The PEGylation significantly decreases the attachment of serum proteins to a

(PLB16-5/Hep)n film (Table 4-3). The ΔF shift which is proportional to the deposited

mass is 5-11 Hz for PEGylated surfaces vs. 40 Hz for surfaces without enhanced

PEGylation.

Table 4-3: Binding of serum proteins on modified polyelectrolyte films.

Serum protein binding				
Assembly on (PLB16-5/HEP)n	**Bilayers (n)**	**dF, Hz**	**Absorbed mass, $\mu g/cm^2$**	**Adsorbed serum protein thickness*, nm**
No additional PEGylation	4.5	50.9	0.89	7.4
PEG 5kDa	7.5	5.7	0.1	1.7
PEG 5kDa	4.5	4.7±4.2	0.1	1.7
PEG 20kDa	7.5	11.0	0.2	0.8
PEG 20kDa	4.5	11.0	0.2	5.9

* - using 1.2 g/cm^3 film density [94-96].

4.3.4   Colloidal stability of nanocapsules

One of the major parameters of nanocapsule applicability for intravenous administration is their colloidal stability in physiologically relevant buffer and the size remaining < 200 nm.

The CPT nanocores coated only with BSA have low colloidally stable for 2 h in PBS buffer both at pH 3 and 7.4. The samples with 5 bilayers of (HEP/PLB16-5) shell (positive outermost layer) had a hydrodynamic diameter within 130±10 nm for at least 7 days, while the size of the sample coated with 7 bilayers of (HEP/PLB16-5) increases to 300 nm (Figure 4-6a). The CPT colloids with a shell that have negative HEP layer on the top are to some extent more stable than that with positive PLB16-5 (Figure 4-6b). One possible explanation is that HEP macromolecules deposited atop PLB16-5 act as spacers between PEG tails and keep them straighter than that with PLB16-5 on the top, thus providing better steric hindrance.

However, if a PLB16-5 terminated shell is additionally PEGylated, the obtained nanoparticles had the hydrodynamic diameter of 123±2 nm for 48 h, and after 7 days

their size increased only by 70 nm, proving that the availability of free amine groups on

the surface of CPT nanocapsules is the main reason of their colloidal instability. Attached

PEG chains increase nanoparticles hydrophilicity and therefore stability of the colloids.
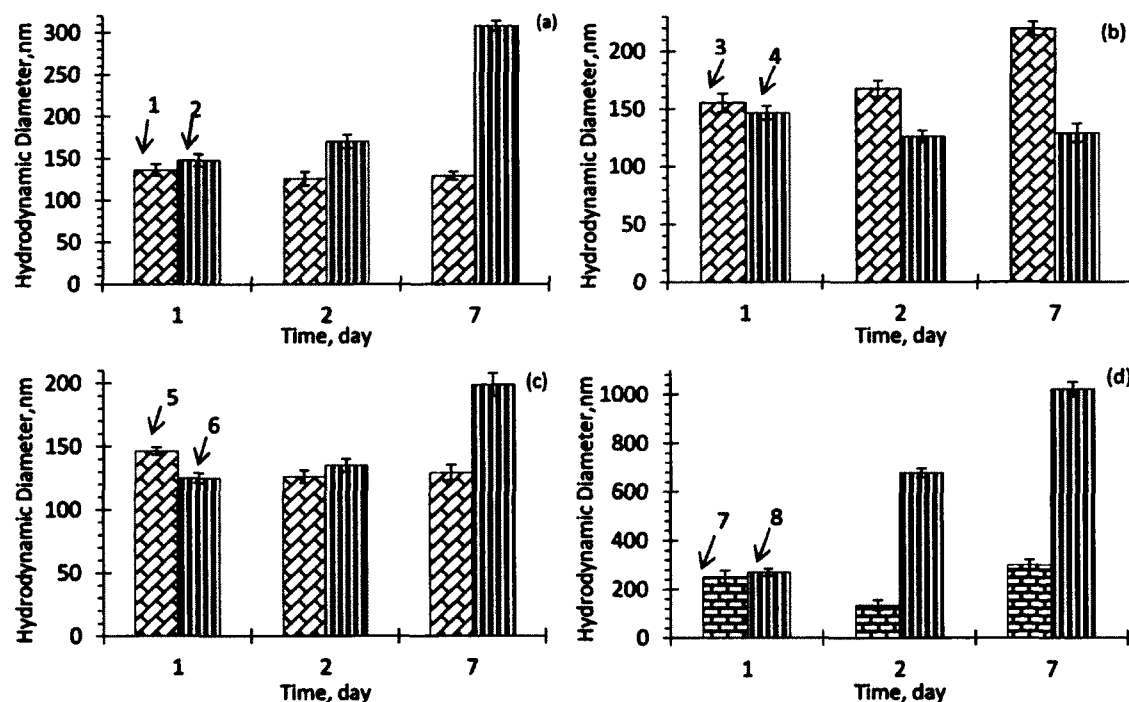
Figure 4-6: Colloidal stability of nanocapsules in PBS buffer, pH 7.4 with varying: a) number of bilayers: 1 - (Hep/PLB16-5)5.0 and 2- (Hep/PLB16-5)7.0 ; b) outermost layer: 3 - (Hep/PLB16-5)5.0 and 4 – (Hep/PLB16-5)5.5; c) PEGylation: 5- (Hep/PLB16-5)5.0 and 6 - (HEP/PLB16-5)5.0/mPEG5kDa; d) molecular weight of PEGylator on a (Hep/PLB16-5)8.0 shell: 7 – mPEG5kDa and 8 – mPEG20kDa.

At the same time, apparent stability of the CPT colloids that are additionally

PEGylated with mPEG20kDa-SVA is not as good as that of colloids treated with 5 kDa

PEGylator and even worse than the expected stability of PLB16-5 terminated

nanoparticles. This difference might be caused by increasing viscosity in the vicinity of

the nanoparticle surface caused by high molecular weight PEG chains slowly protruding

into the solution with time. Long irregular PEG chains can also support self-assembly of the nanoparticles into more complex structures [104, 105].

One can conclude that the best encapsulation is for 5 bilayers with extra PEGylation of shorter length PEG tails, 5 kDa. To make a slower release, we will further make the LbL wall thicker by adding two more bilayers onto the shell.

4.3.5   Chemical stability of CPT in nanocapsules at different pH

CPT has two forms, lactone and carboxylate. Lactone is less toxic and a more active form of CPT for inhibiting Topoisomerase I [106-108]. The lactone group of the substance easily hydrolyses to carboxylate at neutral and slightly alkaline conditions.

In PBS, at all studied pH except pH 9, the lactone form of CPT in nanocapsules was preserved at least for 17 h with a light decrease of its content to 97-98% during next 5 h (Figure 4-7a).
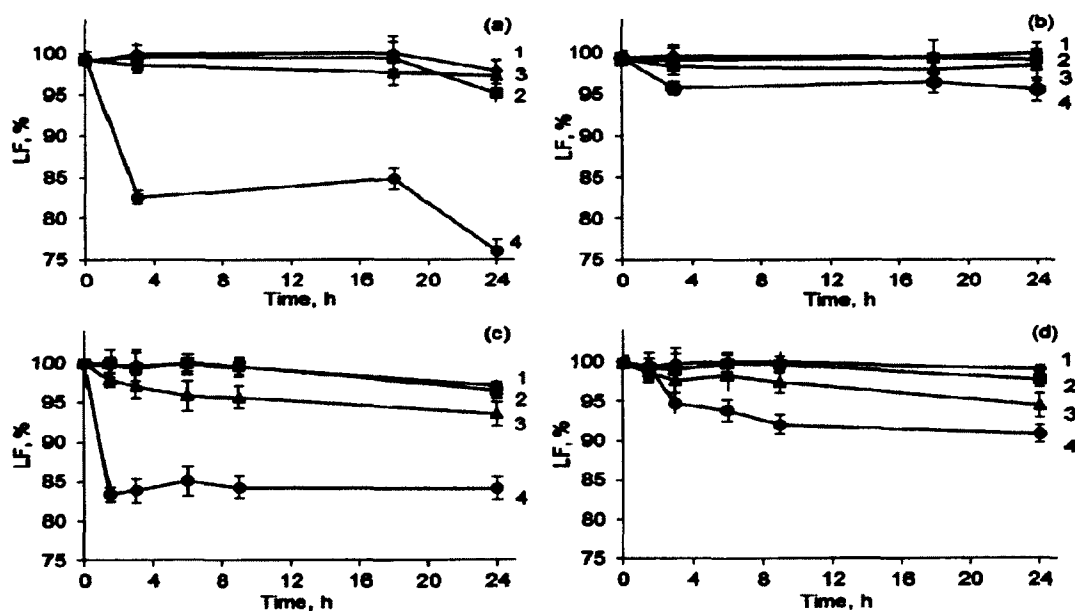
Figure 4-7: Chemical stability of CPT in the nanocapsules (a,b) and free CPT (c,d) in PBS (a, c) and in PBS with 25 mg/mL BSA (b, d). pH: 1- 3.0; 2-5.0; 3- 7.4; 4- 9.0.

At the same time, free CPT added to the release medium as a solution in DMSO degrades faster at all pH, including pH 3-5 (Figure 4-7c). In the presence of 25 mg/mL BSA, lactone in CPT nanocapsules is stable over a wide range of pH, including pH 9.0 (Figure 4-7b), LF is ~96% after 24 h. Moreover, the lactone form is more preserved than that in PBS alone (Figure 4-7a). The improved chemical stability of CPT in LbL capsules makes such formulation less toxic than free CPT.

4.3.6   Release of CPT in PBS and FBS

In PBS buffer supplemented with 2% w/v Polysorbate 80, an initial burst of drug released into the medium leads to 25-30% dissolution of nanoparticles for 1.1-1.6 µg/mL of CPT, and 60% release for 0.5 µg/mL was observed. It is followed by slowing down the drug dissolution during the next 3 h (Figure 4-8a). After that, the released percentage of drug did not change significantly. For the lowest concentration of CPT, 0.5 µg/mL, that is eighteen times lower than the CPT solubility (ca. 9.4 µg/mL), the release reaches the maximum of ~ 70% after 24 h. No sufficient difference in release profile was observed at pH 5 as compared to pH 7.4 at a 1.6 µg/mL CPT concentration.
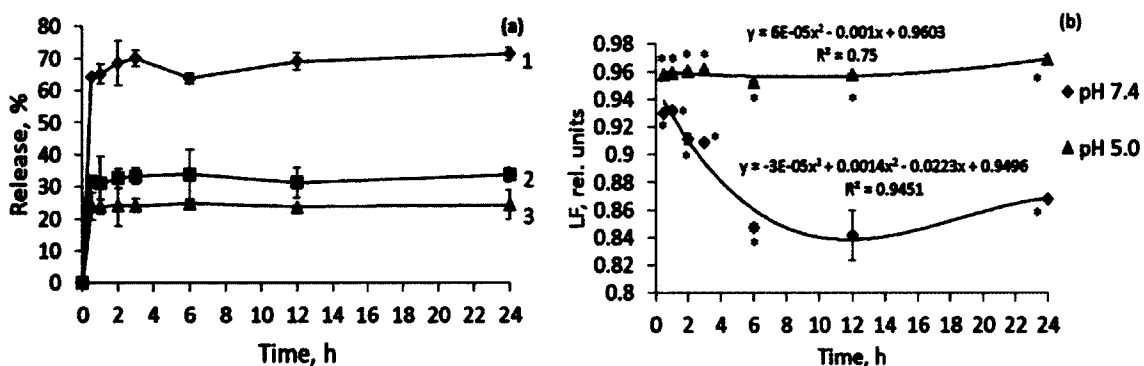
Figure 4-8: Release of CPT from nanocapsules with a (HEP/PLB16-5)5 shell in PBS with 2% w/v Polysorbate 80, (a) cumulative release of CPT, C (CPT), µg/mL: 1- 0.5, 2- 1.1, 3-1.6. (b) lactone fraction remaining in the release medium at pH 7.4 and 5.0 as a function of time. C (CPT) = 1.6 µg/mL. *P < 0.01.

However, after the drug is being released from the nanocapsules at pH 7.4, a slow

hydrolysis of the lactone form of CPT to the carboxylic one takes place. After 6 h, up to

16% of the drug is converted to the carboxylic form (Figure 4-8b). On the other hand, up

to 96% of released CPT retains the lactone form after 24 h if released at pH 5.

The release profile of CPT from (HEP/PLB16-5)5 nanocapsules in FBS differed

from that in PBS (Figure 4-9). An initial fast release up to 85% takes place within the

first 30 min. However, the concentration of CPT in the release medium decreases and the

apparent percent of released drug diminishes to 25-30%. Apparently, this trend was due

to initial aggregation of non-extra-PEGylated nanoparticles with the serum proteins. It

has a lower CPT solubility limit in FBS (6.7 µg/mL) as compared to that in PBS. Similar

release profiles were obtained for different concentrations of CPT nanocapsules

(Appendix A, Figure A-1).
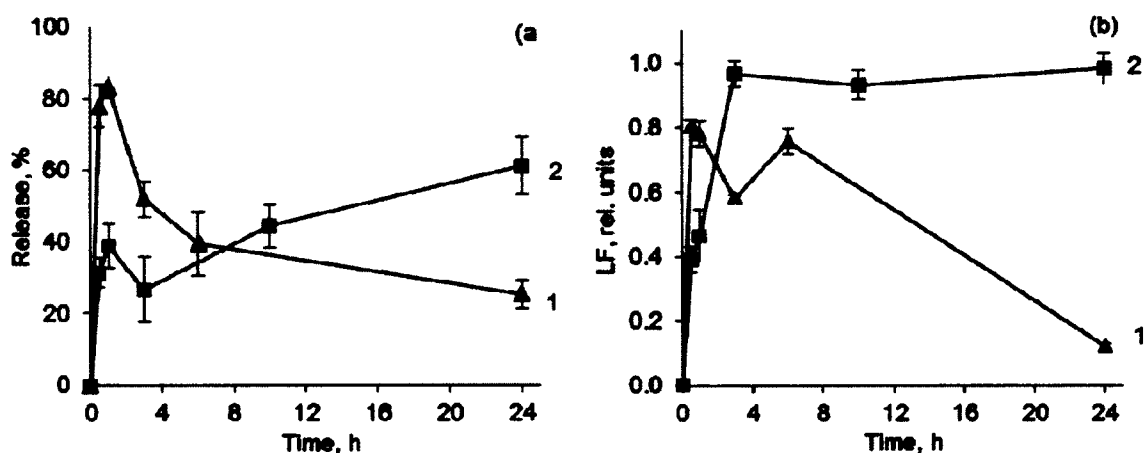
Figure 4-9: Detectable CPT concentration depending on time due to release from
(HEP/PLB16-5)5 (1) and (HEP/PLB16-5)5/mPEG5kDa (2) nanocapsules in FBS (a) and
lactone fraction retained in the released medium (b) as a function of time. C(CPT) =
2.27µg/mL.

It was assumed that the released CPT molecules interact with proteins from the bovine serum. As the time of release increased, a growing volume of the sediment was observed upon separation of nanoparticles from the release medium by centrifugation. A sufficient part of the precipitate was found to be the proteins. The interaction with CPT seems to enhance aggregation of the serum proteins or their attachment to the walls of polyelectrolyte capsules.

The hydrophilic PEG layer formed on the surface of nanocapsules after treatment with mPEG-SVA shields them from the FBS proteins, thus minimizing their attachment and stabilizing the colloid in FBS. The initial release of CPT from the nanocapsules with enhanced PEGylation attains only 40% of the drug after 1 h, and then almost a linear increase of CPT concentration in the release medium was found (Figure 4-9). After 24 h, the released amount of drug reaches 60%. The apparent thickness of the extra PEG layer is comparable with the thickness of (PLB16-5/HEP)7.5 bilayers shell beneath it (Table 4-2); therefore, a lower initial burst and prolonged time of release for the treated capsules are not surprising.

Apart from the much higher initial CPT release rate in the serum, the hydrolysis of the drug in the serum is also faster. For nanocapsules without enhanced PEGylation, the highest fraction of the lactone form, ~0.9, was observed in FBS immediately after the initial burst, and then it decreases almost to 0.1 (Figure 4-9b). The difference in the hydrolysis rates in PBS and the serum can be related to the presence of a high concentration of albumin that accelerates the conversion of lactone to carboxyl [89-93]. For the sample with an extra PEGylated surface due to a much lower initial CPT release rate, the lactone fraction reaches its maximum after 3 h, indicating that at the earlier

stages lactone interacts with the serum components and hydrolyses faster than it accumulates in the tumor cells. Due to the prolonged character of release from the PEGylated nanocapsules, a new portion of lactone CPT is supplied into the supernatant during a long period of time, thus supporting its high relative concentration.

4.3.7 *In vitro* cell culture studies

The treatment of *CRL2303* glioblastoma cells with both free CPT and nanocapsules with extra PEGylated shell causes prominent changes in their morphology that indicate a disappearance of cellular processes, while after the addition of comparable volume of PBS buffer the cells proliferate (Figure 4-10). After 40 h, the treatment with CPT led to clear disruption of cell membranes and necrosis of the cells.

Figure 4-10: Effect of free CPT (2 and 3) and CPT nanocapsules with (HEP/PLB16-5)7/mPEG5kDa shells (4 and 5) on Rat brain glio-blastoma cells after 16 (upper row, a) and 40 h (lower row, b) treatment. 1) Negative control (PBS buffer), 2, 4) 1.0 μM, 3, 5) 10.0 μM. Images shown are representative of multiple wells (≥ 6) and multiple platings of cells for each condition tested. In collaboration with Dr. M. DeCoster, Louisiana Tech University, Ruston, LA.

4.3.8 Effect of CPT nanocapsules on glioblastoma cells viability

Both CPT nanocapsules and free drug inhibit *CRL2303* glioblastoma cell growth

after 16 h of incubation; the decrease of cell viability depends on the applied

concentration of CPT (Figure 4-11). The prolongation of the incubation up to 40 h

increases the effect except for the case of 10 nM free drug that has been apparently

hydrolyzed in the course of long cell incubation. The nano-formulation cytotoxic effect is

mostly observed in the case of medium drug concentration, 100 nM (circled in the Figure

4-11). For 100 nM CPT nanocapsules, a clear delayed effect is observed, with a decrease

in tumor cell viability down to about 30% by 40 hours (Figure 4-11).
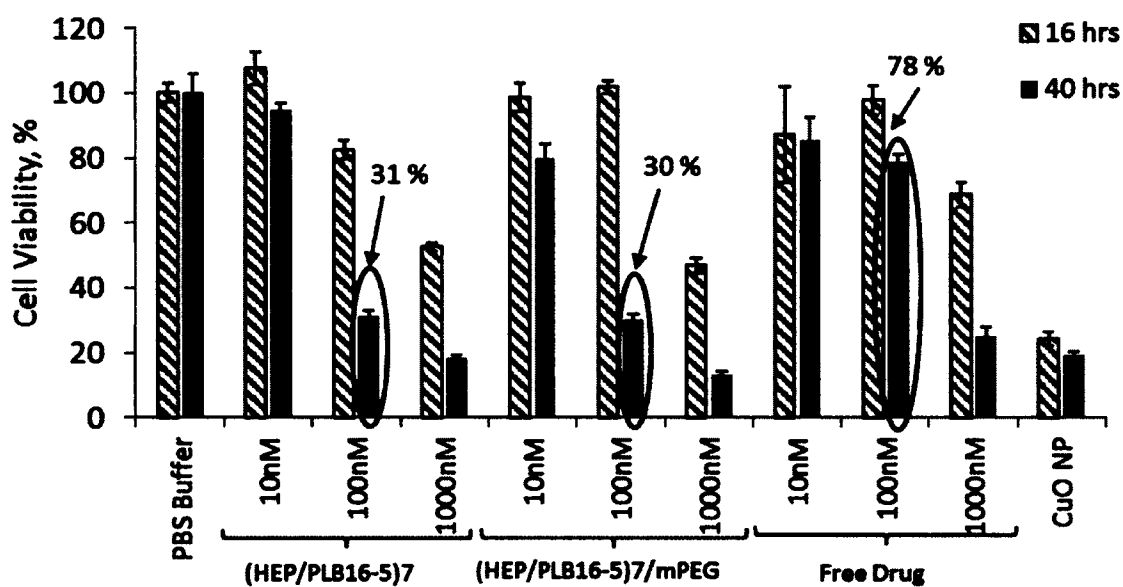
Figure 4-11: Effect of different concentrations of free CPT, and CPT nanocapsules with (Hep/PLB16-5)7 and (Hep/PLB16-5)7/mPEG5kDa shells on CRL2303 glioblastoma cell viability. Data shown are representative of multiple wells ($\geq$ 6) and multiple platings of cells for each condition tested. The percentage values of 100nM are indicated. In collaboration with Dr. M. DeCoster, Louisiana Tech University, Ruston, LA.

The difference between cell growth inhibition activities of CPT nanocapsules with

(HEP/PLB16-5)7 bilayers and (HEP/PLB16-5)7/mPEG5kDa is negligible. The

corresponding IC_{50} values are ca. 103.8 and 103.5 nM (Appendix A, Figure A-2). At the same time, when free CPT is less active, IC_{50} is ca. 146.3 nM. We presume that after free CPT is added to the cell culture medium, a sufficient part of the drug is quickly hydrolyzed into less active carboxylic form, while the lactone CPT in nanocapsules is preserved and releases slowly in the course of the cell incubation.

4.3.9   Prevention of BSA loss from the core

In order to improve CPT loading capacity, we slightly modified the existing method as later mentioned. The nanocores of the CPT were formed as per the previous protocol. The LbL assembly of HEP/PLB16-5 on the CPT nanocores was changed with a total number of 4 bilayers. Now the outermost layer deposited on the CPT nanocore was PLB16-5 at pH 3. Then the nanoparticles were washed once using centrifugation at a speed of 11,000 rpm (Eppendorf 5804R centrifuge) for 10 min and resuspended in PBS at pH 7.4. Furthermore, another two bilayers were deposited at pH 7.4 to form the entire shell composition with a total of six bilayers of HEP/PLB 16-5. The PEGylation step was the same as the earlier process. See Table 4-4.

Table 4-4: Zeta potential values before and after washing step after 4 bilayers.

Description	pH	Zeta potential, mV	%BSA in core
CPT- $(hep/PLB_{16-5})_{4.0}$	3	14 ± 2	100
CPT-$(hep /PLB_{16-5})_{4.0}$	7	-7 ± 4	-
CPT-$(hep/PLB_{16-5})_{4.0}$ / $(hep /PLB_{16-5})_{0.5}$	7	-25 ± 5	-
CPT-$(hep /PLB_{16-5})_{4.0}$ / $(hep /PLB_{16-5})_{2}$	7	14 ± 2	96.7
CPT-$(hep /PLB_{16-5})_{4.0}$ / $(hep /PLB_{16-5})_{2}$ /mPEG$_{5kDa}$	7	1 ± 1	77.8
CPT-$(hep /PLB_{16-5})_{3.5}$ / $(hep /PLB_{16-5})_{3.5}$ / mPEG$_{5kDa}$	7	3 ± 2	56

After resuspension of nanoparticles from pH 3 to 7.4, zeta potential was measured as -7 ± 4 mV. It was observed the release of BSA due to change in the pH. The change in

zeta potential after switching the pH can be explained as re-deposition of BSA on the outermost layer of PLB16-5. See Table 4-4. In the usual method, the loading capacity of the CPT was approximately 56%. Due to change in outermost layer during pH change led to increase in loading capacity of CPT to ~76% (Figure 4-12a). The particle size was measured ca. 210±2 nm and the lactone fraction (LF) was restored to LF ~ 0.998 after 3 days (Figure 4-12a). The percentage of lactone fraction of the CPT in the core was estimated by formula (2) in Section 4.2.5.
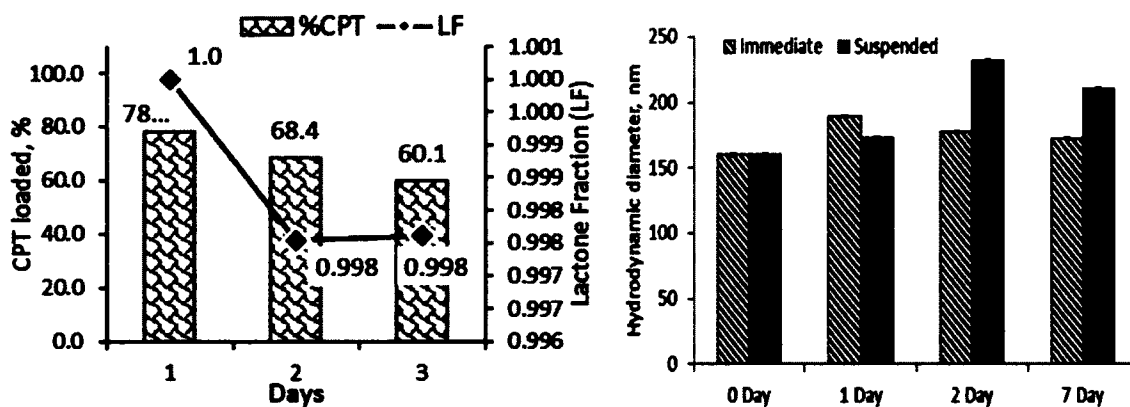
Figure 4-12: (a) % CPT loading and lactone fraction (LF) for 3 days study; (b) The colloidal stability of sample after extra PEGylation for (1) prior suspended, (2) pre-suspended in PBS pH7.2 just before taking reading.

The reduction of loss of BSA was also confirmed by the QCM studies. See APPENDIX A, Table A-1. In changing the outermost layer from HEP to PLL during pH change from 3.0 to 7.2, a significant loss in mass deposition is seen. There is mass loss of -0.866 $\mu g/cm^2$ for HEP at the outermost layer and a mass gain of 0.618 $\mu g/cm^2$ for PLL. This clearly indicates that the new approach has reduced the BSA loss and thus CPT drug loss from the core.

The colloidal stability of such extraPEGylated LbL coated softcores after 7 days

of study was observed to be 172±2 nm by taking immediate reading from the dispersion,

and was 210±2 nm after keeping it suspended in the dilution of 100X in PBS pH 7.2

(Figure 4-12b).

4.4   Conclusion

The objectives of using LbL formulation technique to encapsulate CPT were to

preserve the lactone form of the drug; to attain < 200 nm mono-dispersed stable colloid

dispersion at a high concentration of 0.5 mg/mL; to get a sustained release of the drug for

at least 24 h with good lactone fraction and, finally, to have a better *in vitro* cancer cell

growth inhibition effect than the uncoated CPT drug.

160 nm capsules were formulated with CPT in the core and BSA covering it,

followed by a 7-8 bilayer of alternating anionic heparin (HEP) and cationic PEGylated

polylysine (PLB16-5). By attaining non-washing LbL assembly at two pH values

(starting from lower pH 3 to preserve lactone form and proceeding at pH 7.4),

nanocapsules were formulated with a loading capacity of approximately 60 w % and as

high as 99% lactone CPT fraction. Colloidal stability of the nanocapsules was improved

by incorporating mPEG 5 kDa tails on the outermost layer of PLB16-5. The

encapsulation of the CPT in the shells of polyelectrolytes modified with PEG reduces the

rate of hydrolysis of lactone to carboxylic form compared with free drug at neutral and

alkaline media. The modification of the nanocapsule's outer surface with additional

mPEG 5 kDa tails increases protein-resistance of the shell, decreases initial drug burst,

and prolongs the release time in biologically relevant media. It allows preserving the

active lactone form of the CPT in the course of the nanocapsules' incubation with cancer

cell. As a result, the activity of CPT encased into LbL nanocapsules towards *CRL2303*

glioblastoma cell is improved three-fold. By changing the architecture of the PE

assembly, the CPT loading capacity was increased to ~ 78%. In the next chapter, a step

forward in applying LbL assembly for delivery of more nanomicelle core of PTX is

described.

CHAPTER 5

APPLICATION OF LAYER-BY-LAYER ASSEMBLY FOR NANOMICELLAR CARRIER OF LOW SOLUBLE ANTICANCER DRUG WITH IMPROVED COLLOIDAL STABILITY AND BIOAVAILIBILITY

5.1   Introduction

Chapter 4 describes the application of the developed washless LbL assembly for

encapsulation of more poorly soluble drug PTX loaded in nanomicelle cores. Three step

approaches were tried to reduce the hydrodynamic size along with colloidal stability of

PTX LbL formulation: 1) drug encapsulation in the nanomicelle core; 2) assembly of PEs

on top of it; and 3) conjugation of a PEG trail on the outermost surface of the PTX

formulation to prevent any serum protein adhesion. In a previous work by Shutava *et al.*

[11], a nano-colloidal core of PTX was formulated along with dioctyl sodium

sulfosuccinate (AOT), an anionic surfactant, poly vinyl pyrrolidone (PVP), a non-ionic

surfactant, and Tween 80, with the drug being in its meso-crystalline form. It was further

coated LbL assembly of cationic PEs, Poly L-lysine, PLB16-5, PLB16-20 and Heparin,

and extra PEGylated with mPEG-SVA. The LbL architecture was optimized, and it was

found that PLB16-5/HEP assembly obtained a colloidal stability of ~200 nm for 7-8 days.

A maximum of 7.5 bilayers (PLB16-5/Heparin) was assembled. Such a previous study

helped to select the cationic and anionic PEs which could be used for effective 100-200

65

nm scaled formulations. The QCM studies indicated that higher concentration (0.5 mg/mL) and longer tails of PEG grafted to poly-L-lysine, significantly resisted serum protein (FBS) adsorption. These concepts from Shutava *et al.* [11] and Parekh *et al.* [12] were applied for further improvement of the delivery system for PTX. The main aim was to have smaller particle size of ~100 nm, a better colloidal stability of more than 14 days, high drug loading capacity between 30-50%, ability to preserve the anticancer activity of PTX, thus showing a significant anti-tumor effect, if possible an improved circulation time of > 4 h, and better bioavailability of drug in a mice model. In addition to these objectives, an attempt was also made to optimize the shell structure of PTX nanocolloidal formulation, a previous work in Shutava *et al.* [11], by using different anionic polyelectrolytes for reduced immune response and longer circulation.

5.2   Materials and Methods

5.2.1   Materials

PTX was obtained from L.C. Laboratories, tocopherol polyethylene glycol 1000 succinate (TPGS), dioctyl sulfosuccinate sodium salt (AOT) from Sigma Aldrich. The other polyelectrolytes and poly ethylene glycol molecule were the same as mentioned in Chapter 4.

5.2.2   Core nanomicelle formation

AOT (Dioctyl sulfosuccinate sodium; an anionic surfactant), 3.8 mg/mL and TPGS (D -α-Tocopherol polyethylene glycol (1 kDa) succinate, a non-ionic surfactant), 1.5 mg/mL, were taken in different ratios and dissolved in $CHCl_3$. This mixture was then dried under N_2 purge to form a thin film. The film was resuspended in 2.5 mL PBS pH 7.2 and sonicated for 2-3 min. Then the PTX stock solution in acetone was added drop-

by-drop with continuous sonication to form a final PTX concentration of 1.25 mg/mL.

The sonication was continued for 15 min, until the mixture became transparent. The zeta

potential was measured, which was expected to be negative. Further in the article, this

PTX nanocore is referred to as AGCX.

5.2.3   LbL assembly on nano-core

After the nano-core is formed, 2.5 bilayers of alternating PLB 16-5 and HEP were

assembled (final mass being ~1.31 to 1.03 mg/layer/mg of PTX). For the initial bilayer,

each layer has to be sonicated for a longer time, i.e. 5 min, than the rest of the layers,

which was for 2 min. After 1 hr of ageing, the sample was washed at 14,000 rpm

(Eppendorf 5804R centrifuge) for 10 min. The supernatant obtained was the final sample

of interest, indicated as AGCX-LbL. The pellet was resuspended in the same volume of

PBS, pH 7.2, i.e. 2.5 mL and re-dispersed under continuous sonication. For extra

PEGylation, dry powder of mPEG5kDa-SVA (Laysan Bio Inc.) was added directly after

the last PE layer of heparin i.e. (PLB16-5/HEP) 3.0 bilayers. It was followed by

sonication to have a final PEG concentration of 20 mg/mL.

After overnight ageing, the dispersion was washed similarly at 14000 rpm

(Eppendorf 5804R centrifuge) for 10 min. The supernatant collected was the final extra

PEGylated sample, i.e. AGCX-LbL-PEG. The pellet was re-dispersed in the same way as

before. For both AGCX-LbL and AGCX-LbL-PEG samples, the dispersion after pellet

re-suspension was used for measuring the % drug loading capacity. Procedure and

calculations of it are described in Section 5.2.4.1. Various ratios of both surfactants and

PTX drug were tried during optimization of formulation, details of which are mentioned

in APPENDIX B, Table B.1-1. The stability and zeta potential values of these nano-

micelle cores are shown in Figure 5-4. The final concentrations of each reagent and PTX

drug for the optimized formulation is listed in Table 5-1. The above formulation process

was also tried with another anticancer drug, Lapatinib, which has more solubility than

PTX. Due to the difficulty in determining the amount of Lapatinib, the formulation was

made for PTX. The chemical stability of Lapatinib was analyzed by HPLC (Agilent

1100), in Figure B.2-2 and Figure B.2-3. For more details, see APPENDIX B, Section

B.2.

Table 5-1: Composition of AGCX formulation: LbL coating on PTX loaded
nanomicelle.

Sample	Individual Concentration			AOT/ PTX	TPGS/ PTX	TPGS/ AOT	(Total NI+I Surf*)/ PTX	Avg. PE**/ layer per PTX
	C(AOT) mg/mL	C(TPGS) mg/mL	C(PTX) mg/mL					
AGCX	3.765	1.51	1.255	3	1.203	0.401	4.203	1.3

* NI- Non Ionic, I- Ionic; **PE- Polyelectrolyte (HEP or PLB16-5)

5.2.4   Percentage calculations

5.2.4.1   Percentage drug encapsulation

Since the drug was encapsulated in a nano-micelle, it was retrieved in the

supernatant after the washing step. The pellet was re-dispersed in the same volume of

PBS pH 7.2. A small aliquot (20 μL) of this dispersion was diluted 100 times in acetyl

nitrile. It was then washed at 14,000 rpm (Eppendorf 5804R centrifuge) for 10 min. The

% drug encapsulated was calculated using the following formula:

$$\% \ Drug \ encapsulation = \frac{Inital \ Conc \ of \ PTX \ used - Conc \ of \ PTX \ in \ residue}{Initial \ conc. of \ PTX \ used \ for \ formulation} \times 100 \ \% \quad Eq. \ 5-1$$

The UV absorbance of the supernatant was measured at 227 nm ($\varepsilon = 28845.93$ M^{-1}cm^{-1} or 33.781 mg^{-1}cm^{-1}mL) in acetyl nitrile.

5.2.4.2   Estimation of amount of TPGS, %

It was also important to analyze the percentage of other reagents present in the final formulation of AGCX-LbL and AGCX-LbL-PEG. For TPGS analysis, the pellet dispersion after the washing step of LbL or extra PEGylation was re-dispersed in acetyl nitrile, 101 dilutions, and washed again. This supernatant was analyzed at 273 nm for its absorbance. Similarly, before washing, AGCX-LbL was analyzed at 273 nm. The % of TPGS present in the formulation was calculated by the following formula:

TPGS (Absorbance 273nm),% =

$$\left(\frac{\textit{Non washed AGCX LbL} - \textit{Dispersed pellet AGCX LbL or AGCXLbL PEG}}{\textit{Non washed AGCX LbL}}\right) \times 100 \ \%. \quad \textbf{Eq. 5-2}$$

5.2.5   SEM and cryo-TEM sample preparation

The drug dispersion was dropped on a clean silicon wafer, and was dried at room temperature. The silicon wafer and the dried sample were then coated with 20 nm of gold and then examined with the SEM. Cryo TEM samples were prepared and vitrified by using Vitrobot manufactured by FEI and the samples were run on cryo TEM, FEI Tecnai G2 F30 Twin. Cryo TEM was done to preserve the soft core of nanomicelles during electron microscope imaging.

5.2.6   Colloidal stability in FBS

Colloidal stability in FBS was estimated for the following samples individually: 1) AGCX nanocore, 2) LbL coated nanocore as AGCX(PLB/HEP)2.5, and 3) Extra PEGylated nanocore as AGCX(PLB/HEP)2.5_mPEG-SVA. 30 µL of corresponding PTX

sample was added in 2 mL of FBS (pH7.4) and mixed well. It was then immersed in a

water bath at 37.5° C. The study was done for a total of 48 h, under continuous stirring at

1000 rpm (Eppendorf 5804R centrifuge). At different time intervals, samples were

analyzed for the hydrodynamic size and zeta potential.

5.2.7   *In vitro* release study Tween 80

Release studies for extra PEGylated AGCX samples were done in PBS at pH 7.4

with 2% w/v Tween 80 at 37.5° C. Different volumes of PTX dispersion were taken from

the stock and added to 30 mL of preheated PBS mixture. The release medium was kept

under continuous stirring. The PTX concentrations studied were 24, 12 and 3 μg/mL. At

release time periods of 0.5, 1, 3, 6, 12, and 24 hrs, 200 μL aliquots of release medium

were extracted and replaced with the same volume of PBS, pH 7.4 with 2% Tween 80.

5.2.8   Percentage drug released calculation

It was necessary to calculate the amount of free drug released in the release

medium to analyze the release of the drug at individual time points. For the UV study, out

of 200 μL of released medium collected at different time points, aliquots of 20 μL were

diluted in 2 mL of Acetyl Nitrile and were centrifuged at 14,000 rpm (Eppendorf 5804R

centrifuge) for 10 min. The supernatant was then analyzed in UV vis at 270 nm

wavelengths, with extinction coefficient being 482817.8 $M^{-1}cm^{-1}$ or 565.42 mL $mg^{-1}cm^{-1}$.

The solubility of PTX in the water is less than 12 μM or 10 μg/mL [109].

5.2.9   Cytotoxicity studies

4T1 breast cancer cells purchased from The American Type Culture Collection

(ATCC; Manassas, VA) were grown and maintained in RPMI, pH 7.4, supplemented

with 10% (v/v) FBS and 1% of penicillin/streptomycin stock solution in a humidified, 5%

(v/v) $CO2$ atmosphere at 37° C. The cytotoxicity studies were observed in 4T1 breast cancer cell lines, 4000 cells/well. The control used was Cremaphor-EL vehicle. The cells were treated with: 1) free PTX, 2) LbL coated AGCX nanocores, and 3) extra PEGylated AGCX nanocores. The concentration range used was from 16 ng/mL to 1 µg/mL. Cell titer blue cell viability assay was performed for cell viability studies.

5.2.10   *In vivo* mice studies

The *in vivo* mouse and cell culture studies were done in Northeastern University, Department of pharmaceutical sciences, at Dr. Torchilin's laboratory in Boston, MA.

5.2.10.1   Mouse model

4T1 cells (2 x 106) were inoculated subcutaneously in the left flank of female Balb/c mice. PTX drug formulation were injected intraperitoneally (i.p.) to the mice when the tumor volumes were about 200 mm^3. LbL samples and extra PEGylated samples of PTX (AGCX core) were injected, each to 8 mice, with 4 injections on alternated days. Each injection was of 0.5 mg/mL, 0.5 mL in PBS solvent, pH 7.4. Simultaneously, 2 mice were injected with 0.5 mL of the same concentration of heparin PE present in PTX sample i.e. 0.9375 mg/mg of PTX. For animal studies only, instead of 2.5 bilayers, 1.5 bilayers of PLB16-5/HEP were assembled as an LbL coating. Fewer bilayers were used to minimize the process steps and reduce the use of PEs by 33 wt. %. Tumor volumes, tumor weight, and body weight were monitored every alternate day.

Animals that completed the entire study successfully were only included in the analysis. Mice were constantly monitored and allowed for free access to food and water (following the animal care protocol no. 13-1242 R. approved by Northeastern University Institutional Animal Care and Use Committee, in accordance with the "Principles of

laboratory animal care," NIH publication no. 85-23, revised in 1985). The tumor volume

was calculated using the formula V = 0.5 (length × width^2) by measuring the dimensions

of the tumor at regular time intervals. Statistical analysis included a one-way ANOVA

followed by Tukey's post-hoc test and Kruskal-Wall test.

5.2.10.2 Tumor growth inhibition

The treatments of tumor-bearing mice started 7 days after 4T1 cell inoculation.

All 4 doses were of 12.5 mg PTX/kg every 2 days administered via tail vein. Each

treatment group consisted of 5-6 mice. Tumor volume was estimated as V = 0.5 (length ×

width^2) every 2 days from the beginning of treatments. At +8 days after the first injection,

mice were sacrificed, and tumors were excised and weighed. The control group was

treated with PBS, pH 7.4. The injections were of Taxol (free PTX drug), AGCX-LbL,

and AGCX-LbL-PEG.

5.3   Results and Discussion

5.3.1   Morphological characterization of nanomiceller LbL formulation

The AGCX-LbL and AGCX-LbL-PEG samples are shown after the washing steps

in Figure 5-1. Both of the dispersions seem to be translucent. AGCX-LbL sample seems

to be more clear than extraPEGylated ones.
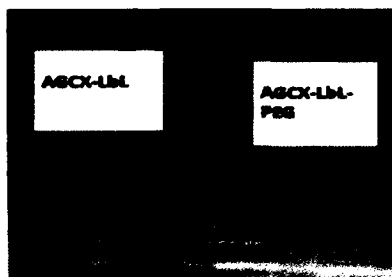
Figure 5-1: AGCX-LbL and AGCX-LbL-PEG samples after washing steps.

The SEM images confirmed that after LbL assembly, the supernatant had the nano-micelles. They had a bit of irregular border due to the non-uniform LbL coating, as seen in Figure 5-2(a). It had an average hydrodynamic diameter of 127 ± 5 nm after 7 days. While the resuspended pellet after washing exhibited the nano-crystalline core as seen in Figure 5-2(b). As seen in Figure 5-2(c) and (d), the extra PEGylation had made the surface look more uniform and spherical.
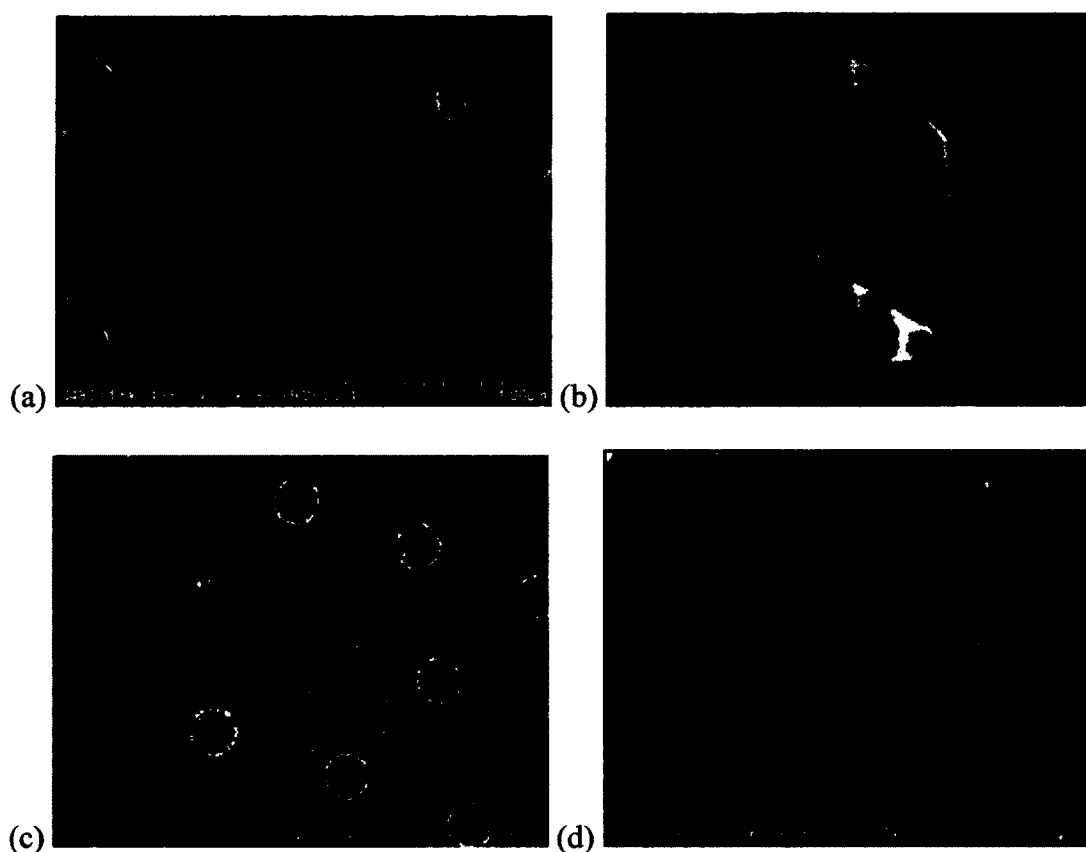
Figure 5-2: SEM of AGCX(PLB/HEP)2.5bilayer – (a) Supernatant; (b) pellet re-dispersed; (c) and (d) extra-PEGylated (7th day). Done at Tulane University, New Orleans, LA.

Since the nanocores were confirmed to be nanomicelles, cryo-TEM was used to confirm the exact shape in cryo state. Figure 5-3(a, b) shows that the border of the nanocores were bit irregular. After LbL assembly, it smoothes out (Figure 5-3c).

Furthermore, extra PEGylation on top of LbL coating seems to fill the gaps between irregular PE/s LbL assemblies, thus making the nanocores more uniformly spherical, as seen in Figure 5-3d. The thick lines seen in the TEM images are the channels of the sample grid.
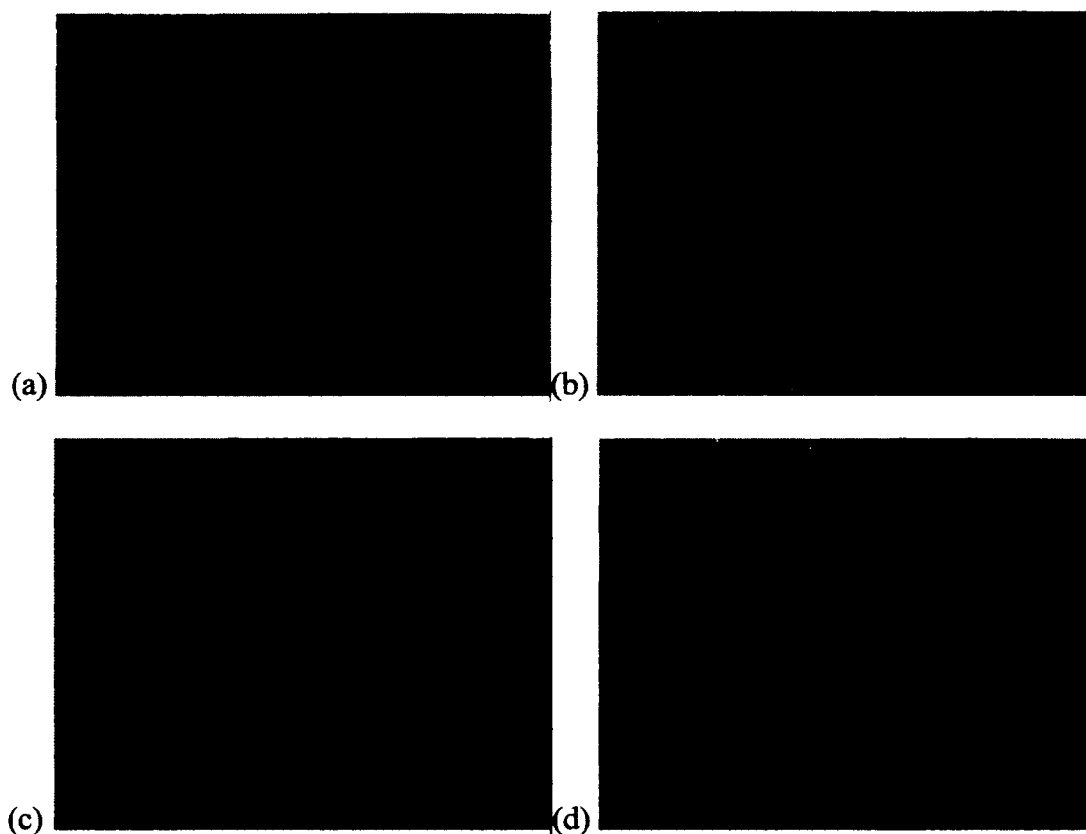
Figure 5-3: Cryo TEM of AGCX: (a) and (b) nanomicelle core; (c) LbL coated; (d) extra PEGylated on LbL assembly. Done at Tulane University, New Orleans, LA.

5.3.2   Optimization of PTX a nano-micellar LbL formulation

Various ratios of TPGS, AOT and PTX were analyzed in the formulation for optimization. Further increase in the amount of surfactant is required for higher drug encapsulation. Best colloidal stability was observed for low TPGS/AOT ratio of 0.401 and a low total surfactant (ionic + non-ionic) to PTX ratio of 4.203. See Table B.1-1 in

APPENDIX B. An unexpected decrease in particle size was observed with an increase in the initial PTX concentration (Figure 5-4).
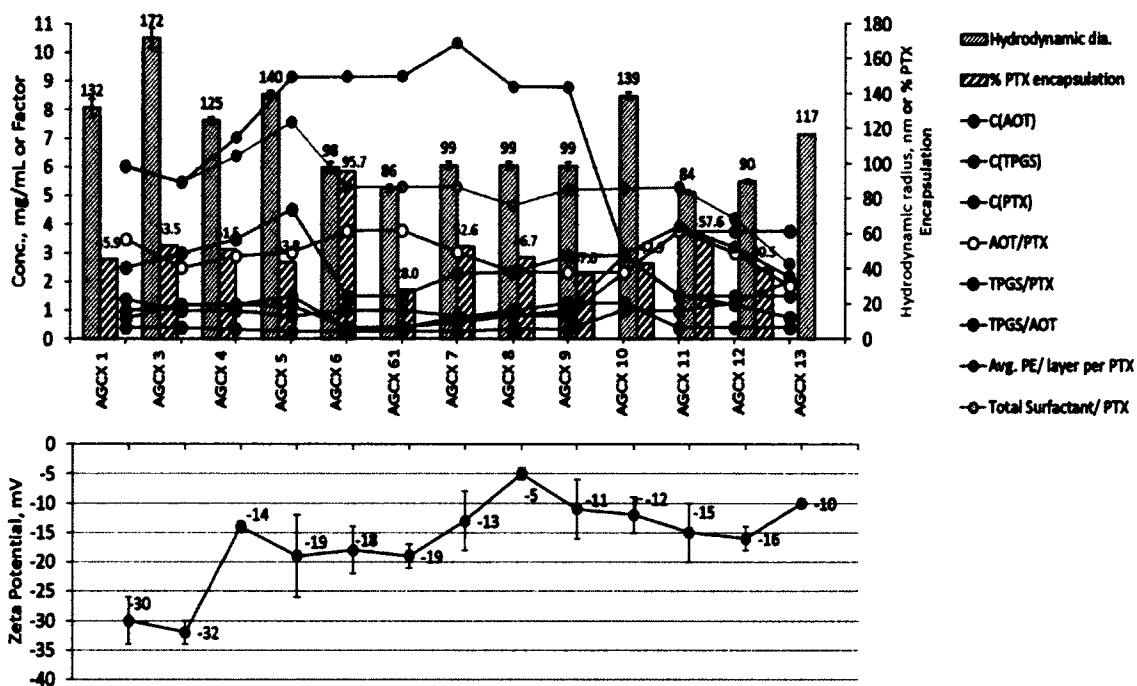
Figure 5-4: The upper graph – composition a hydrodynamic size of the nano-micelle core, %PTX encapsulation of the final formulation after LbL assembly; the lower graph – the zeta potential of surface just after nano-micelle core formation.

As the concentration of the PTX drug was increased, the approximate amount of polyelectrolyte required for a PE layer deposition was almost the same. This trend was especially seen along the samples AGCX9 to AGCX13. The amount of PE per PTX for one layer assembly decreases simultaneously from 8.79 to 2.17 mg/ [PTX]. See Figure 5-4. When the zeta potential of nano-micelle core was sufficiently negative, $-20 < \zeta < -15$ mV, smaller particle size was achieved after 2.5 bilayers of PEs assembly. Further layer deposition lead to insufficient charge reversal. It indicated the destabilization of the LbL assembly. This destabilization could be caused by aggregation of counter free PEs floating in the dispersion mixture.

The negative zeta potential value of -38 ± 2 mV, just after the core AGCX

formation, was due to dominance of excess of sulfate ion heads of AOT pointing out of

the micelle core (Figure 5-5a). Such a high negative potential will support further LbL

assembly of PEs. The amount of PEs required for the first layer, i.e. PLB16-5 is in the

high 60 mg/mL, 70 µL in 2.5 mL of dispersion or final concentration of 1.31 mg/mL. The

amount of PEs for other layers is approximately 1.03 mg/mL. The amount of PEs

required for nanomicelle coating is higher than that in the previous formulation of CPT

(CHAPTER 4). The larger amount can be explained on the basis that the hydrodynamic

size is smaller (approx 100 nm) than that of CPT (150 nm). The % PTX encapsulation

calculated using Eq. 5-1, and it was approximately 60-70% for both AGCX-LbL and

AGCX-LbL-PEG. The % TPGS calculated using Eq. 5-2 was 70-80% (Table 5-2). The

UV absorbance graph for the sample can be seen in Figure B.1-1 in APPENDIX B.

Table 5-2: Details of samples: Zeta potential, Particle size, % PTX concentration, % TPGS concentration.

Sample	% PTX Encapsulation	%TPGS
AGCX_LbL_mPEG	62	74
AGCX_LbL	66	73
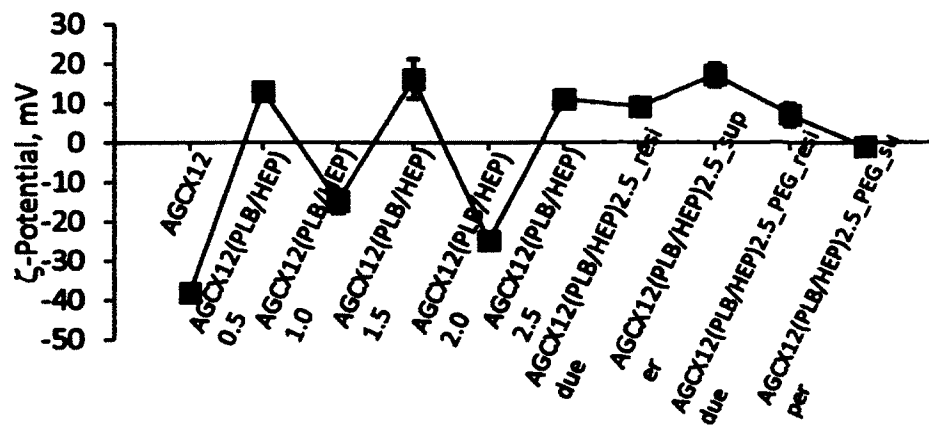
(a)
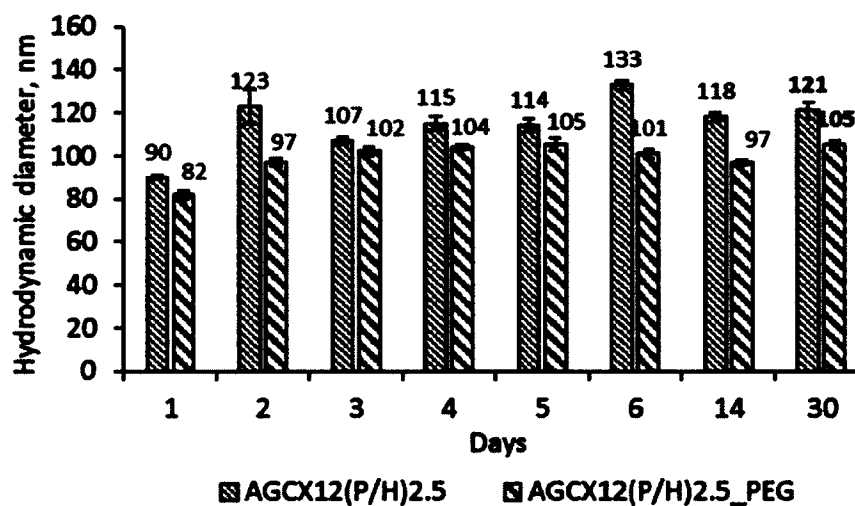
(b)

Figure 5-5: (a) Zeta potential of AGCX during formulation process and (b) Hydrodynamic diameter of AGCX12 after LbL coating and extra PEGylation in PBS pH 7.4. Colloidal stability study of 30 days.

5.3.3   Colloidal stability of LbL coated nanomicellar core

The colloidal stability of extra PEGylated sample in PBS at pH 7.4 was good for

AGCX core, with a hydrodynamic size of 97±2 nm after a 14-day study, while after 30

days it was still 105 nm. See Figure 5-5b. Colloidal stability in FBS also contained

studies of AGCX-LbL and AGCX-LbL-PEG and the AGCX core. Along with particle

size distribution for a 48 h stability study, zeta potential was also measured. For all of

them an exponential increase in hydrodynamic size (Figure 5-6, values for 100% AUC

are indicated due to bi-phasic distribution) was observed in the following order: AGCX-

LbL-PEG > AGCX-LbL > AGCX-core, with AGCX-LbL-PEG having max peak at 481

nm, AGCX-LbL at 1010 nm, and AGCX-core at 1455 nm. As the colloidal stability

decreases, the zeta potential value also dips more; as for the case of AGCX-LbL

(AGCX(P/H)2.5), the change in Z.P. value from 0 h to 48 h is ~ 33 mV, and for AGCX-

LbL-PEG (AGCX(P/H)2.5_PEG), it is ~ 20 mV.
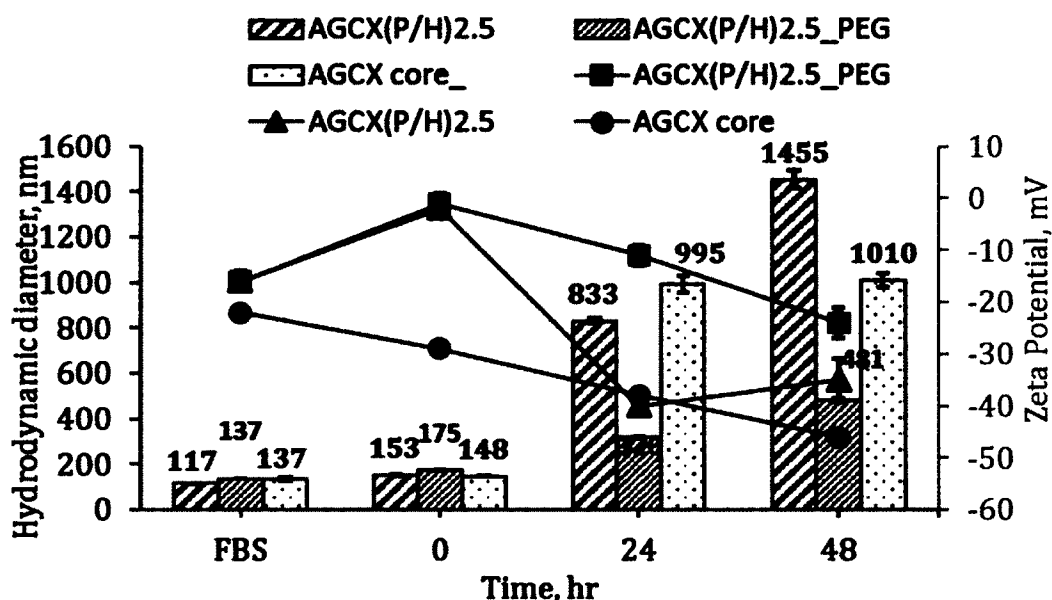
Figure 5-6: Colloidal stability of AGCX low and high PEGylated samples in FBS, pH 7.4, at 37.5° C. Maximum peak values of hydrodynamic size with % AUC =100 indicated.

5.3.4   Release study of LbL and PEGylated nanomicelle

As per the release profile of high PEGylated AGCX nanoparticles, all the

concentrations (0.003 to 0.024 mg/mL) seem to have a similar profile. The highest

concentration of AGCX NPs have the lowest release. This trend can be explained. As the

solubility limit of PTX is 0.008 mg/mL, most of the PTX released gets precipitated, thus leading to lower % of PTX release. See Figure 5-7. All the release profiles seem to increase a bit, if the release was run for more hours.
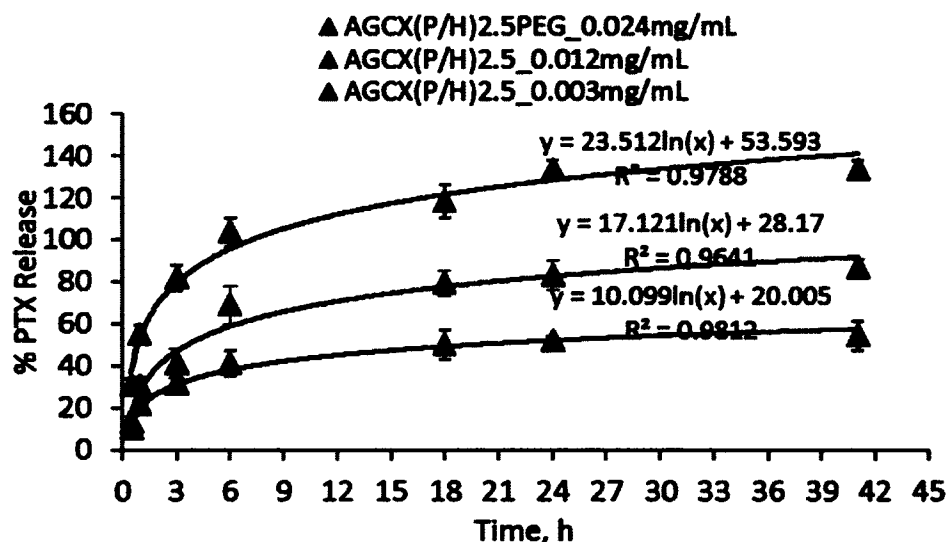
Figure 5-7: Release study of high PEGylated AGCX in PBS with 2% Tween 80, pH 7.4 at 37.5° C.

5.3.5 Cell culture studies on 4T1 breast cancer cell lines

IC_{50} concentrations strongly decreased for LbL coated and extra PEGylated AGCX cores, as compared to free PTX (Taxol). See Table 5-3.

Table 5-3: IC50 of AGCX formulation and its comparison with Free PTX (Taxol), in μg/mL and nM.

Drugs	IC_{50}, μg/mL	IC_{50}, nM
Taxol	0.846	991.05
AGCX_2.5	0.189	221.07
AGCX_2.5_mPEG	0.131	152.85

The values were obtained from the cytotoxicity experiment on 4T1 breast cancer cells. LbL coating improved the cytotoxicity ~4.5 times having an IC_{50} of 221 nM, while

that of Taxol was found to be 991 nM. Cytotoxicity improved slightly after extra

PEGylation with mPEG-SVA on the LbL coating, reducing the IC_{50} to 153 nM. The IC_{50}

values are calculated from the cytotoxicity results shown in Figure B.1-2, Appendix B.

5.3.6   *In vivo* mice studies

The results in Figure 5-8 are analyzed taking only those mice into consideration,

which have a tumor volume in the range of 80-200 mm³ at 0 h time of study. The rest

have been excluded. Instead of standard deviation, standard error has been indicated for

each data point, where Standard Error = Standard Deviation /√n, and "n" is the number of

mice taken into consideration i.e. n = 6.
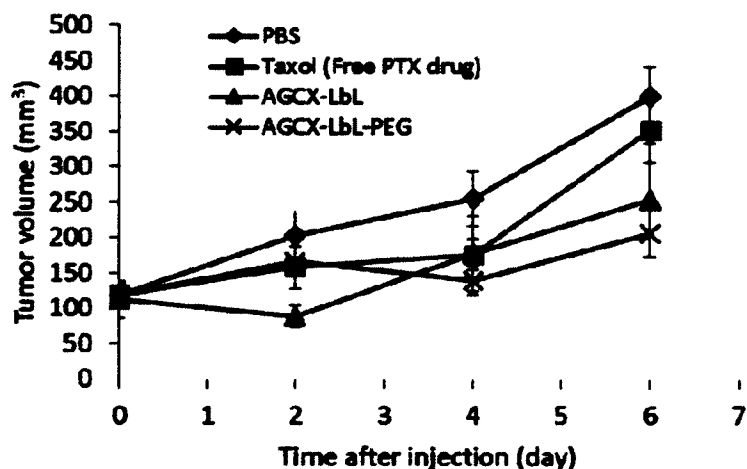
Figure 5-8: Tumor activity (mm3) study of 8 days: injected with 1) PBS as control; 2) Taxol (Free PTX drug), 3) AGCX-LbL, and 4) AGCX-LbL-PEG, on mice injected with 4T1 breast cancer cells. A study of 8 days. Standard Error (SE) values have been shown and n = 6.

The results have been shown for 3 injections, i.e. 6 days. The average tumor

volume at 0 h was 112-119 mm³. The control mice injected with PBS showed an

exponential increase in tumor volume at a rate of ~44.6 mm³/day, while for Taxol it was

~36.1 mm³/day, for AGCX-LbL ~25.7 mm³/day and for AGCX-LbL-PEG ~11.8

mm^3/day. Until 2 injections the tumor volume remains almost the same for Taxol and AGCX-LbL-PEG. After the 3rd injection, tumor volume increased steeply. After the 4th injection, some cases of toxicity led to hemorrhaging in the stomach and colon. Earlier reports have suggested that the administration of tocopherol acetate or Vitamin E may increase the risk of hemorrhaging [110], but still the correct explanation and confirmation of the data has not been found. A specific reason for the toxicity was not determined in the mentioned mice experiments due to shortage of mice for further experiments.

5.4   Conclusion

A significant improvement in the LbL process for low soluble drug encapsulation has been made. The number of process steps were reduced by: 1) coating with only 2.5 bilayers of PE to attain such a high colloidally stable formulation, 2) high PEGylated samples had no washing step just after the LbL assembly, as it was the step for CPT [12] in CHAPTER 4 and for PTX in Shutava *et al.* [11]. A significantly improved colloidally stable formulation for LbL coated samples of 121 nm and a highly PEGylated sample of 105 nm were attained even after 30 days in PBS pH 7.4. It had a high drug encapsulation capacity of 30-40% and ~6.5 times higher cytotoxicity against 4T1 breast cancer cells, with an IC$_{50}$ of 153 nM. Injection of such PTX nano formulation to mice was safe (survival mice rate was ca. 85%) and showed an improved antitumor effect in mice. Toxicity was found in some mice, the reason for which can be studied in the future to improve the formulation.

In the next chapter, the techniques of washless LbL assembly from CHAPTER 4 and assembling less layers of LbL with fewer washing steps from CHAPTER 5 are

combined, to improve the circulation time significantly, and bioavailability of nano lipid

carrier (NLC) for anticancer drug DOX.

CHAPTER 6

ENHANCED PHARMACOKINETICS AND TUMOR GROWTH INHIBITION USING A NANOSTRUCTURED LIPID CARRIER LOADED WITH DOXORUBICIN AND MODIFIED IN A LAYER-BY-LAYER POLYELECTROLYTE FORMULATION

In this chapter, a step further has been taken in the application of washless technique of LbL assembly for improving the colloidal stability by narrowing down the particle size distribution of lipid nanoparticles, such as solid nanoparticles (SLN) and nanostructured lipid carriers (NLC). The study also adopts the concept of using fewer PE layers for LbL coating, making the process shorter, simpler, and thus cheaper. Such an approach is expected to increase the circulation time in the blood, lower accumulation in the liver, and increase accumulation in tumors while improving the tumor growth inhibition effect.

This work was done in collaboration with Center for Pharmaceutical Biotechnology and Nanomedicine, Northeastern University, Boston at Dr. Torchilin's lab. The NLC-DOX core were developed, and the cytotoxicity and *in vivo* mice experiments were done at Dr. Torchilin's lab. Furthermore, the rest of the stabilization process by LbL assembly process was done at Institute for Micromanufacturing, Louisiana Tech University at Dr. Lvov's lab. A manuscript from this work has been submitted at International Journal of Pharmaceutics and is under review [25].

6.1   Introduction

Many reports have described the advantages of lipid nanoparticles such as solid lipid nanoparticles (SLN) and nanostructured lipid carriers (NLC). These nanoparticles have been widely described as promising drug delivery systems for the treatment of cancer. Previously the co-encapsulation of DOX and docosahexaenoic acid (DHA) in SLN and NLC for the enhancement of drug antitumor effects has been proposed [13, 111]. The SLN co-loaded with DOX and DHA were more cytotoxic than free drugs against the human lung A549 cancer cell line in monolayer cultures [111]. The developed NLC co-loaded with DOX and DHA were more cytotoxic against the sensitive MCF-7 breast cancer cell line and even more potent against the drug resistant MCF-7/Adr cell line than the free drugs. The higher cytotoxicity against the MCF-7/Adr was also verified in a cultured spheroid model. It was suggested that the NLC overcame drug resistance due to a bypass of the glycoprotein P bomb efflux effect [13, 112].

To further improve the anticancer effect of the NLC co-loaded with DOX and DHA and to improve the colloidal stability by narrowing the particle size distribution, the surface modification of the nanoparticles with an LbL technique involving an alternate adsorption of polycation and polyanion on a charged substrate was considered [11]. The LbL film promotes a controlled release of drug by controlling the diffusion of drug from the solid core to the external medium [12]. NLC loaded with DOX is a solid lipid core with a sufficient surface negative charge to support a LbL architecture [13, 113]. LbL polymeric films are typically uniform and sufficiently adherent to charged surfaces [11, 12].

Recently, a washless technique of polyelectrolyte adsorption has been developed

based on the addition of each shell layer in a precise amount, determined by titration, that

leads to almost complete charge reversals (+/–15 mV). This method avoids intermediate

washing after each layering and significantly reduces the process time. Additionally, the

reduction of total polyelectrolytes used lowers the cost of the whole process [11, 12]. Its

recent application in encapsulation of drugs with low solubility such as PTX [11] and

CPT [11, 12] improved their colloidal stability and cytotoxicity.

For this study, the surface of NLC co-loaded with DOX and DHA has been

modified by the LbL technique to evaluate drug release, characteristics of the

nanoparticles, cytotoxicity against human and murine cancer cell lines, and *in vivo*

biodistribution and tumor growth inhibition.

6.2 Materials and Methods

6.2.1 Materials

DOX hydrochloride was purchased from LC Laboratories (Woburn, MA).

triethanolamine (TEA), oleic acid (OA), polyvinyl pyrrolidone, 10 kDa (PVP) and the

negative polyelectrolyte (PE), heparin sulfate (HEP) were purchased from Sigma-

Aldrich. Positive PE as poly-L-lysine 16 kDa and block co-polymer-polyethylene glycol,

5 kDa (PLB16-5) were from Alamanda Polymers, Inc. Additional PEGylation was done

with methoxy polyethylene glycol 5 kDa, succinimidyl valeric acid (mPEG5kDa-SVA)

from Laysan Bio, Inc. Glyceryl behenate (Compritol 888 ATO®) was kindly provided by

Gattefossé (Rhône-Alpes, France). Monooleate of sorbitan ethoxylated (Super refinedTM

polysorbate 80; Tween TM 80) and docosahexaenoic acid (DHA) as triglyceride

(Incromega™ DHA 500TG) were kindly provided by Croda, Inc. Dulbecco's modified

eagle medium (DMEM), antibiotic stock solution (10,000 I.U. of penicillin + 10,000 µg/mL of streptomycin) and 0.25% Trypsin-EDTA were purchased from CellGro. Heat inactivated FBS was purchased from Atlanta Biologicals. Centrifugation devices used were Amicon® Ultra - 4 100 k, Millipore. The Cell Titer Blue assay kit and CytoTox 96® Non-Radioactive Cytotoxicity Assay were purchased from Promega. All other chemicals were of analytical grade.

6.2.2   Preparation of Nanostructured Lipid Carrier (NLC) of Doxorubicin

The nanostructured lipid carrier (NLC) loaded with DOX was prepared at Northeastern University. The preparation and the composition of the formulations were previously described [13]. A batch was of 5 ml of formulation. The oily phase (OP) was prepared with 100 mg of Tween 80, 10 mg of oleic acid, 5 mg of DOX, 6 mg of triethanolamine and 150 mg of matrix lipid composed of 110 mg of Compritol and 40 mg of DHA (0.4% w/v). This formulation was referred to as "NLC-DOX". The aqueous phase (AP) was composed of purified water. After preparation, the pH was adjusted to 7.0-7.5 and a final volume of 5 mL. First, the OP and the AP were heated separately to 80° C. After OP melting, the AP was added drop-wise into the OP and homogenized using a glass rod for 1 min. This emulsion was immediately subjected to intense probe sonication (8 Watts) for 5 minutes, using a high intensity ultrasonic processor (Fisher F60 Sonic Dismembrator Fisher F-6; Fisher Scientific, Pittsburgh, PA). The pH was adjusted to 7.0 with 0.1 M HCl and 0.1 M NaOH. The formulation was stored at 4° C, protected from light in a nitrogen atmosphere. The NLC-DOX cores were formulated at Northeastern University, Dept. of Pharmaceutical Science.

6.2.3   Layer-by-Layer assembly

NLC-DOX (3 mL, with approx. 1 mg/mL of DOX encapsulated) was added to a

small glass bottle. To form NLC-DOX-PVP (NDP), approximately 4 mg of PVP was

added with simultaneous sonication, for a final concentration of 1.31 mg/mL. The

sonication was continued for an additional 10 minutes to stabilize these NLC cores. Zeta

potential measurements confirmed the negative charge (−15 to −20 mV) necessary for a

proper LbL poly electrolyte (PE) assembly. The first layer assembled was with a positive

PE (~4.8 mg of PLB16-5) added to the NDP mixture under continuous sonication.

Similarly, a total of 2.5 bi-layers of alternating HEP/ PLB16-5 were assembled by adding

lower amounts of each PE, ~1.9 mg, with the final outermost layer of HEP. Each

assembled layer was sonicated for 2 to 3 min. The complete process was conducted in a

deionized (DI) water medium, maintained at pH 7.4. For an extra-PEGylated sample, a

dry powder of mPEG5kDa-SVA was added directly to the above LbL formulation with

PLB16-5 as the outermost layer. Sonication was done in cold water at 10° C to ensure a

temperature lower than the melting point of OP, i.e. 80° C [13]. The succinimidyl

valerate (SVA) group in mPEG5kDa-SVA was an N-hydroxyl succinimidyl ester group

(-NHS ester) conjugated to methoxy PEG. It readily conjugates mPEG group with excess

−NH$_2$ groups on a surface side by releasing free NHS in the medium [114]. The final

concentration of mPEG5kDa-SVA added to the dispersion was 20 mg/mL. The mixture

was sonicated for 5 min and then kept overnight for ageing [12]. The mixture was spun at

14,000 rpm (Eppendorf 5804R centrifuge) for 10 min, and the supernatant was collected;

the pellet was discarded. The NDP LbL formulation has a lipid-based core. Thus, it was

suspended in the supernatant. This supernatant, NDP(PLB16-5/HEP)2.5/mPEG was

finally termed "NLC-DOX-LBL-PEG". For just the LBL sample with no extra PEGylation, 3 bilayers of (PLB16-5/HEP) were assembled, i.e. HEP as the outermost layer was similarly washed. The obtained supernatant NDP(PLB16-5/HEP)3.0 was termed "NLC-DOX-LBL". Zeta potential was measured after each additional layer deposition to confirm complete charge reversal between -15 and +15 mV.

The formulations were further purified prior to the *in vitro* and *in vivo* studies to remove the unloaded DOX and the unattached polymers by ultrafiltration using Amicon® Ultra-4, 100 kDa MWCO centrifugal filter devices (Sigma-Aldrich). About 2 ml of formulations were added to the devices and centrifugation performed for 15 min at 5,000 rpm (Eppendorf 5804R centrifuge) and 4° C. The retantate was resuspended in a 5% glucose solution.

6.2.4   Characterization of formulation

The mean particle diameter and zeta potential were measured by dynamic light scattering (DLS) and electrophoretic mobility, respectively, using the Zeta PLUS particle size analyzer (Brookhaven Instruments; Holtsville, NY). All measurements were performed in triplicate.

The encapsulation efficiency (EE) and drug loading (DL) of DOX in NLC were determined by an ultrafiltration method using Amicon® Ultra-0.5 mL, 100 kDa MWCO centrifugal devices (Sigma-Aldrich) with the membrane passivated with a 5% aqueous solution of Tween™ 20 to eliminate DOX binding as previously described [111]. The EE and DL were calculated using the following equations:

$$EE\ (\%) = (C_T - C_{AP})/C_T\ x100. \qquad\qquad \textbf{Eq. 6-1}$$

Where C_T = total DOX concentration in NLC, C_{AP} = DOX concentration in aqueous phase (non-encapsulated).

$$DL\ (mg/g) = W_{DL}/W_{NP}. \hspace{3cm} \textbf{Eq. 6-2}$$

Here W_{DL} = mg of drug loaded in nano-particles and W_{NP} = grams of nanoparticles (lipids).

Briefly, the C_T, C_{AP} and W_{DL} were evaluated as follows. The C_T was determined by dissolving an aliquot of 200 µL the NLC dispersion in 5 mL of a mixture of tetrahydrofuran (THF)/methanol (MeOH) 4:6 v/v, centrifugation for 10 min at 2,400 × g and analysis of the supernatant by spectrophotometry at 480 nm (UV-mini 1240; Shimadzu, Japan). The C_{AP} was evaluated from an aliquot of the aqueous phase separated from the NLC dispersion by ultrafiltration (10 min at 2,400 g), dilution with THF/ MeOH and analysis by UV-visible. The WDL was derived using the calculated EE × mg total of DOX added.

6.2.5   Colloidal stability study

The colloidal stability was checked by diluting the dispersion 100 times in PBS, pH 7.4. The hydrodynamic size was measured by particle size analysis on the 1st, 7th, and 14th storage day for both LbL and PEGylated samples. The average values were from 20 readings taken on each sample to confirm the particle size distribution (PSD).

6.2.6   SEM sample preparation

The dispersion was diluted 10 times in distilled water, pH 7. A drop of each sample was allowed to dry on a clean silicon wafer at room temperature. Before SEM imaging, a 12 nm thickness of gold was sputtered at 40 mA run for 30 sec. The FE-SEM was observed at 1.5 kV to prevent burning of polymer coated samples.

6.2.7   Transmission electron microscopy

Nanoparticles were negatively stained with 1.5% uranyl acetate, and images were

taken using a JEOL TEM-1010 transmission electron microscope (JEOL USA, Inc.,

Peabody, MA) operating at an acceleration voltage of 80 kV. The images were captured

at a 20,000x magnification.

6.2.8   Release of doxorubicin from NLC

The release study was performed at Northeastern University by analysis of

dialysis in PBS, pH 7.4 [13]. Cellulose ester membrane dialysis tubing with a cutoff size

of 100 KDa (Spectrum Laboratories; Rancho Dominguez, CA) were filled with 3 mL of

formulations loaded with DOX or DOX aqueous solution (~0.5 mg/mL) diluted in the

buffer 1:2, sealed and incubated with 50 ml of the media for up to 24 h at 37° C with

continuous 250 rpm (Eppendorf 5804R centrifuge). At various time points, 1 mL of

solution was withdrawn and replaced with an equal volume of the media. The DOX

concentrations were measured by spectrofluorimetrically with a Synergy HT Multi-Mode

Microplate Reader (Biotek; Winnooski, VT) at 485/590nm ex/em wavelengths. The

values were plotted as percentage of cumulative drug release.

6.2.9   _In vivo_ studies

Cells, 4T1, purchased from The American Type Culture Collection (ATCC;

Manassas, VA) were grown and maintained in RPMI, pH 7.4, supplemented with 10%

(v/v) FBS and 1% of penicillin/streptomycin stock solution in a humidified 5% (v/v) CO2

atmosphere at 37° C.

For subcutaneous injection over the left flank region, a 100 μL suspension of

2×10^6 4T1 cells in RPMI serum free were injected in 6-8 week old BALB/c mice for

biodistribution and tumor growth inhibition studies. The time for the initial detection of a tumor was about 7 days when tumors were about 100-150 mm^3. Mice were regularly monitored and allowed for free access to food and water following an animal care protocol (13-1242 R) approved by the Northeastern University Institutional Animal Care and Use Committee in accordance with the "Principles of laboratory animal care", NIH publication no. 85-23, revised in 1985). Tumor volumes were calculated using the formula V = 0.5 (length × width^2) by caliper measurements of tumors at regular time intervals.

6.2.10   Biodistribution study

Groups of 4-5 animals bearing 4T1 tumors were injected on day +7 with a single dose equivalent of 5 mg/mL of DOX. The treatments were as follows: (1) Free DOX; (2) NLC-DOX; (3) NLC-DOX-LBL, and (4) NLC-DOX-LBL-PEG via the lateral tail vein. At 0.5, 1, 2, and 4 h post-injection, blood was collected from anesthetized mice by cardiac puncture into a heparinized (1 U) tube. The blood was centrifuged at 1000 g for 10 min at 4° C followed by collection of the upper plasma layer and storage at −80° C until use. Liver and tumors were harvested for DOX analysis. The amount of the DOX was quantified as previously described by Wang *et al.*, 2014 [115]. Briefly, weighed tissue homogenates of 10% (w/v) or 25% plasma (200 μL) were added to a mixture of 100 μL of 10% (v/v) Triton X-100, 200 μL of water, and 1.5 mL of acidified isopropanol (0.75 N). Following the extraction of DOX overnight at -20° C, samples were warmed to room temperature, vortexed for 5 min, centrifuged at 15,000 g for 20 min and stored at 80° C until analysis. DOX was quantified fluorometrically (ex/em 470/590 nm). Standard curves were prepared using tissues or plasma of mice not treated with DOX.

6.2.11   Tumor growth inhibition

The treatments of tumor-bearing mice started 7 days after 4T1 cell inoculation. The first two doses were of 2.5 mg DOX/kg every 2 days and then 3 doses of 1.25 mg DOX/kg every 2 days administered via tail vein. Each treatment group consisted of 5-6 mice. Tumor volume was estimated as $V = 0.5$ (length $\times$ width^2) every 2 days from the beginning of treatments. At +12 days after the first injection, mice were sacrificed, and tumors were excised and weighed. The control group was treated with PBS, pH 7.4.

6.3   Results and Discussion

6.3.1   Layer-by-Layer coated NLC characterization

Figure 6-1 and Table 6-1 show the hydrodynamic sizes and zeta potential of nanoparticles with each layer addition. At the first polymer addition, the average size increased from 89 nm to 127 nm, and then remained unchanged. The final average size for NLC-DOX-LBL was about 138 nm, and for NLC-DOX-LBL-PEG it was 128 nm. These samples showed a particle size distribution with a single sharp peak and a low polydispersity.

Table 6-1: Zeta potential and hydrodynamic size of NLC-DOX, NLC-DOX-LBL and NLC-DOX-LBL-PEG.

Sample	Zeta Potential, mV	Average hydrodynamic diameter, nm	Poly Dispersity	Max Peak/s, nm (%AUC)
NLC-DOX	-40 ± 2	89 ± 3	0.291	63(100%), 149(80%)
NLC-DOX-LBL	-14 ± 2	138 ± 2	0.092	115(100%)
NLC-DOX-LBL-mPEG	5 ± 3	128 ± 1	0.098	129(100%)

Figure 6-2 shows the SEM and TEM images. Both NLC-DOX-LBL and NLC-DOX-LBL-PEG samples are irregularly shaped with an average diameter of 150 nm and 100 nm, respectively. The extra-PEGylated NLC were more uniformly spherical, smaller in size and had less standard deviation. The larger, more irregular particles represent agglomerates of free, oppositely charged polyelectrolytes. The bright white halos seen in the SEM images around most structures represent an edge effect caused by a generation of secondary electrons from the curved circumferences of spherical structures [116]. The sizes appear to differ between Figure 6-1 and Figure 6-2. The measurements shown in Figure 6-1 were taken immediately after the preparation, while the SEM images reported in Figure 6-2 were taken 7 days after sample preparation.

The zeta potential of the NLC-DOX lipid core was highly negative, i.e. $\sim$ -40 mV (Table 6-1). For this reason, the initial amount of PE (PLB16-5) required to reverse surface charge (4.8 mg) was high. For subsequent layers, the amount of HEP or PLB16-5 needed was lower, (2.4 mg) for complete charge reversal. After each LbL sample was washed, surface charge changed slightly due to separation of loosely bound electrolytes. The formation of some precipitates was verified. It may have been due to interaction of free oppositely charged polymers in the solution. They were removed with the pellet during centrifugation steps.
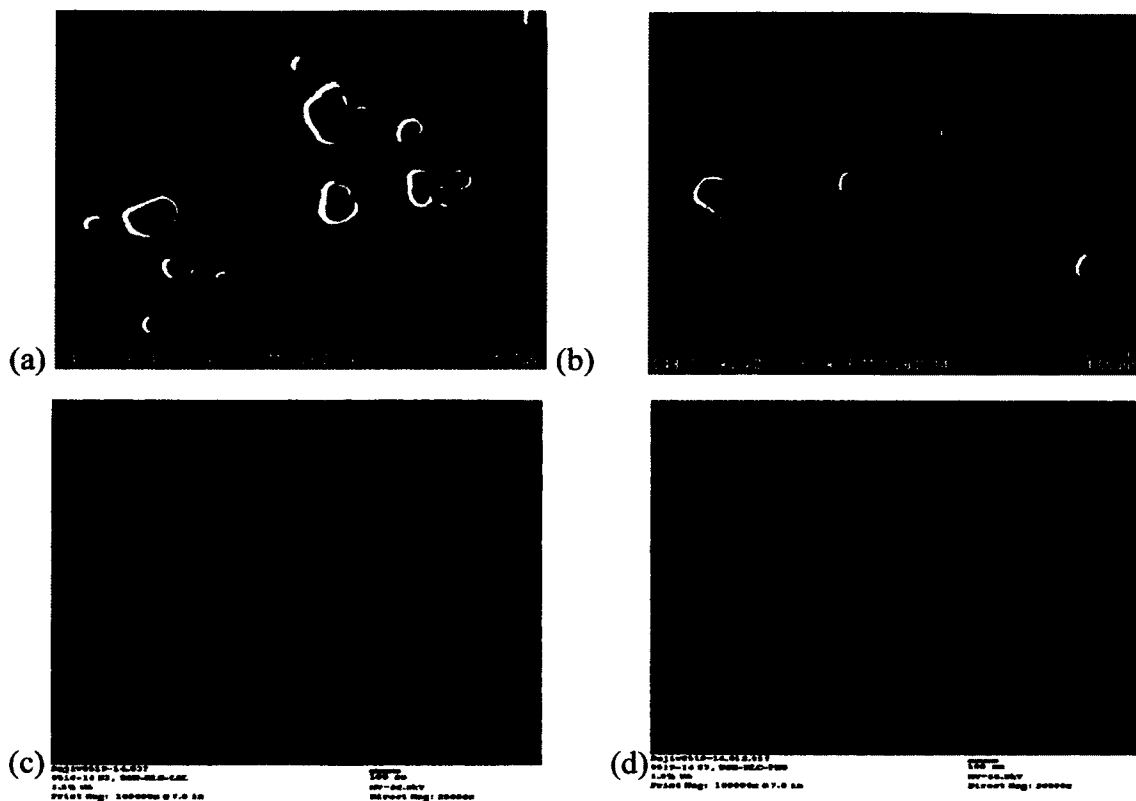
Figure 6-1: SEM and TEM images: (a) SEM of NLC-DOX-LBL (outermost layer being HEP); (b) SEM of NLC-DOX-LBL-PEG (with extra PEGylation), (c) TEM of NLC-DOX-LBL, and (d) NLC-DOX-LBL-PEG.
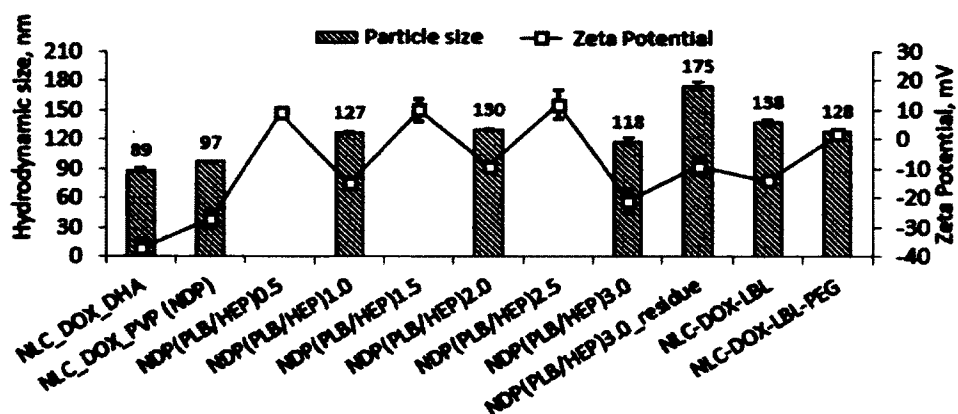
Figure 6-2: Hydrodynamic size and zeta potential along the LbL assembly process and extra PEGylation of NLC-DOX. Where, NDP(PLB16-5/HEP)2.5/mPEG is indicated as NLC-DOX-LBL-PEG and NDP(PLB16-5/HEP)3.0 as NLC-DOX-LBL.

The conjugation of mPEG-SVA to amine groups of the NDP (PLB/HEP)2.5 was

confirmed by a reduction of the zeta potential from high to low positive values, i.e. +5 to

+2 mV (See Figure 6-1). The colloidal stability of the extra PEGylated sample was better

compared to the LbL-coated NDP cores (See Figure 6-3).
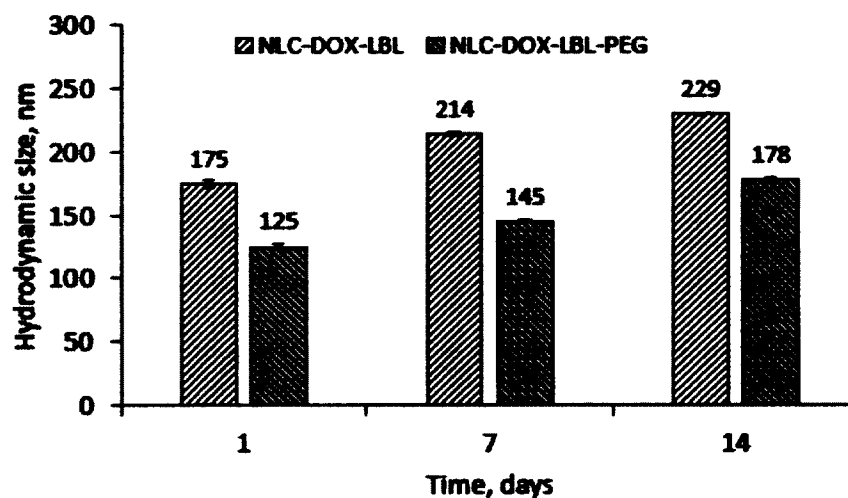
Figure 6-3: Colloidal stability of NLC-DOX-LBL and extra NLC-DOX-LBL-PEG. The maximum peak values of the PSD are indicated as in MSD summary having maximum intensity weighted size obtained from Non-negatively constrained Least Squares (NNLS) algorithm.

There was a gradual increase in the particle size distribution (PSD) values

between the 1st and 14th days of the study for both LbL-coated and extra PEGylated NDP

cores. After 14 days, LbL samples showed a bimodal PSD with a polydispersity of 0.158

and maximum peaks at 229 nm (100%) and 91 nm (38%). In the extra PEGylated

samples, the PEG tails outside the LbL assembly improved the colloidal stability due to

its steric hindrance property [12] as indicated by its narrow unimodal PSD of 178 nm

with polydispersity of 0.108 after 14 days.

6.3.2   Drug Release in PBS pH 7.4

The results of the drug release assay performed by dialysis with PBS, pH 7.4 are

included in Figure 6-4. The released DOX from NLC-DOX was 22 ± 1% in the first 30

min and increased to 35 ± 2%, 49 ± 2%, and 57 ± 4% at 1 h, 2 h, and 4 h, respectively,

following which there was no significant release for up to 24 h. In contrast, for NLC-

DOX-LBL and NLC-DOX-LBL-PEG, the release at 30 min was 10 ± 1% and 9 ± 1%,

respectively, and increased to 21 ± 1% in 1 h. The release profiles of NLC-DOX-LBL

and NLC-DOX-LBL-PEG were similar and showed improved capacity to retain the drug

compared to NLC-DOX (35 ± 2% and 37 ± 0% at 2 h, 41 ± 3% and 47 ± 1% at 4 h,

respectively). Within 2 hours, almost 90% of Free DOX had been released.
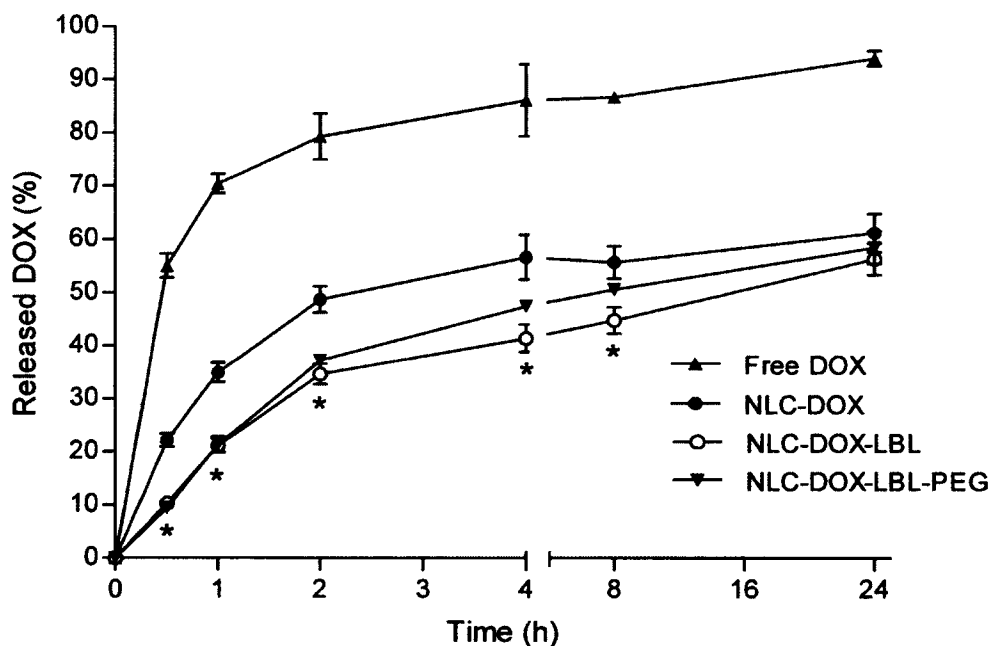
Figure 6-4: DOX release in complete PBS, pH 7.4 by dialysis using a cellulose ester
membrane (100 Kda MWCO). The released DOX measured in the media was analyzed
by fluorescence. N = 3; Mean ± SD; *P < 0.05 for the comparison of NLC-DOX-DHA-
LBL/ NLC-DOX-DHA-LBL-PEG against NLC-DOX and Free DOX. In collaboration
with Dr. V. Torchilin at Northeastern University, Boston, MA.

6.3.3   <u>Pharmacokinetic studies</u>

An evaluation of the drug concentration in plasma, liver and tumor for mice injected IV with Free DOX, NLC-DOX, NLC-DOX-LBL, and NLC-DOX-LBL-PEG are shown in Figure 6-5. The plasma concentrations of free DOX and NLC-DOX were 6.5 ± 0.9 µg/mL and 8.8 ± 1.1 µg/mL at 30 min; at 2 h, they were 3.8 ± 0.8 µg/mL and 5.3 ± 0.7 µg/mL, and at 4 h, 2.2 ± 0.5 µg/mL, and 4.4 ± 0.5 µg/mL, respectively. NLC-DOX-LBL and NLC-DOX-LBL-PEG retained a higher plasma DOX concentration over the 4 h period at 10.4 ± 0.6 µg/mL and 12.5 ± 0.5 µg/mL at 30 min, at 8.6 ± 0.6 µg/mL and $11.5 \pm 1\%$ at 2 h, and 5.6 ± 0.1 µg/mL and 8.7 ± 0.7 µg/mL by 4 h, respectively (Figure 6-5a). The formulations with the LbL polymers attached (NLC-DOX-LBL and NLC-DOX-LBL-PEG) showed longer longevity in the blood for DOX compared to free drug and the plain NLC-DOX formulation. Similar results were seen for solid lipid nanoparticles loaded only with DOX and modified with Layer-by-Layer, but using different polymers [113]. The percent of injected dose in plasma over this time period is consistent with the relatively greater retention of DOX for the NLC-DOX-LBL and NLC-DOX-LBL-PEG over Free DOX and NLC-DOX (Figure 6-5b).

Figure 6-5c shows the level of accumulation of DOX in the liver and its decline over a 4 h period. It remained highest for the NLC-DOX treatment. NLC-DOX-LBL and NLC-DOX-LBL-PEG treatments resulted in lower accumulation than NLC-DOX and Free DOX. At 4 h the levels were 0.132 ± 0.01 µg/g, 0.510 ± 0.02 µg/g, $0.177 \pm 0,03$ µg/g, and 0.228 ± 0.06 µg/g for Free DOX, NLC-DOX, NLC-DOX-LBL and NLC-DOX-LBL-PEG, respectively. The lower accumulation in the liver of LbL formulations may have been associated with the generally low level of toxicity observed, while the

associated higher concentration of DOX in tumors enhanced the antitumor effects. In

addition to the higher retention of the drug by these formulations, another factor to

consider is related to the fact that the attached polymers are hydrophilic and may have

protected these nanoparticles from the mononuclear phagocytic system [13] (Torchilin,

2006).
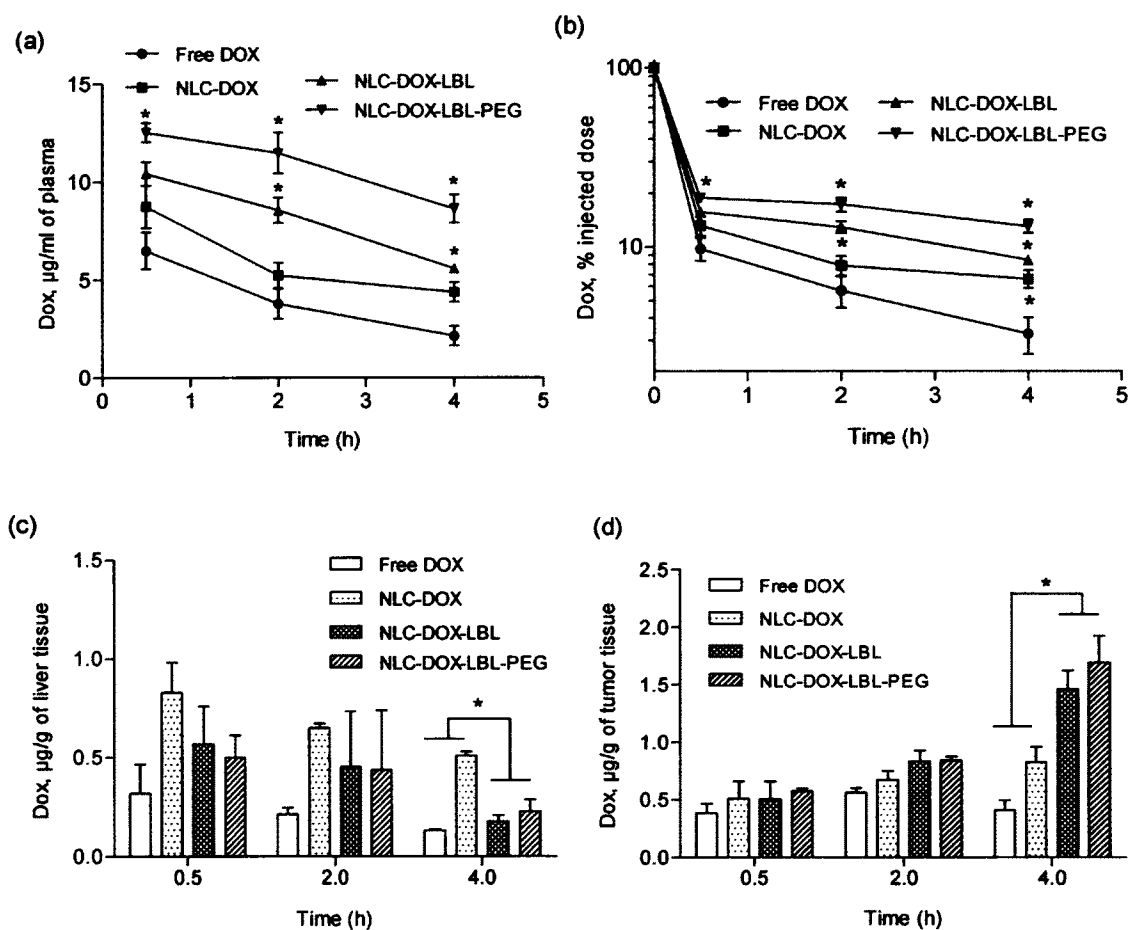
Figure 6-5: Evaluation of DOX concentration in plasma (a, b), liver (c) and tumor (d) after administration of Free DOX, NLC-DOX, NLC-DOX-LBL and NLC-DOX-LBL-PEG. The time point for collection of samples were 30 min, 2 h and 4 h. N = 4-5; Mean ± SD; *P < 0.05. In collaboration with Dr. V. Torchilin at Northeastern University, Boston, MA.

Figure 6-5d represents the accumulation of DOX formulations in mouse tumors. At 30 min after administration, there was no difference of drug concentration in tumors among the groups. However, by 2 h, NLC-DOX-LBL-PEG was higher in concentration compared to Free DOX. At 4 h, the concentrations in tumors for all NLC-DOX treatments was clearly greater than for Free DOX. Additionally, LbL-containing formulations were approximately double that of the NLC-DOX levels ($p < 0.05$). No difference was observed between NLC-DOX-LBL and NLC-DOX-LBL-PEG.

6.3.4   Tumor growth inhibition

The evaluation of the effect of treatment on tumor volumes in mice is outlined in Figure 6-6a. At the end of the treatment (day 12), the relative tumor volumes were 10.7 ± 3.4 mm^3, 8.3 ± 2 mm^3, 6.5 ± 1 mm^3, 3.6 ± 0.3 mm^3, and 2.9 ± 0.1 mm^3 for vehicle controls, Free DOX, NLC-DOX, NLC-DOX-LBL and NLC-DOX-LBL-PEG, respectively. The more efficient treatments for inhibition of tumor growth contained NLC-DOX-LBL-PEG, which was most apparent by day 12. Plain NLC-DOX were somewhat more effective than Free DOX. The NLC-DOXs formulated with LbL clearly ($p < 0.05$) inhibited the tumor's growth.

Figure 6-6b shows the tumor weights after excision at day +12. The tumors of mice treated with NLC-DOX-LBL and NLC-DOX-LBL-PEG had a consistently lower weight. There was no tumor weight difference among vehicle controls, free DOX and NLC-DOX, and little effect of DOX. These results were consistent with the tumor volume data.
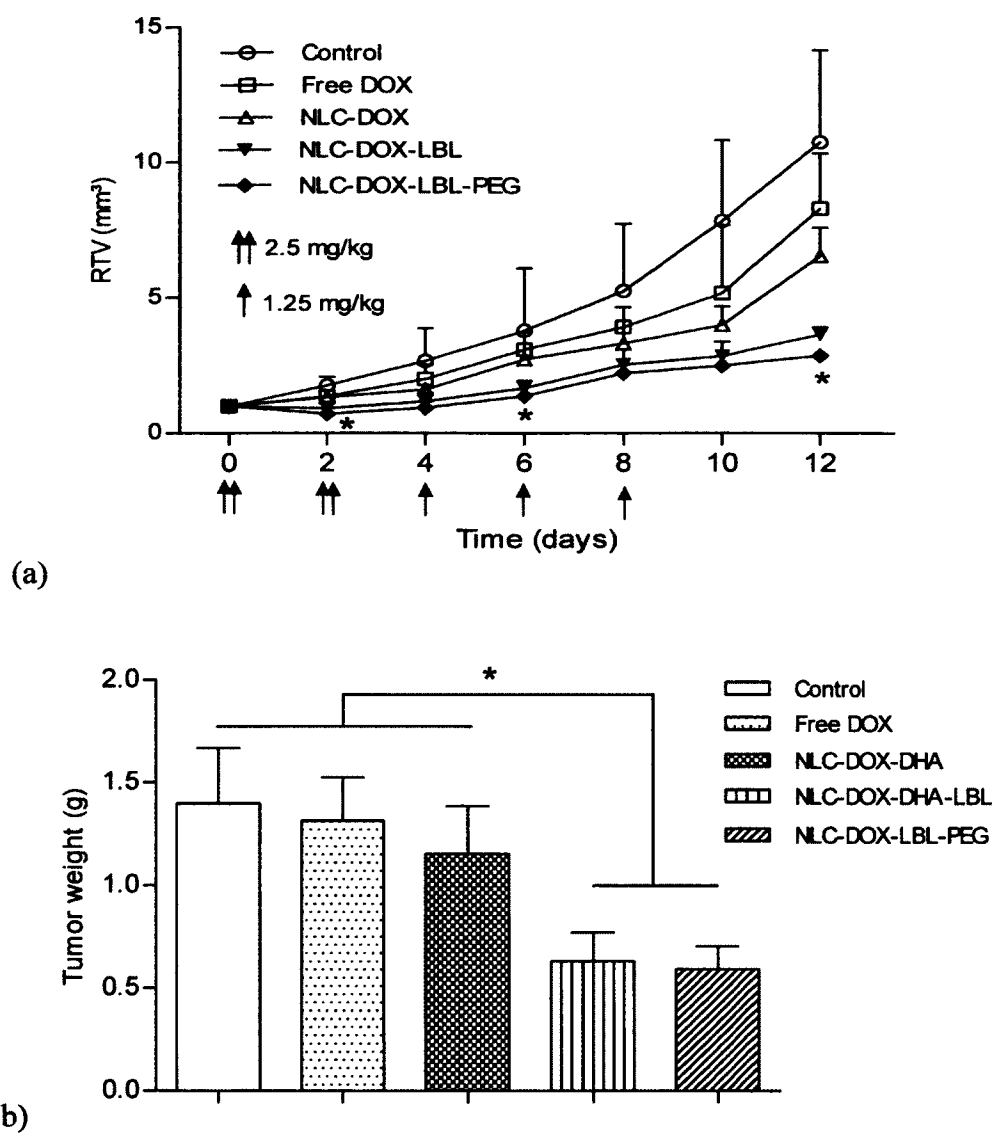
Figure 6-6: (a) Evaluation of the relative tumor volume and (b) tumor weight excised at day 12. The mice were inoculated with 4T1 cells and treated with Saline (Control), Free DOX, NLC-DOX, NLC-DOX-LBL or NLC-DOX-LBL-PEG. N= 5-6. Average ± SD. One way ANOVA was used considering day by day. The post test was Newman-Keuls. In collaboration with Dr. V. Torchilin at Northeastern University, Boston, MA.

6.3.5 Mice evaluation

Mice were monitored for significant signs of toxicity using observations of behavior and body weight changes. Figure 6-7 describes the variation of the mouse's weight from day 0 baseline over the 12-day treatment period. The control group

maintained a consistent increase in body weight of almost a gram. With the exception of

the NLC-DOX-LBL-PEG, which had an initial weight loss followed by a late recovery,

the DOX-treated groups had only small weight fluctuations.
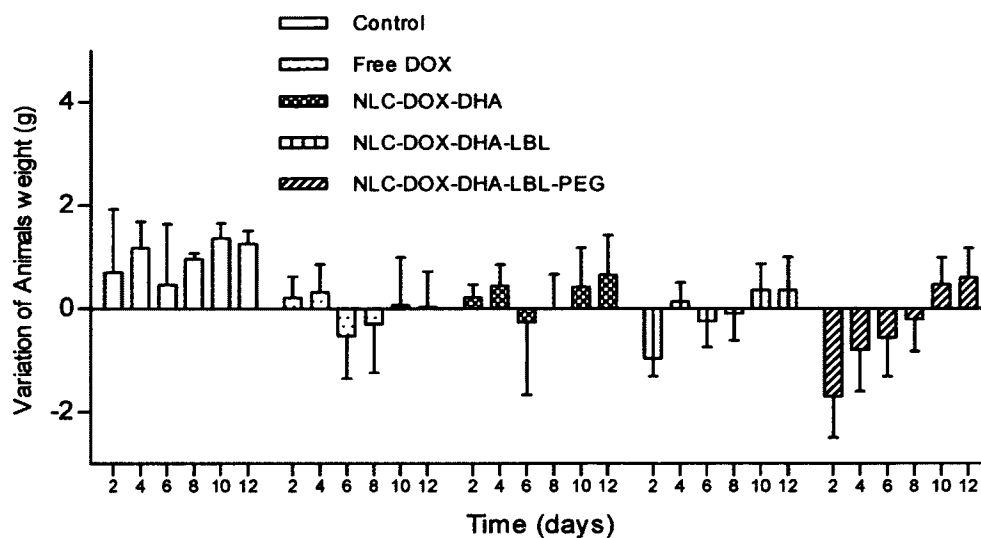
Figure 6-7: Variations of the mice weight according to the treatment. N = 3 to 6. Average ± SD. One way ANOVA with Newman-Keuls post test. In collaboration with Dr. V. Torchilin at Northeastern University, Boston, MA.

6.4   Conclusion

Our proposed core shell nanostructured lipid carrier (NLC) loaded with DOX and

DHA and modified with LBL show the size, zeta potential, and stability characteristics

needed for a controlled release after parental administration. The NLC-DOX-LBL and

NLC-DOX-LBL-PEG had a better size distribution of 128±2 nm, with a polydispersity of

0.098, a more sustained DOX release, improved pharmacokinetics, a higher plasma

concentration of DOX in LbL and PEG samples approximately 2.5 and 3.0 times

respectively against NLC-DOX samples. It showed approximately 2.9 and 2.2 lower

accumulation in the liver for LbL and PEG samples respectively as compared to NLC-

DOX samples. Simultaneously, it showed approximately 1.5 and 1.75 higher accumulation in tumors for LbL and PEG samples, respectively, as compared to NLC-DOX samples, and an enhanced effect on tumor growth inhibition. Thus, the attachment of LbL to the surface of NLC loaded with DOX represents a potential improvement in anticancer therapy. The steps in the process of LbL coating can be reduced by optimizing conditions with the exact amount of polyelectrolyte needed per layer so that multiple layers can be assembled with fewer steps more rapidly and efficiently.

In conclusion, the concepts of: 1) washless LbL for encapsulation of nanocores, as learned in CHAPTER 4, and 2) reduction of the number of PE layers (e.g. 2.5 bilayers on nano lipid cores) have been applied to achieve a narrow particle size distribution with high colloidal stability of 100-120 nm hydrodynamic size.

CHAPTER 7

CONCLUSION AND FUTURE WORK

7.1   Conclusion

1)   An essential step forward has been taken in the application of LbL self-assembly

for effective 100-170 nm encapsulation of low soluble anticancer drugs with a loading of

40-60 wt. % in various forms of nano-cores: meso-crystalline drug soft cores,

nanomiceller carriers, and nanostructured lipid cores incorporating low soluble drugs.

LbL polymer assembly acts as an adjustable interface between the drug loaded matrix

core and the external environment of the blood. It provides a colloidal stability of nano

structures in a dispersion. It acted as an effective modality to functionalize the outermost

surface with long tails of poly ethylene glycol (PEG) for longer circulation, and

monoclonal antibodies. It thus proves a basis for targeted delivery of low soluble drugs,

with prolonged circulation in serum and improved biodistribution to the targeted organ.

All the polymers used are biocompatible substances that are FDA approved which was

another challenge as compared with earlier developed LbL encapsulation technique based

on synthetic polyelectrolytes.

2)   LbL assembly technique was for the first time used for encapsulation of low

soluble drug under two-step of pH, from pH 3 to 7.2. It is performed specifically to

preserve the active form of an anticancer drug, CPT, i.e. lactone form. Employment of

washless LbL assembly technique and optimization of PE architecture helped to attain a

high drug loading capacity of 78 w %, retained the active form of CPT by 99 % lactone fraction. The PEG tails modified surface further provided the high protein resistance, decreased the initial burst of drug release and prolonged the overall release time in the serum for more than 4 h. By preserving the active lactone form, it simultaneously improved the cytotoxicity against glioblastoma cell lines, *CRL2303*, three-fold.

3)   Concepts learned from CPT LbL formulation have been well applied for encapsulating a nano miceller PTX core. The milestones achieved were: reducing the number of process steps, attaining high colloidal stability of ~100 nm for 30 days, high drug loading capacity of 30-40%, an approximate 6.5 times higher cyctotoxicity than free drug, an improved injectable for delivery into mice model (tumor injected) with a survival rate ca. 85% and finally showing a significantly improved antitumor effect. Mice experiments were performed in collaboration with Northeastern University, Department of Pharmaceutical Science.

4)   Finally, the above concepts were applied to improve the anticancer therapy of nanostructured lipid carrier (NLC) loaded with DOX and DHA. This was the first time that LbL technique has been merged with lipid carrier-based drug delivery. It was experimentally shown that LbL assembly improved the colloidal stability by narrowing the particle size distribution of 128±2 nm with a polydispersity of 0.098. The LbL and high PEGylated NLC-DOX cores proved to have approximate 1.5 times improved capacity to preserve the antitumor effect, compared to NLC-DOX. An improved biodistribution by 1.5 and 1.75 times higher accumulation in the tumors was observed for LbL and high PEGylated samples, respectively.

7.2   Future Work

Washless LbL assembly has been well explored for the encapsulation of low soluble drug in different forms of nano cores. From these approaches, it has been learned that it acts as a good encapsulating agent and a cage like structure for different carriers; maintaining the colloidal stability as low as 100 nm for weeks is successful in keeping the chemical form of the drug along with its function (in this case the anticancer activity). Pharmacokinetic improvement in systemic delivery of the drug as injectable has been shown to some extent.

Still more pathological study for the toxicity issues has to be studied, as was observed in the case of PTX LbL nanomicelles. This work will help us understand the cause for survival rate of ca. 85%. It will guide us in the right direction to improve the formulation.

A new approach can be developed to form a dual drug delivery system by assembling a nanoencapsulation of a Drug I (e.g. nanomicelle of Lapatinib), <100 nm, on top of a larger nanoparticle of Drug II (e.g. LbL formulation of CPT), ~ 160 nm. It will be important to develop a way to analyze both drugs separately. Such electrostatic bound drug cores will be a novel way to deliver multiple drugs at the same time.

Furthermore, washless LbL technique with fewer PE assembly layers has brought a milestone in simplifying the tedious process of LbL assembly technique. It can be used for large scale processing of coating microbial agents for application in food industries. The administration of low soluble protein or protein derivatives (e.g. whey proteins, insoluble amino acids – leucine, isoleucine) supplements for oral administration are in the form of drinkable shakes (suspensions) and dry powder (by spray drying).

APPENDIX A

LAYER-BY-LAYER NANOENCAPSULATION OF CAMPTOTHECIN WITH IMPROVED ACTIVITY
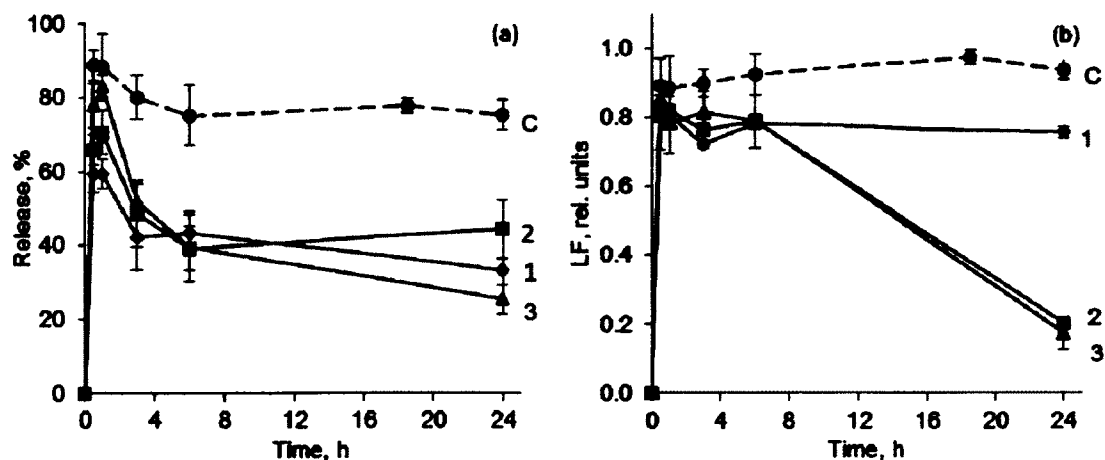
Figure A-1: Release profiles of CPT from (Hep/PLB16-5)5 nanocapsules in FBS (1) and lactone fraction retained in the released medium (2) as a function of time. C(CPT), µg/mL: 1- 6.7, 2- 4.5, 3- 2.27 µg/ml. C- free CPT (control), 6.7 µg/mL.

Table A-1: QCM estimation of BSA loss from the core of CPT formulation.

Sample description	Steps	pH	ΔF, Hz	ΔR, Ω	$\Delta R/\Delta F$, Ω/Hz	*Δm, µg/cm^2
[CPT(HEP/PLB16-5)$_{3.5}$]$^{pH3.0}$/[(PLB16-5/HEP)$_{4.0}$/mPEG]$^{pH7.2}$	PLL/HEP	3	-41.25	0.667	0.016	0.729
	pH change from 3 to 7.2	7.2	49	9	-0.184	-0.866
[CPT(HEP/PLB16-5)$_{4.0}$]$^{pH3.0}$/[(PLB16-5/HEP)$_{3.5}$/mPEG]$^{pH7.2}$	PLL/HEP	3	-40.325	0.127	0.003	0.712
	pH change from 3 to 7.2	7.2	-35	2.67	0.076	0.618

* $\Delta m = -(\Delta F/56.6)$
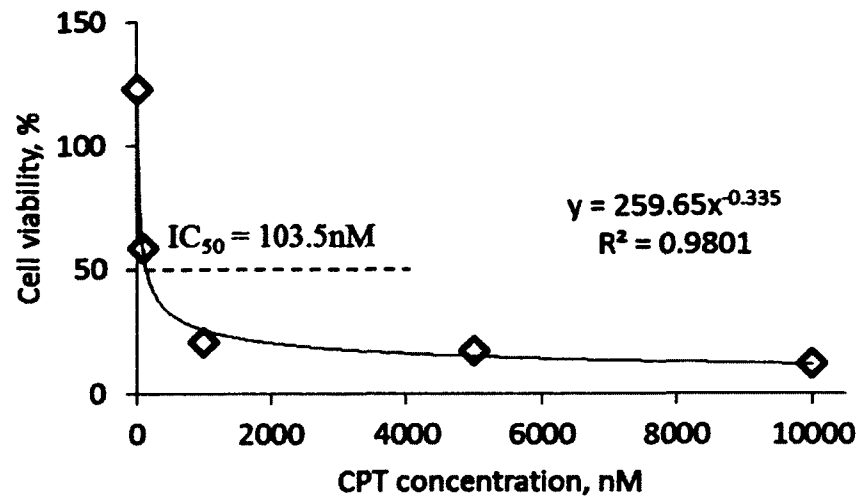
Figure A-2: % Cell viability vs CPT concentration in extra PEGylated nanocapsules treatments; IC50 is indicated.

APPENDIX B

APPLICATION OF LAYER-BY-LAYER ASSEMBLY FOR NANOMICELLAR CARRIER OF LOW SOLUBLE ANTICANCER DRUG WITH IMPROVED COLLOIDAL STABILITY AND BIOAVAILIBILITY

B.1 Nanomicellar LbL based Paclitaxel formulation

Table B.1-1: Variation of composition of formulation during optimization of PTX loaded nanomicelle LbL. Best formulation is highlighted. # AGCX12 is the optimized formulation and is indicated as AGCX.

Sample	C(AOT) mg/mL	C(TFCS) mg/mL	C(PTX) mg/mL	AOT/ PTX	TFCS/ PTX	TFCS/ AOT	(Total NI+I*Surf)/ PTX	Avg. PE**/ layer per PTX
AGCX1	1.589	0.992	0.397	3.5	2.5	0.714	6	6.048
AGCX3	0.992	1.191	0.397	2.5	3	1.2	5.5	5.473
AGCX4	0.992	1.191	0.341	2.91	3.488	1.2	6.395	7.033
AGCX5	0.794	1.191	0.262	3.030	4.545	1.5	7.576	9.164
AGCX6	0.992	0.397	0.262	3.788	1.515	0.4	5.303	9.164
AGCX61	0.992	0.397	0.262	3.788	1.515	0.4	5.303	9.164
AGCX7	0.794	0.595	0.262	3.030	2.273	0.75	5.303	10.309
AGCX8	0.794	0.794	0.341	2.326	2.326	1	4.651	8.791
AGCX9	0.794	0.992	0.341	2.326	2.907	1.25	5.233	8.791
AGCX10	2.341	2.936	1.007	2.325	2.916	1.25	5.240	2.979
AGCX11	3.75	1.504	0.991	3.783	1.517	0.40	5.299	5.934
AGCX12#	3.75	1.51	1.255	3	1.200	0.401	4.200	5.205
AGCX13	3.75	1.504	2.016	1.861	0.746	0.401	2.607	2.173

* NI- Non Ionic, I- Ionic; **PE- Polyelectrolyte (HEP or PLB16-5)
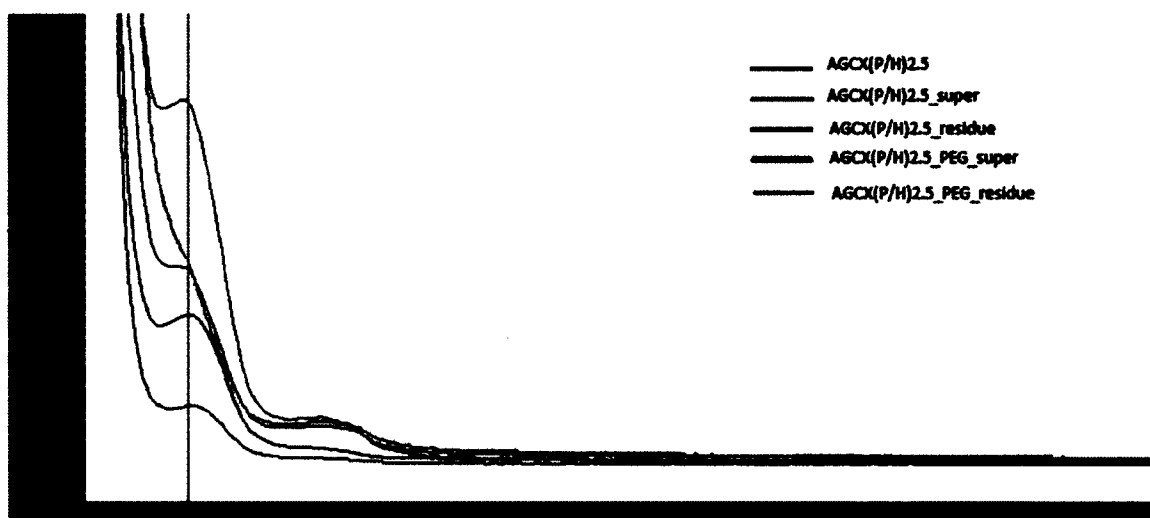
Figure B.1-1: UV visible spectra of AGCX-LbL (indicated as AGCX(P/H)2.5_super).
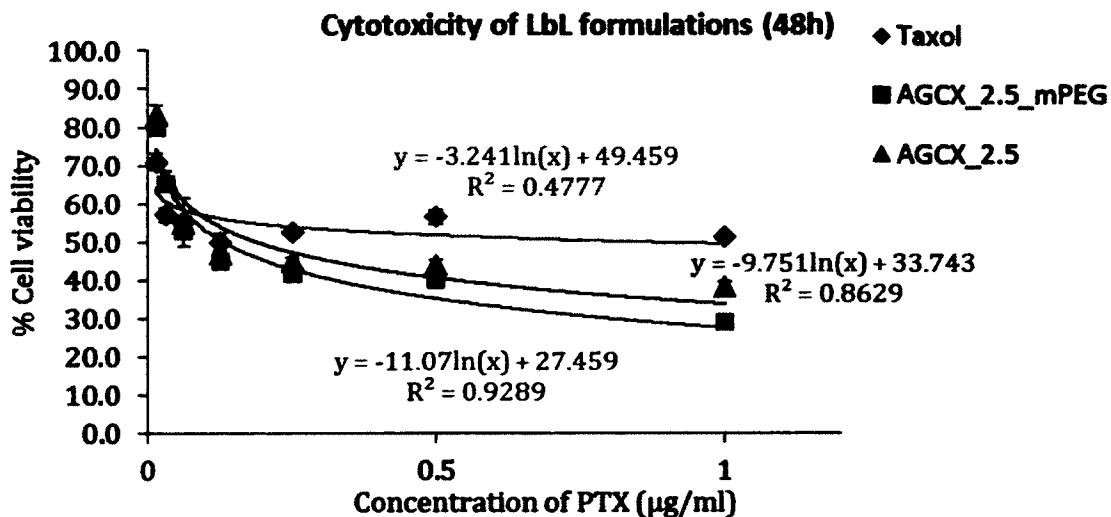
Figure B.1-2: Cytotoxicity results in 4T1 breast cancer cell lines, 4000 cells/well.

B.2   Nanomicellar LbL based Lapatinib formulation

B.2.1   Formulation preparation

First, TPGS was dissolved in CHCl3. It was then dried under N2 gas till all the

CHCl3 disappears and a thin film of TPGS is formed. PVP in separate container was

dissolved in 2.5 mL of PBS, 80 mg/mL, 50 µL (approximately 1.43 mg/mL of total 2.5

mL sample), followed by sonication for 2 min. This mixture was added to the dried

TPGS film. It was sonicated for 3 min to make a final concentration of approximately

1.78 mg/mL. Next, Lapatinib (Ltb) drug in DMSO, 7 mg/mL, 200 µL (DMSO)

(approximately 0.5 mg/mL of total 2.5 mL sample) was added to the above mixture and

sonicated for an additional 15 min. This nano-miceller core is mentioned as PGL. After

that, alternating 2.5 bilayers of PLB16-5 and Dextran Sulfate, DS were assembled, with

PLB16-5 as the outermost layer; 500 µL of this dispersion was extra PEGylated with

mPEG-SVA (5 kDa) followed by 1 min of sonication (final mPEG-SVA concentration

being 20 mg/mL). The samples were washed and the supernatant was recovered since the

color of the supernatant was yellowish (same as the drug). The % Lapatinib encapsulation

was measured by using calibration curve in the presence of the same concentration of

TPGS in Ethanol, 0.0864 mg/mL; extinction coefficient 20.241 $cm^{-1}mg^{-1}$ mL or

$18732.34M^{-1}cm^{-1}$ at 333 nm.

Table B.2-1: Lapatinib formulation core composition.

	PVP	TPGS	Ltb	Ratio, mg/mg	
Final concentration, mg/mL	1.43	1.78	0.5	**PVP/Ltb**	**TPGS/Ltb**
				2.86	3.57
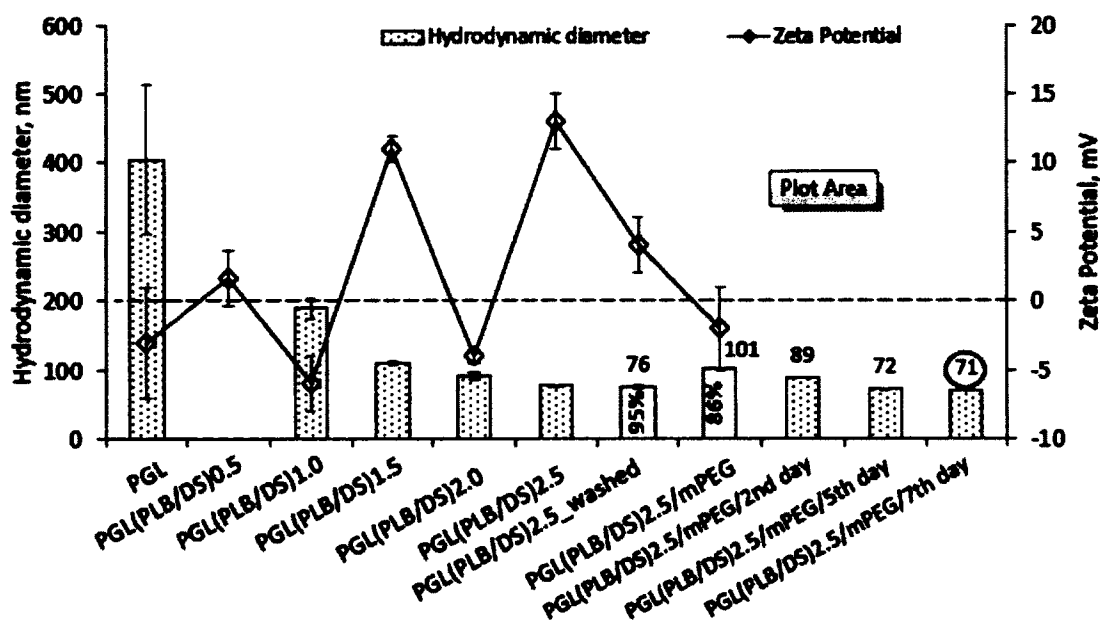
Figure B.2-1: Zeta potential and hydrodynamic diameter along the formulation process. The Ltb % encapsulation is indicated inside the column bars for washed samples of PGL(PLB/DS)2.5 and PGL(PLB/DS)2.5/mPEG.

B.2.2   HPLC results

The calibration curve of Lapatinib was run in the mobile phase of Acetyl nitrile / Methanol 50:50 v/v, absorbance observed at 232 nm, with a solvent flow rate of 1

mL/min. The Lapatinib solution was dissolved in methanol. In the presence of polyelectrolytes and polyethylene glycol (PEG) tails, the retention time of Lapatinib had shifted. This complicated the analysis of the Lapatinib concentration after LbL assembly and extra PEGylation.
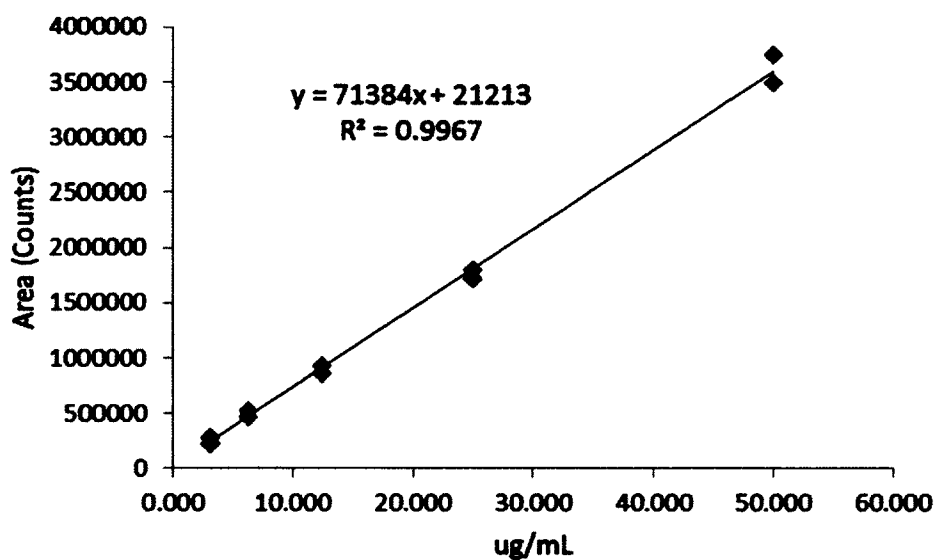
Figure B.2-2: Calibration curve of Lapatinib in HPLC (Agilent 1100).
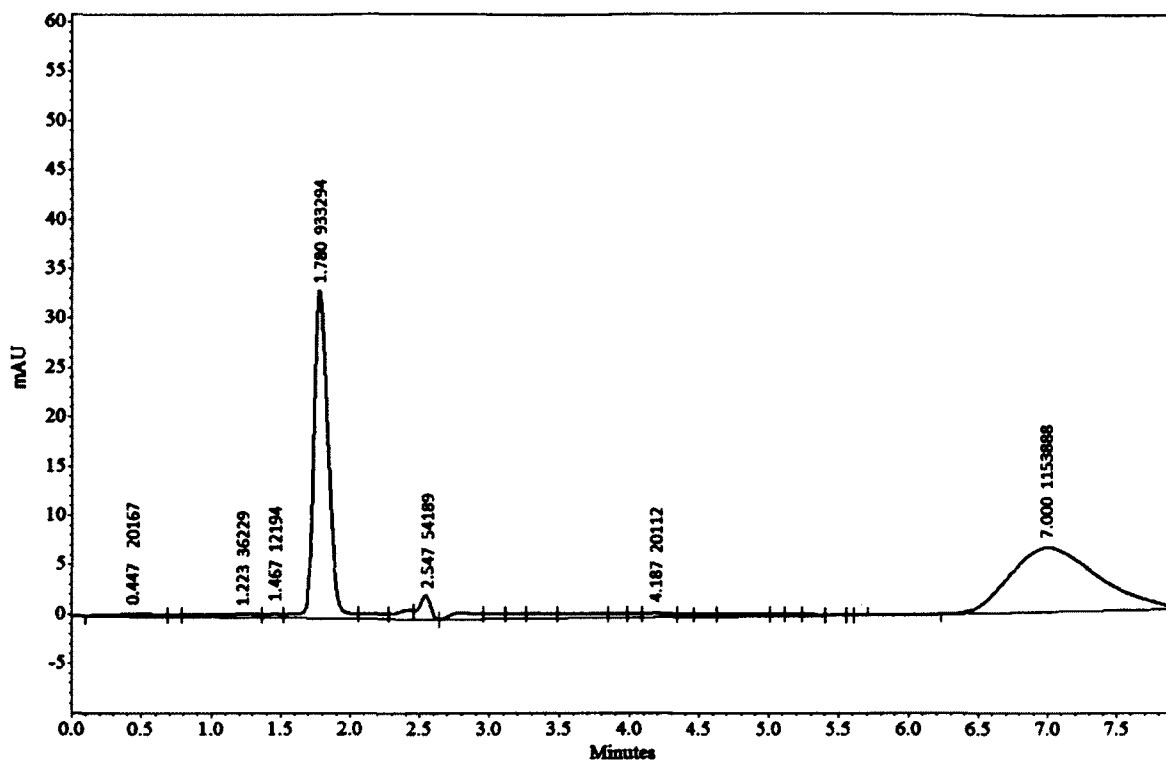
(a)
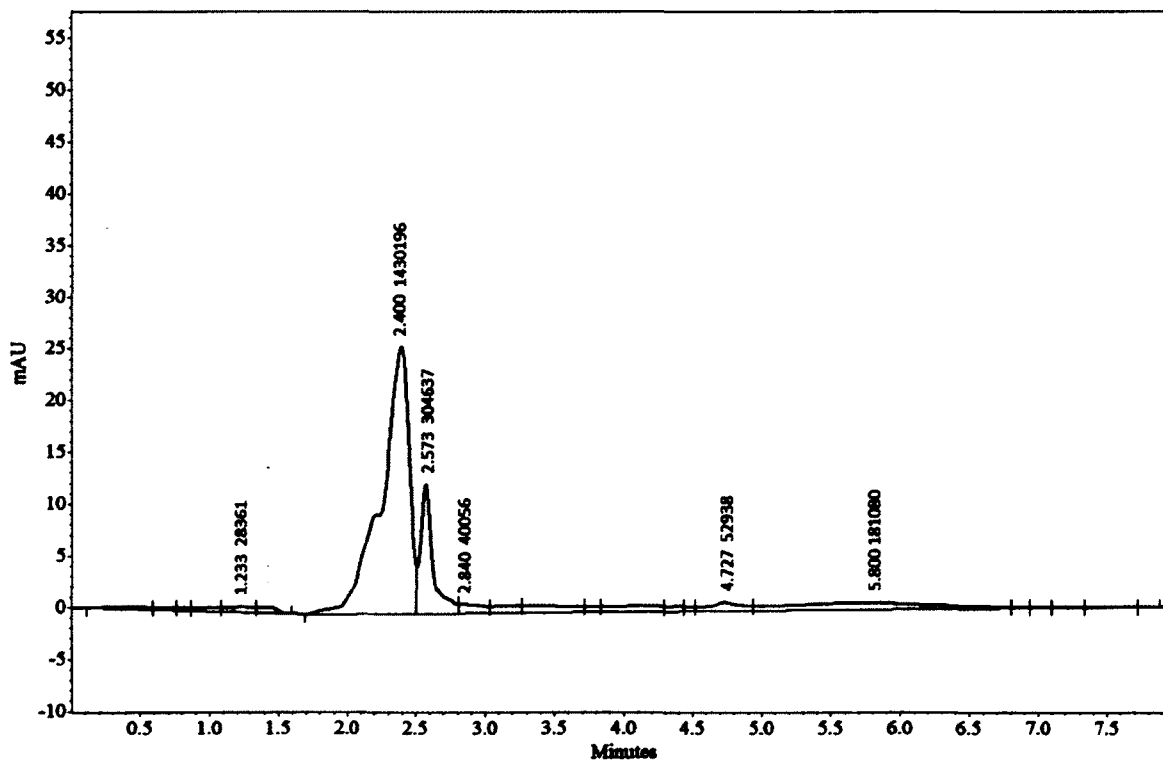
(b)
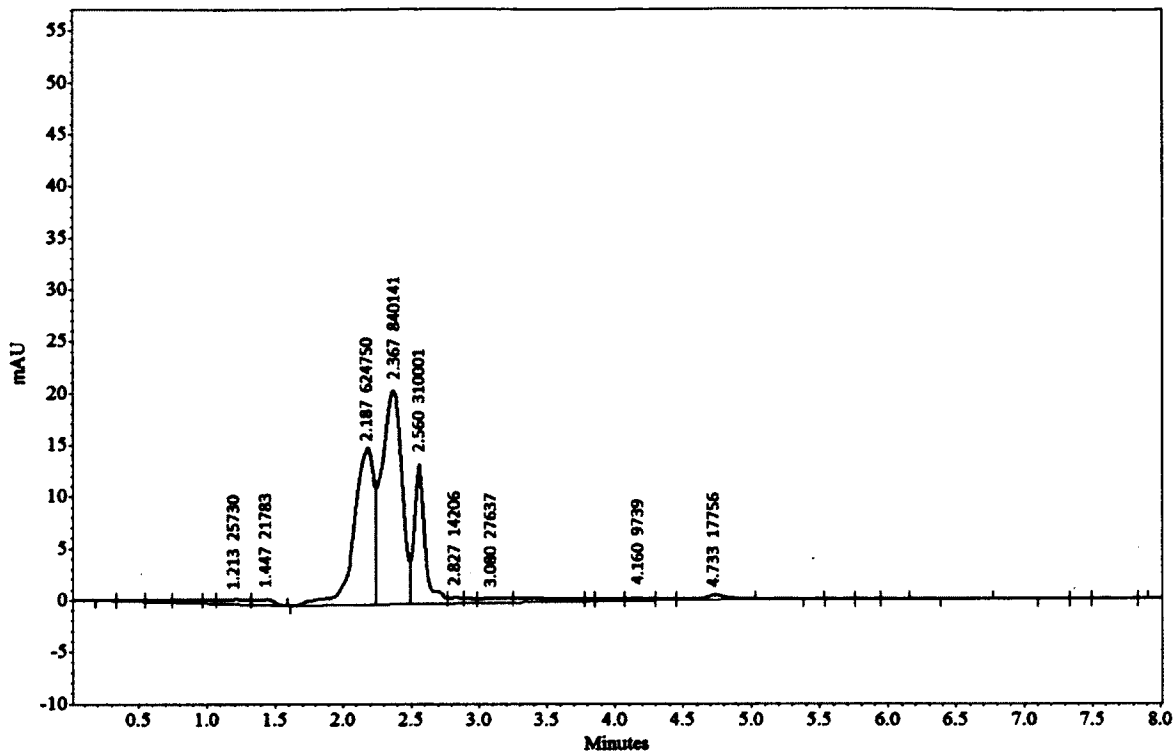
(c)

Figure B.2-3: Chromatograms of: (a) Lapatinib 25 ug/mL, (b) LbL samples (Low PEGylated), (c) PEGylated samples (High PEGylated) in mobile phase Acetyl Nitrile/Water 40/60.

REFERENCES

[1]   M. M. DeVilliers, D. P. Otto, S. J. Strydom, and Y. M. Lvov, "Introduction to nanocoatings produced by Layer-by-Layer (LbL) self-assembly," *Advanced Drug Delivery Reviews*, vol. 63, no. 9, pp. 701–715, 2011.

[2]   K. Ariga, Y. M. Lvov, K. Kawakami, Q. Ji, and J. P. Hill, "Layer-by-Layer self-assembled shells for drug delivery," *Advanced Drug Delivery Reviews*, vol. 63, pp. 762–771, 2011.

[3]   B. M. Wohl, and J. F. J. Engbersen, "Responsive Layer-by-Layer materials for drug delivery," *Journal of Controlled Release*, vol. 158, pp. 2–14, 2012.

[4]   J. Lee, J. Y. Choi, and C. H. Park, "Characteristics of polymers enabling nanocomminution of water-insoluble drugs," *Int. J. Pharm.*, vol. 355, no. 1-2, pp. 328-326, 2008.

[5]   H. Chen, C. Khemtong, X. Yang, X. Chang, and J. Gao, "Nanonization strategies for poorly water-soluble drugs," *Drug Discov. Today*, vol. 16, pp. 354-360, 2010.

[6]   Z. Zheng., X. Zhang, D. Carbo, C. Clark, C. A. Nathan and Y. Lvov, "Sonication-assisted synthesis of polyelectrolyte-coated curcumin nanoparticles," *Langmuir*, vol. 26, no. 11, pp. 7679–7681, 2010.

[7]   A. Agarwal, Y. Lvov, R. Sawant, and V. Torchilin, "Stable nanocolloids of poorly soluble drugs with high drug content prepared using the combination of sonication and Layer-by-Layer technology," *Journal of Controlled Release*, vol. 128, pp. 255–260, 2008.

[8]   D. Vergara, C. Bellomo, X. Zhang, V. Vergaro, A. Tinelli, V. Lorusso, R. Rinaldi, Y. M. Lvov, S. Leporatti, and M. Maffia, "Lapatinib/Paclitaxel polyelectrolyte nanocapsules for overcoming multidrug resistance in ovarian cancer," *Nanomedicine: Nanotechnology, Biology, and Medicine*, vol. 8, pp. 891-899, 2012.

[9]   V. Vergaro, F. Scarlino, C. Bellomo, R. Rinaldi, D. Vergara, M. Maffia, F. Baldassarre, G. Giannelli, X. Zhang, Y. M. Lvov, and S. Leporatti, "Drug-loaded polyelectrolyte microcapsules for sustained targeting of cancer cells," *Advanced Drug Delivery Reviews*, vol. 63, no. 9, pp. 847–864, 2011.

[10] Y. M. Lvov, P. Pattekari, X. Zhang, and V. Torchilin, "Converting poorly soluble materials into stable aqueous nanocolloids," *Langmuir*, vol. 27, no. 3, pp. 1212–1217, 2011.

[11] T. G. Shutava, P. P. Pattekari, K. A. Arapov, V. P. Torchilin, and Y. M. Lvov, "Architectural Layer-by-Layer assembly of drug nanocapsules with PEGylated polyelectrolytes," *Soft Matter*, vol. 8, no. 36, pp. 9418–9427, 2012.

[12] G. Parekh, P. Pattekari, C. Joshi, T. Shutava, M. DeCoster, T. Levchenko, V. Torchilin, and Y. Lvov, "Layer-by-Layer nanoencapsulation of camptothecin with improved activity," *International Journal of Pharmaceutics*, vol. 465, no. 1-2, pp. 218–227, 2014.

[13] S. V. Mussi, R. Sawant, F. Perche, M. C. Oliveira, R. B. Azevedo, L. A. Ferreira, and V. P. Torchilin, "Novel nanostructured lipid carrier co-loaded with doxorubicin and docosahexaenoic acid demonstrates enhanced *in vitro* activity and overcomes drug resistance in MCF-7/Adr cells," *Pharmaceutical Research*, vol. 31, no. 8, pp. 1882-1892, 2014.

[14] Y. Lvov, T. Shutava, K. Arapov, V. Torchilin, and M. DeVilliers, "Micro and nano Layer-by-Layer drug encapsulation with polyelectrolytes: progress and challenges," *Pharma Focus Asia*, vol. 15, pp. 28-32, 2011.

[15] C. O. Rangel-Yagui, A. Pessoa-Jr, and L. C. Tavares, "Micellar solubilization of drugs," *J. Pharm. Pharmaceut. Sci.*, vol. 8, no. 2, pp. 147-163, 2005.

[16] A. Hua, "Layer-by-Layer capsules for magnetic resonance imaging and drug delivery," *Advanced Drug Delivery Reviews*, vol. 63, no. 9, pp. 772-788, 2011.

[17] S. Schwarz, J. E. Wong, J. Bornemann, M. Hodenius, U. Himmelreich, W. Richtering, M. Hoehn, M. Zenke, and T. Hieronymus, "Polyelectrolyte coating of iron oxide nanoparticles for MRI-based cell tracking," *Nanomedicine: Nanotechnology, Biology, and Medicine*, vol. 8, pp. 682-691, 2012.

[18] B. Mu, W. Zhong, Y. Dong, P. C. Du, and P. Liu, "Encapsulation of drug microparticles with self-assembled Fe3O4/alginate hybrid multilayers for targeted controlled release," *J. Biomed. Mater. Res. B: Appl. Biomater.*, vol. 100, no. 3, pp. 825–831, 2012.

[19] G. Bantchev, Z. Lu, and Y. Lvov, "Layer-by-Layer nanoshell assembly on colloids through simplified washless process," *J. Nanosci. Nanotechnol.*, vol. 9, pp. 396-403, 2009.

[20]   Y. Lvov, P. Pattekari, and T. Shutava, "Making Aqueous Nanocolloids from Low Soluble Materials: LbL Shells on Nanocores," Ch.14 in book: "Multilayer Thin Films: Sequential Assembly of Nanocomposite Materials," Eds. G. Decher, J. Schlenoff, Wiley-VCH, NY, London. 2012 in press

[21]   O. Tsuneo, and S. Mitsuhiro, "Absorption of Polyelectrolytes on Colloidal Surfaces as Studied by Electrophoretic and Dynamic Light-Scattering Techniques," *Journal of Colloid and Interface Science*, vol. 213, no. 2, pp. 565–571, 1999.

[22]   N. Laugel, C. Betscha, M. Winterhalter, J. C. Voegel, P. Schaaf, and V. Ball, "Relationship between the growth regime of polyelectrolyte multilayers and the polyanion/polycation complexation enthalpy," *J. Physical Chemistry B*, vol. 110, no. 39, pp. 19443-19449, 2006.

[23]   C. C. Buron, C. Filiâtre, F. Membrey, C. Bainier, L. Buisson, D. Charraut, A. Foissy, "Thin Solid Films: Surface morphology and thickness of a multilayer film composed of strong and weak polyelectrolytes: Effect of the number of adsorbed layers, concentration and type of salts," *Thin Solid Films*, vol. 517, no. 8, pp. 2611–2617, 2009.

[24]   S. Hirsjärvi, Y. Qiao, A. Royere, J. Bibette, and J. P. Benoit, "Layer-by-Layer surface modification of lipid nanocapsules," *European Journal of Pharmaceutics and Biopharmaceutics*, vol. 76, no. 2, pp. 200–207, 2010.

[25]   S. V. Mussi, G. Parekh, P. Pattekari, T. Levchenko, Y. Lvov, L. A. M. Ferreira, and V. P. Torchilin, "Improved pharmacokinetics and enhanced tumor growth inhibition using a nanostructured lipid carrier loaded with doxorubicin and modified by the Layer-by-Layer polyelectrolyte coating," *International Journal of Pharmaceutics*, Manuscript submitted on April 2015 and under review

[26]   O. C. Farokhzad, J. M. Karp, and R. Langer, "Nanoparticle-aptamer bioconjugates for cancer targeting," *Expert Opin. Drug Delivery*, vol. 3, no. 3, pp. 311-324, 2006.

[27]   A. G. Cuenca, H. Jiang, S. N. Hochwald, M. Delano, W. G. Cance, and S. R. Grobmyer, "Emerging implications of nanotechnology on cancer diagnostics and therapeutics," *Cancer*, vol. 107, no. 3, pp. 459-466, 2006.

[28]   G. Schneider, and G. Decher, "From functional core/shell nanoparticles prepared via Layer-by-Layer deposition to empty nanospheres," *Nano Letters*, vol. 4, no. 10, pp. 1833–1839, 2004.

[29]   Y. Li, J. Xia, P. L. Dubin, "Complex formation between polyelectrolytes and oppositely charged mixed micelles: static and dynamic light scattering. Study of the effect of polyelectrolyte molecular weight and concentration," *Macromolecules*, vol. 11, pp. 2486-2492, 1994.

[30] C. C. Buron, C. Filiâtre, F. Membrey, C. Bainier, L. Buisson, D. Charraut, and A. Foissy, "Surface morphology and thickness of a multilayer film composed of strong and weak polyelectrolytes: Effect of the number of adsorbed layers, concentration and type of salts," *Thin Solid Films*, vol. 517, no. 8, pp. 2611–2617, 2009.

[31] P. Chodanowski, and S. Stoll, "Polyelectrolyte adsorption on charged particles: ionic concentration and particle size effects—a Monte Carlo approach," *J. Chem. Phys.*, vol. 115, pp. 4951, 2001.

[32] Z. S. Haidar, "Bio-Inspired/-Functional Colloidal Core-Shell Polymeric-Based NanoSystems: Technology Promise in Tissue Engineering, Bioimaging and NanoMedicine," *Polymers*, vol. 2, no. 3, pp. 323-352, 2010.

[33] S. W. Morton, K. P. Herlihy, K. E. Shopsowitz, Z. J. Deng, K. S. Chu, C.J. Bowerman, J. M. DeSimone, and P. T. Hammond, "Scalable Manufacture of Built-to-Order Nanomedicine: Spray-Assisted Layer-by-Layer Functionalization of PRINT Nanoparticles," *Advanced Materials*, vol. 25, no. 34, pp. 4707–4713, 2013.

[34] E. M. Shchukina, and D. G. Shchukin, "LbL coated microcapsules for delivering lipid-based drugs," *J. Advanced Drug Delivery Reviews*, vol. 63, pp. 837-846, 2011.

[35] B. De Geest, G. Sukhorukov, and H. Möhwald, "The pros and cons of polyelectrolyte capsules in drug delivery," *Expert Opin. Drug Deliv.*, vol. 6, pp. 613–624, 2009.

[36] T. Boudou, P. Kharkar, J. Jing, R. Guillot, I. Paintrand, R. Auzely-Velty and C. Picart, "Polyelectrolyte multilayer nanoshells with hydrophobic nanodomains for delivery of Paclitaxel," *J. Control Release*, vol. 159, no. 3, pp. 403-412, 2012.

[37] D. Vergara, C. Bellomo, X. Zhang, V. Vergaro, A. Tinelli, V. Lorusso, Ross Rinaldi, Y. M. Lvov, S. Leporatti, and M. Maffia, " Lapatinib/Paclitaxel polyelectrolyte nanocapsules for overcoming multidrug resistance in ovarian cancer," *Nanomedicine: Nanotechnology, Biology, and Medicine*, vol. 8, pp. 891-899, 2012.

[38] L. Nilsson, and B. Bergenstahl, "Adsorption of Hydrophobically Modified Starch at Oil/Water Interfaces during Emulsification," *J. Colloid Interface Sci.*, vol. 308, pp. 508-513, 2007.

[39] D. Guzey, and D. McClements, "Formation, stability and properties of multilayer emulsions for application in the food industry," *Adv. Colloid Interface Sci.*, vol. 128, pp. 227-248, 2006.

[40]   K. Szczepanowicz, H. J. Hoel, L. Szyk-Warszynska, E. Bielanska, A. M. Bouzga, G. Gaudernack, C. Simon and P. Warszynski, "Formation of Biocompatible Nanocapsules with Emulsion Core and Pegylated Shell by Polyelectrolyte Multilayer Adsorption," *Langmuir*, vol. 26, pp. 12592-12597, 2010.

[41]   V. Torchilin, "Multifuctional nanocarriers," *Adv. Drug Delivery Rev.*, vol. 58, pp. 1532-1555, 2006.

[42]   A. Domb, Y. Tabata, M. R. Kumar, and S. Farber, "Nanoparticles for Pharmaceutical Applications," *American Scientific*, Publishers: Stevenson Ranch, CA, pp. 5-158, 2007.

[43]   S. De Koker, B. G. De Geest, C. Cuvelier, L. Ferdinande,W. Deckers, W. E. Hennink, S. C. De Smedt and N. Mertens, "In Vivo Cellular Uptake, Degradation and Biocompatibility of Polyelectrolyte Microcapsules," *Adv. Funct. Mater.*, vol. 17, pp. 3754–3763, 2007.

[44]   T. Shutava, S. Balkundi, P. Vangala, P. O'Neal, J. Steffan, R. Bigelow, J. Cardelli, and Y. Lvov, " Layer-by-Layer-Coated Gelatin Nanoparticles as a Vehicle for Delivery of Natural Polyphenols," *ACS Nano*, vol. 3, 1877-1885, 2009.

[45]   L. Zhang, F. X. Gu, J. M. Chan, A. Z. Wang, R. S. Langer, and O. C. Farokhzad, "Nanoparticles in Medicine: Therapeutic Applications and Developments," *Clin. Pharmaco. and Ther.*, vol. 83, pp. 761-769, 2008.

[46]   K. Ariga, J. P. Hill, and Q. Ji, "Layer-by-Layer Assembly as a Versatile Bottom-Up Nanofabrication Technique for Exploratory Research and Realistic Application," *Phys. Chem. Chem. Phys.*, vol. 9, pp. 2319-2340, 2007.

[47]   K. Ariga, J.P. Hill, M. V. Lee, A. Vinu, R. Charvet, and S. Acharya, "Challenges and breakthroughs in recent research on self-assembly," *Sci. Technol. Adv. Mater.*, vol. 9, pp. 1-96, 2008.

[48]   C., S. Kobierski, R. Mauludin, and R. Muller, "Second generation of drug nanocrystals for delivery of poorly soluble drugs: smartCrystal technology," *Dosis*, vol. 2, pp. 124-128, 2008.

[49]   I. Parikh, and U. Selvaraj, "Composition and method of preparing microparticles of water-insoluble substances," *US Pat.*, 5922355, 1999; R. H. Muller, C. Jacobs and O. Kayser, in *Pharmaceutical Emulsions and Suspensions. Drugs and the Pharmaceutical Sciences*, vol. 105; ed. F. Nielloud and G. Marti-Mestres, Marcel Dekker, pp. 383, 2000.

[50]   V. P. Torchilin, "Micellar nanocarriers: Pharmaceutical perspective," *Pharmaceutical Research*, vol. 24, no. 1, pp. 1-16, 2006.

[51] S. Khapli, J. R. Kim, J. K. Montclare, R. Levicky, M. Porfiri, and S. Sofou, "Frozen cyclohexane in water emulsion as a sacrificial template for the synthesis of multilayered polyelectrolyte microcapsules," *Langmuir*, vol. 25, no. 17, pp. 9728–9733, 2009.

[52] N. Larsona, and H. Ghandehari, "Polymeric conjugates for drug delivery," *Chem. Mater.*, vol. 24, no. 5, pp. 840-853, 2012.

[53] C. Lipinski, "Poor aqueous solubility - An industry wide problem in drug discovery," *Am. Pharm. Rev.*, vol. 5, no. 3, pp. 82–85, 2002.

[54] F. Caruso, "Nanoengineering of particle surfaces," *Adv. Materials*, vol. 13, pp. 11-23, 2001.

[55] X. Qiu, S. Leporatti, E. Donath, and H. Möhwald, "Studies on the Drug Release Properties of Polysaccharide Multilayers Encapsulated Ibuprofen Microparticles," *Langmuir*, vol. 17, pp. 5375-5380, 2001.

[56] Y. Lvov, A. Antipov, A. Mamedov, H. Möhwald, and G Sukhorukov, "Urease Encapsulation in Nanoorganized Microshells," *Nano Letters*, vol. 1, pp. 125-128, 2001.

[57] G. Sukhorukov, "Multilayer Hollow Microspheres," in *Dendtrimers*, R. Arshady, and A. Guyot, (Eds.), MML Series, Citrus Books, New York, vol. 5, pp. 111-147, 2002.

[58] H. Chen, C. Khemtong, X. Yang, X. Chang, and J. Gao, "Nanonization strategies for poorly water-soluble drugs," *Drug Discovery Today*, vol. 16, no. 7-8, pp. 354-360, 2011.

[59] I. Erel-Unal, and S. A. Sukhishvili, "Hydrogen-bonded hybrid multilayers: film architecture controls release of macromolecules," *Macromolecules*, vol. 41, pp. 8737–8744, 2008.

[60] A. G. Skirtach, A. Muñoz Javier, O. Kreft, K. Köhler, A. Piera Alberola, H. Möhwald,W. J. Parak, and G. B. Sukhorukov, "Laser-induced release of encapsulated materials inside living cells," *Angew. Chem. Int. Ed.*, vol. 45, pp. 4612–4617, 2006.

[61] Z. Zhu, and S. A. Sukhishvili, "Temperature-induced swelling and small molecule release with hydrogen- bonded multilayers of block copolymer micelles," *ACS Nano*, vol. 3, pp. 3595–3605, 2009.

[62] Z. S. Haidar, M. Tabrizian, and R. C. Hamdy, "A hybrid rhOP-1 delivery system enhances new bone regeneration and consolidation in a rabbit model of distraction osteogenesis," *Growth Factors*, vol. 28, pp. 44–55, 2010.

[63] Z. S. Haidar, R. C. Hamdy, and M. Tabrizian, "Biocompatibility and safety of a hybrid core-shell nanoparticulate OP-1 delivery system intramuscularly administered in rats," *Biomaterials*, vol. 31, pp. 2746–2754, 2010.

[64] Z. S. Haidar, F. Azari, R. C. Hamdy, and M. Tabrizian, "Modulated release of OP-1 and enhanced preosteoblast differentiation using a core-shell nanoparticulate system," *J. Biomed. Mater. Res. A*, vol. 91, pp. 919–928, 2009.

[65] G. L. Amidon, H. Lennernas, V. P. Shah, and J. R. Crison, "A theoretical basis for a biopharmaceutic drug classification: the correlation of *in vitro* drug product dissolution and in vivo bioavailability," *Pharm. Res.*, vol. 12, no. 3, pp. 413–420, 1995.

[66] D. O. Grigoriev, T. Bukreeva, H. Möhwald, and D. G. Shchukin, "New method for fabrication of loaded micro- and nanocontainers: emulsion encapsulation by polyelectrolyte Lb-L deposition on the liquid core," *Langmuir*, vol. 24, pp. 999–1004, 2008.

[67] S. Leporatti, A. Voigt, R. Mitlöhner, G. Sukhorukov, E. Donath, and H. Möhwald, "Scanning force microscopy invertigation of polyelectrolyte nano- and microcapsule wall texture," *Langmuir*, vol. 16, pp. 4059–4063, 2000.

[68] Y. Han, D. Radziuk, D.G. Shchukin, and H. Möhwald, "Stability and size dependence of protein microspheres prepared by ultrasonication," *J. Mater. Chem.*, vol. 18, pp. 5162–5166, 2008.

[69] N. Pargaonkar, Y. Lvov, N. Li, J. Steenekamp, and M. de Villiers, "Controlled Release of Dexamethasone from Microcapsules Produced by Polyelectrolyte Layer-by-Layer Nanoassembly." *Pharmaceutical Res.*, vol. 22, pp. 826-835, 2005.

[70] K. S. Suslick, "Sonochemistry," *Science*, vol. 247, pp. 1439-1445, 1990.

[71] K. S. Suslick, R. E. Cline Jr., and D. A. Hammerton, "The Sonochemical Hot Spot," *J. Am. Chem. Soc.*, vol. 108, 5641-5642, 1986.

[72] K. S. Suslick, E. B. Flint, M. W. Grinstaff, and K. A. Kemper, "Sonoluminescence from Metal Carbonyls," *J. Phys. Chem.*, vol. 97, 3098-3099, 1993.

[73] B. Borkent, S. Gekle, A. Prosperetti, and D. Lohse, "Nucleation threshold and deactivation mechanisms of nanoscopic cavitation nuclei," *Phys. Fluids*, vol. 21, no. 102003, pp. 1-8, 2009.

[74] E. Dibbern, F. Toublan, and K. Suslick, "Formation and Characterization of Polyglutamate Core–Shell Microspheres," *J. Am. Chem. Soc.*, vol. 128, 6540-6541, 2006.

[75]   H. M. Santos, C. Lodeiro, and J. L. Capelo-Martinez, "The power of ultrasound," in *Chemistry: analytical applications*, J. L. Capelo-Martinez, KGaA, Weinheim, Germany: Wiley-VCH Verlag GmbH and Co., 2009, pp. 1-16.

[76]   G. B. Sukhorukov, E. Donath, S. Davis, H. Lichtenfeld, F. Caruso, V. I. Popov, and H. Möhwald, "Stepwise polyelectrolyte assembly on particle surfaces: a novel approach to colloid design," *Polym. Adv. Technol.*, vol. 9, no. 10–11, pp. 759–67, 1998.

[77]   D. J. McClements, "Theoretical analysis of factors affecting formation and stability of multilayered colloidal dispersions," *Langmuir*, vol. 21, pp. 9777–9785, 2005.

[78]   T. Shutava, P. Pattekari, G. Parekh, and Y. Lvov, "Improving efficiency of Layer-by-Layer coating on nanosized particles with non-washing assembly technique," in *Physics, Chemistry and Applications of Nanostructures: Reviews of Short Notes to Nanomeeting-2013, World Scientific*, 2013, pp. 267-270.

[79]   J. Rashba-Step, T. Scott, R. Darvari, Y. Lvov, and T. Shutava, "Surface-modified microparticles and method of forming the same," US Patent 20060260777, Nov.23, 2006.

[80]   K. W. Mattison, P. L. Dubin, and I. J. Brittain, "Complex formation between bovine serum albumin and strong polyelectrolytes: effect of polymer charge density," *J. Phys. Chem. B*, vol. 102, pp. 3830–3836, 1998.

[81]   T. Tsuzuki, "Commercial scale production of inorganic nanoparticles," *Int. J. Nanotechnol.*, vol. 6, no. 5/6, pp. 567-578, 2009.

[82]   T. Sivasankar, and B. Kumar, "Role of nanoparticles in drug delivery system," *Int. J. Res. Pharm. Biomed. Sci.*, vol. 1, no. 2, pp. 41-66, 2010.

[83]   M. Kahlweit, "Ostwald ripening of precipitates," *Adv. Colloid Interface Sci.*, vol. 5, pp. 1-35, 1975.

[84]   S. Kim, J. Y. Kim, K. M. Huh, G. Acharya, and K. Park, "Hydrotropic polymer micelles containing acrylic acid moieties for oral delivery of paclitaxel," *J. Control. Release*, vol. 132, no. 2, pp. 222-229, 2008.

[85]   Y. W. Cho, J. Lee, S. C. Lee, K. M. Huh, and K. Park, "Hydrotropic agents for study of *in vitro* paclitaxel release from polymeric micelles," *J. Control. Release*, vol. 97, no. 2, pp. 249–257, 2004.

[86]   X. H. Wei, Y. P. Nui, Y. Y. Xu, Y. Z. Du, F. Q. Hu, and H. Yuan, "Salicylic acid-grafted chitosan oligosaccharide nanoparticle for paclitaxel delivery," *J. Bioact. Compat. Polym.*, vol. 25, no. 3, pp. 319-335, 2010.

[87]   Y. Lvov, "Electrostatic Layer-by-Layer assembly of proteins and polyions," in *Protein Architecture: Interfacial Molecular Assembly and Immobilization Biotechnology*, Lvov, Y., Möhwald, H. (Eds.), Marcel Dekker Publ., New York, 2000, pp. 1–394.

[88]   A. V. Vertegel, R. W. Siegel, and J. S. Dordick, "Silica nanoparticle size influences the structure and enzymatic activity of absorbed lysozyme," *Langmuir*, vol. 20, no. 16, pp. 6800-2807, 2004.

[89]   A. Hatefi, and B. Amsden, "Biodegradable injectable in situ forming drug delivery systems," *J. of Controlled Release*, vol. 80, no. 1-3, pp. 9-28, 2002.

[90]   P. A. McCarron, W. M. Marouf, D. J. Quinn, F. Fay, R. E. Burden, S. A. Olwill, and C. J. Scott, "Antibody targeting of camptothecin-loaded PLGA nanoparticles to tumor cells," *Bioconj. Chem.*, vol. 19, no. 8, pp. 1561–1569, August, 2008.

[91]   N. Sanna, G. Chillemi, L. Gontrani, A. Grandi, G. Mancini, S. Castelli, G. Zagotto, C. Zazza, V. Barone, and A. Desideri, "UV–vis spectra of the anticancer camptothecin family drugs in aqueous solution: specific spectroscopic signatures unraveled by a combined computational and experimental study," *J. Phys. Chem. B*, vol. 113, no. 16, pp. 5369-5375, March, 2009.

[92]   C. Dora, M. Alvarez-Silva, A. Trentin, T. de Faria, D. Fernandes, R. da Costa, M. Stimamiglio, and E. Lemos-Senna, "Evaluation of antimetastatic activity and systemic toxicity of camptothecin-loaded microspheres in mice injected with B16-F10 melanoma cells," *J. Pharm. Pharm. Sci.*, vol. 9, no. 1, pp. 22-31, 2006.

[93]   F. Hausheer, K. Haridas, D. Murali, and D. Reddy, "Formulations and compositions of poorly water soluble camptothecin derivatives," US Pat. 5726181A, March, 1998.

[94]   QCM 200, "Quartz Crystal Microbalance Digital Controller Operation and Service Manual, " *Revision 2.1, Stanford Research Systems Inc.*, pp. 106, 2005.

[95]   K. Marx, "Quartz crystal microbalance: A useful tool for studying thin polymer films and complex biomolecular systems at the solution-surface interface," *Biomacromolecules*, vol. 4, no. 5, pp. 1099-1120, 2003.

[96]   J. Voros, "The density and refractive index of adsorbing protein layers", *Biophys. J.*, vol. 87, no. 1, pp. 553-561, 2004.

[97]   S. Alarifi, D. Ali, A. Verma, S. Alakhtani, and B. A. Ali, "Cytotoxicity and genotoxicity of copper oxide nanoparticles in human skin keratinocytes cells," *Int. J. Toxicity*, vol. 32, no. 4, pp. 296–307, 2013.

[98] F. Bulcke, K. Thiel, and R. Dringen, "Uptake and toxicity of copper oxide nanoparticles in cultured primary brain astrocytes," *Nanotoxicology*, vol. 8, no. 7, pp. 775-785, November, 2014.

[99] C. Joshi, B. Karumuri, J. J. Newman, and M. A. DeCoster, "Cell morphological changes combined with biochemical assays for assessment of apoptosis and apoptosis reversal," in *Current Microscopy Contributions to Advances in Science and Technology*, Mendez-Vilas, A. (Ed.), Formatex Research Center, Badajoz, pp. 756–762, 2012.

[100] Q. Zhao, and B. Li, "pH-controlled drug loading and release from biodegradable microcapsules," *Nanomed. Nanotechnol. Biol. Med.*, vol. 4, no. 4pp. 302–310, December, 2008.

[101] F. Fleury, A. Ianoul, M. Berjot, V. Feofanov, A. J. P. Alix, and I. Nabiev, "Camptothecin-binding site in human serum albumin and protein transformations induced by the drug binding," *FEBS Lett.*, vol. 411, no. 2-3, pp. 215–220, 1997.

[102] B. Selvi, S. Patel, and M. Savva, "Physicochemical characterization and membrane binding properties of camptothecin," *J. Pharm. Sci.*, vol. 97, no. 10, pp. 4379–4390, 2008.

[103] Z. Mi, and T. G. Burke, "Differential interactions of camptothecin by human serum albumin," *Biochemistry*, vol. 33, no. 34, pp. 10325–10336, 1994.

[104] T. Gillich, C. Acikgöz, L. Isa, A. D. Schlüter, N. D. Spencer, and M. Textor, "PEGstabilized core-shell nanoparticles: impact of linear versus dendritic polymer shell architecture on colloidal properties and the reversibility of temperature induced aggregation," *ACS Nano*, vol. 7, no. 1, pp. 316–329, 2013.

[105] L. Cheng, and D. Cao, "Aggregation of polymer-grafted nanoparticles in good solvents: a hierarchical modeling method," *J. Chem. Phys.*, vol. 135, no. 12, 124703, September, 2011.

[106] Y. Pommier, "Topoisomerase I inhibitors: camptothecins and beyond," *Nat. Rev. Cancer*, vol. 6, no. 10, pp. 789–802, 2006.

[107] T. Sivasankar, and B. Kumar, "Role of nanoparticles in drug delivery system," *Int. J. Res. Pharm. Biomed. Sci.*, vol. 1, pp. 41, 2010.

[108] M. E. Wall, M. C. Wani, A. W. Nicholas, G. Manikumar, C. Tele, L. Moore, A. Truesdale, P. Leitner, and J. M. Besterman, "Plant antitumor agents. 30. Synthesis and structure activity of novel camptothecin analogs," *J. Med. Chem.*, vol. 36, no. 18, pp. 2689–2700, September, 1993.

[109] M. S. Surapaneni, S. K. Das, and N. G. Das, "Designing paclitaxel drug delivery systems aimed at improved patient outcomes: Current status and challenges," *ISRN Pharmacology*, pp. 1-15, August, 2012.

[110] T. Westergren, and B. Kalikstad, "Dosage and formulation issues: oral vitamin E therapy in children," *Eur. J. Clin. Pharmacol.*, vol. 66, pp. 109-118, 2010.

[111] S. V. Mussi, R. C. Silva, M. C. Oliveira, C. M. Lucci, R. B. Azevedo, and L. A. Ferreira, "New approach to improve encapsulation and antitumor activity of doxorubicin loaded in solid lipid nanoparticles," *Eur. J. Pharm. Sci.*, vol. 48, no. 1-2, pp. 282-290, 2013.

[112] X. G. Zhang, J. Milao, Y. Q. Dai, Y. Z. Du, H. Yaun, and F. Q. Hu, "Reversal activity of nanostructured lipid carriers loading cytotoxic drug in multi-drug resistant cancer cells," *Int. J. Pharm.*, vol. 361, no. 1-2, pp. 239-244, 2008.

[113] T. Ramasamy, T. H. Tran, J. Y. Choi, H. J. Cho, J. H. Kim, C. S. Yong, H. G. Choi, and J. O. Kim, "Layer-by-Layer coated lipid-polymer hybrid nanoparticles designed for use in anticancer drug delivery," *Carbohydr. Polym.*, vol. 102, pp. 653-661, 2014.

[114] G. Hermanson, "Discrete PEG reagents," in *Bioconjugate Techniques*, 2nd ed., San Diego, CF, Academic Press, ch. 18, pp. 707-733, 2008.

[115] T. Wang, W. C. Hartner, J. W. Gillespie, K. P. Praveen, S. Yang, L. A. Mei, V. A. Petrenko, and V. P. Torchilin, "Enhanced tumor delivery and antitumor activity in vivo of liposomal doxorubicin modified with MCF-7-specific phage fusion protein," *Nanomedicine*, vol. 10, no. 2, pp. 421-430, 2014.

[116] L. Reimer, "Introduction to polymer morphology," in *Scanning electron microscopy, Physics of image formation and microanalysis*, 2nd ed., New York, NY, Springer Verlag, ch. 1, 1998, pp. 7-8.

[117] V. P. Torchilin, "Multifunctional nanocarriers," *Adv. Drug Deliv. Rev.*, vol. 58, no. 14, pp. 1532-1555, 2006.

[118] G. Schneider, and G. Decher, "Functional Core-shell Nanoparticles via Layer-by-Layer Assembly. Investigation of the Experimental Parameters for Controlling Particle Aggregation and for Enhancing Dispersion Stability," *Langmuir*, vol. 24, pp. 1778–1789, 2008.

[119] C. E. Mora-Huertas, H. Fessi, and A. Elaissari, "Polymer-based nanocapsules for drug delivery," *Int. J. Pharmaceutics*, vol. 385, pp. 113-142, 2010.

[120] J. Lee, J. Y. Choi, and C. H. Park, "Characteristics of polymers enabling nano-comminution of water-insoluble drugs," *Int. J. Pharm.*, vol. 355, no. 1-2, pp. 328-336, 2008.

[121] R. H. Muller, C. Jacobs, and O. Kayser, in *Pharmaceutical Emulsions and Suspensions. Drugs and the Pharmaceutical Sciences*, vol.105, F. Nielloud, G. Marti-Mestres Eds., Marcel Dekker, 2000, pp. 383-408.

[122] P. Pattekari, Z. Zheng, X. Zhang, T. Levchenko, V. Torchilin, and Y. Lvov," Top-down and bottom-up approaches in production aqueous nanocolloids of paclitaxel," *Phys. Chem. Chem. Phys.*, vol. 13, no. 19, pp. 9014-9019, 2011.

[123] D. J. McClements, "Structural design principles for improved food performance: nano-laminated biopolymer structures in foods," in *Micro/Nanoencapsulation of Active Food Ingredients, ACS Symposium Series*, vol. 1007, eds., American Chemical Society, Washington, DC, ch. 1, 2009, pp. 3-34.

[124] D. Güzey, and D. J. McClements, "Influence of Environmental Stresses on O/W Emulsions Stabilized by β-Lactoglobulin–Pectin and β-Lactoglobulin–Pectin–Chitosan Membranes Produced by the Electrostatic Layer-by-Layer Deposition Technique," *Food Biophysics*, vol. 1, pp. 30-40, 2006.

[125] S. Mansouri, Y. Merhi, F. M. Winnik, and M. Tabrizian, "Investigation of Layer-by-Layer Assembly of Polyelectrolytes on Fully Functional Human Red Blood Cells in Suspension for Attenuated Immune Response," *Biomacromolecules*, vol. 12, pp. 585-592, 2011.

[126] C. Cortez, J. F. Quinn, X. Hao, C. S. Gudipati, M. H. Stenzel, T. P. Davis, and F. Caruso, "Multilayer Buildup and Biofouling Characteristics of PSS-b-PEG Containing Films," *Langmuir*, vol. 26, pp. 9720–9727, 2010.

[127] R. A. Petros, and J. H. DeSimone, " Strategies in the design of nanoparticles for therapeutic applications," *Nature Reviews Drug discovery*, vol. 9, pp. 615-627, 2010.